UNIVERSITAT DE BARCELONA

Mechanisms and modulation of cortical rhythms and complexity

Almudena Barbero Castillo

IDIBAPS

GOBIERNO DE ESPAÑA · MINISTERIO DE CIENCIA, INNOVACIÓN Y UNIVERSIDADES

Universitat de Barcelona

MECHANISMS AND MODULATION OF CORTICAL RHYTHMS AND COMPLEXITY

Doctoral thesis by Almudena Barbero Castillo

PhD Supervisor: María Victoria Sanchez Vives

2020

INSTITUT D'INVESTIGACIONS BIOMÈDIQUES AUGUST PI I SUNYER

UNIVERSITY OF BARCELONA

THESIS FOR DOCTORAL DEGREE IN BIOMEDICINE

MECHANISMS AND MODULATION OF CORTICAL RHYTHMS AND COMPLEXITY

Author:

Almudena Barbero Castillo

Supervisor:

María Victoria Sánchez Vives, MD, PhD

System Neuroscience

Cortical Network and Event Lab

2020

"Divide each difficulty into as many parts as is feasible and necessary to resolve it."

— René Descartes

Abstract

Doctoral degree in Biomedicine

Mechanisms and modulation of cortical rhythms and complexity

by **Almudena Barbero Castillo**

Throughout various brain states, billions of neurons interact simultaneously, resulting in a variety of cortical rhythms accompanied by switches between consciousness states and brain complexity. The Perturbational Complexity Index can effectively distinguish the level of cortical complexity from humans to *in vitro* cerebral cortex. Through the modulation of cortical activity in isolated cortical slices, we investigated the mechanisms underlying cortical network rhythms and the emergence of cortical complexity *in vitro*. In this Thesis, we reveal that the relevance of inhibitory transmission, the excitatory inhibitory balance, or the importance of cortical excitability all the way to ionic channels, for the maintenance of cortical rhythms and neural complexity at physiological levels.

Summary

Doctoral degree in Biomedicine

Mechanisms and modulation of cortical rhythms and complexity

by **Almudena Barbero Castillo**

Throughout various brain states, billions of neurons interact resulting in a variety of cortical rhythms accompanied by switches between behavioral states (Gervasoni et al., 2004). As a result of the specific (1) structure (layers and columns), (2) connections and (3) components (excitatory and inhibitory neurons expressing receptors and ion channels) within the cortical networks, switches in the cortical network state are possible. From synchronized cortical regimes of slow wave activity (SWA) during deep sleep or anesthesia (Steriade et al., 2001), global activity can change to irregular and spatiotemporally complex cortical activity during arousal states (Duarte et al., 2017; Steriade et al., 2001). If the underlying cellular or molecular regulatory mechanisms of these transitions are altered, aberrant cortical rhythms and behavioral states may appear (e.g., epilepsy or consciousness disorders). Thus, healthy and altered patterns of cortical activity correlate with behavioral states. Many methods have been used to detect the level of consciousness based on cortical activity (spontaneous or evoked activity). The Perturbational Complexity Index (PCI) (Casali et al., 2013) can effectively detect the level of complexity in humans and also in cortical slices *in vitro* (sPCI) (D'Andola et al., 2017) based on the cortical evoked responses after electrical stimulation. Because (1) cortical activity patterns can be simulated in *in vitro* preparations (Compte, 2003; Sanchez-Vives et al., 2010), (2) shifting between cortical rhythms can occur independently of thalamic

inputs, and (3) as a result of neuromodulators acting directly on cortex(Constantinople and Bruno, 2011), we can specifically activate or inactivate ion channels or receptors in order to induce changes in the spontaneous or evoked activity (sPCI) and provide insights into the underlying mechanisms controlling the transition between different cortical rhythms and complexity.

To investigate these, (1) we replicated SWA and awake-like regimes to validate isolated cortical slices as a model of brain states and analyzed sPCI as a methodological tool to quantify network complexity; (2) we studied the contribution of excitatory and inhibitory components to the different cortical network rhythms and complexity; and (3) we identified cellular mechanisms underlying the modulation of cortical states by regulating the levels of different neurotransmitters involved in brain state transitions and complexity.

The main methods used during this doctoral thesis consisted of an *in vitro* preparation of cortical brain slices from ferrets, which spontaneously display SWA. We recorded the cortical activity with a 16-channel array, and modulated the spontaneous and evoked cortical activity by the bath application of agonist/antagonists of ion channels/receptors. We also modulate cortical activity using electrical tools (through direct current stimulation) or photopharmacology tools.

The results exposed within this thesis revealed that isolated cortical slices can display different cortical activity patterns and levels of complexity detected by sPCI (D'Andola et al., 2017). Using this model, we demonstrated that the disruption of inhibitory and excitatory balances has important effects over the regime of cortical activity and the cortical complexity. We demonstrated that inhibition (fast and slow) maintains cortical activity patterns through the modulation of excitability and their oscillatory frequency. In addition, we demonstrated that certain levels of excitability are required to induce higher complexity states. When we induced changes in excitability through (1) K^+ channels or muscarinic acetylcholine receptors; (2) or with inactivation of K^+ channels or blocking

inhibition, the network shifts from the bistable response to more heterogeneous responses (increasing network complexity states) or to a homogeneous epileptic response (decreasing network complexity states), respectively. Thus, these findings suggest that the maintenance of cortical rhythms and neural complexity at physiological levels requires the coordinated contribution of the balance between excitation and inhibition and excitability, parameters that can be modulated by different mechanisms, like neurotransmitters, drugs or exogenous stimulation.

This work was supported by the Spanish Ministry of Science and Innovation through the MICINN under grant TRANSLACORTEX BFU2017-85048-R and co-financed by the European Union Regional Development Fund within the framework of the ERDF/FEDER Operational Program. This project has received funding from the European Union's Horizon 2020 research and innovation programme under grant agreement No 785907 and 945539 (Human Brain Project Flagship).

IDIBAPS is funded by the CERCA program (Generalitat de Catalunya) and the Systems Neuroscience group is supported by the Neurovirtual Group by -AGAUR- (2017 SGR 1296).

Acknowledgments

Los agradecimientos son pocos, y las palabras insuficientes para cada una de las personas que me habéis ayudado y habéis formado parte de este largo camino.

En primer lugar, gracias a Mavi por darme la oportunidad de trabajar en el laboratorio bajo por su supervisión, toda una inspiradora. Ha sido muy importante para mí, pues he comprendido la neurociencia más allá de lo que ya conocía desde mis estudios en biología. Esto ha sido gracias a qué las personas que lo componen provienen de diferentes campos de la neurociencia, lo cual mejora el entendimiento de la misma.

También agradecerle a Vanessa, antigua lab manager, la mama del lab, siempre al tanto de todo, solucionadora de problemas pequeños y grandes, gran persona y un gran apoyo durante los años que compartimos en el laboratorio.

Por supuesto, agradecer a todos los postdocs y predocs con los que he compartido laboratorio en estos años. Se podrían dividir en dos generaciones.

(1) Una primera generación donde soportasteis mis primeros pasos en el entendimiento de la electrofisiología: Pedro compartiendo horas y horas de set up y frustración; Julia, Patricia, Nahuel, Nuria, Alex y Lorena que me ayudaron a comprender las bases de la neurofisiología y la base computacional; la frescura, alegría y positivismo de la gran gurú Cristina con los que tantos ratos he compartido y me han inspirado para ver las cosas de otro modo. Especial agradecimiento de esta primera generación a Bea, Álvaro, Miguel y Sara. Bea por enseñarme tanto de la parte in vitro, del laboratorio y por seguir estando ahí aún, apoyando tanto desde la distancia, un ejemplo a seguir para mí. Álvaro por ser un gran apoyo en la parte computacional y también un gran apoyo fuera del lab, una gran persona y un gran amigo. Miguel, por su ironía gallega, sus ganas de ayudar y sus ganas de enseñar; y mi pollito, Sara, que además de ser una perfecta alumna, ha sido una amiga ideal.

(2) Gracias a la segunda generación, por los que están o hace poco estuvieron en el lab: al equipo computacional Alessandra, Leonardo, Carlos, Arnau, Andrea, Marçcal que siempre habéis estado allí para ayudarme en mis peleas con Matlab; al equipo experimental: Miquel, Jose Manuel y Jose

Miguel que habéis estado en esta última etapa donde hemos luchado por sacar adelante la parte experimental y aún estamos en ello; además agradecer a compis de anécdotas con Brenda, Patricia, Tony y Marta Forcella. He de hacer especial mención también al colaborador estrella en esta tesis, Fabio Riefolo (bajo la supervisión de Pau Gorostiza), el creador de photoswitchable molecules como PAI, BAI, PNZ… hemos pasado tantas horas de set up, luces, y luchas por conseguir el photoswitching… Sin él, gran parte de la tesis no hubiera salido adelante, ¡ni los papers que nos quedan por publicar! Por último y no menos importante gracias a mis chicas Melody y Belén compañeras de "U", de alegrías y frustraciones, de secretos y consejos. Gracias por estar ahí en todo momento.

Agradecer a todos aquellos que me habéis sacado de la rutina diaria para despejar mi mente. Mis chicas de máster Inés y Sheila, con las que tantas tardes de locura y risas hemos pasado. Pedro, un gran amigo, compañero de baile, de momentos inolvidables y gran consejero. Y evidentemente, agradecer mil y una veces por cada fin de semana compartido, horas de comer que acaban en cena y fiesta, y viajes increíbles, y llenar todos esos momentos de felicidad y alegría a: Jacobo, Rodrigo, Adrián, Barri, Clara, Marcos, Elena F, Elena M, Enrique, Janire, Javi, Luis, Marc y María. No cambiaría ninguno de esos momentos y los que no quedan por vivir por nada del mundo.

También a todos aquellos que desde la distancia habéis estado compartiendo los momentos más importantes. Sobre todo a los biólogos David, Pablo, Ale, Juan, Charis, Isma, Irene, Mario y María. Especialmente mencionar a mis incondicionales amigas desde la primaria Natalia, Paula y Carolina, que siempre habéis estado allí para escuchar mis alegrías y penas aunque estuvierais a km de distancia.

Finalmente, agradecer a la GRAN familia que tengo, porque no solo una familia es aquella con la que compartes sangre. En primer lugar, agradeceros a Mamá, Isabel y Oscar que siempre me habéis estado apoyando y guiando en los momentos más difíciles, dando fuerzas para llegar hasta el final de esta etapa. También a Angelines, a mis primos y tios, Asún, Alberto, Fran y Jorge que siempre se han preocupado por mi desde la distancia; y a mi familia catalana Conxita y Ato por apoyarme tanto al final de este camino. Finalmente, agradecerle a Ernest, que siempre ha estado para escuchar mis alegrías y penas, apoyándome y esforzándose en que viera lo realmente capaz que soy de sacar todo lo que me proponga. Gracias por creer en mí.

Contents

List of Publications

- Barbero-Castillo A, Weinert JF, Camassa A, Perez-Mendez L, Caldas-Martinez S, Mattia M, Sanchez-Vives M V. (2019) Proceedings #31: Cortical Network Complexity under Different Levels of Excitability Controlled by Electric Fields. *Brain Stimul 12, e97–e99.* https://doi.org/10.1016/j.brs.2018.12.200.

- Barbero-Castillo A, Riefolo F, Matera C, Caldas-Martínez S, Mateos-Aparicio P, Weinert JF, Claro E, Sánchez-Vives MV, Gorostiza P (2020) Control of brain state transitions with light. *bioRxiv 793927.* https://doi.org/10.1101/793927. *Submitted to Advance Science.*

- Mateos-Aparicio P, Barbero-Castillo A, Porta LD, Camassa A, Perez-Mendez L, Sanchez-Vives M V. Impact of $GABA_A$ and $GABA_B$ receptors on cortical dynamics and perturbational complexity during synchronous and asynchronous activity. *Submitted to Cerebral Cortex.*

- Sanchez-Vives M V., Barbero-Castillo A, Perez-Zabalza M, Reig R (2020) $GABA_B$ Receptor-modulation of Thalamocortical Dynamics and Synaptic Plasticity. *Neuroscience.* https://doi.org/10.1016/J.NEUROSCIENCE.2020.03.011.

- Barbero-Castillo A, Camassa A, Dasilva M, Masvidal-Codina E, Guimerà-Brunet A, Bosch M, Demirtas M, Sanchez-Vives M V. Brain state discrimination across levels of anesthesia using chronic full-band cortical recordings with graphene microtransistors arrays. *In preparation.*

List of Figures

List of Abbreviations

4-AP	4-aminopyridine
ACh	Acetylcholine
AChR	Acetylcholine receptor
ACSF	Artificial cerebro-spinal fluid
AI	Appendix I
AII	Appendix II
a.u.	Arbitrary units
BMI	Bicuculline methiodide
CCh	Carbachol
CGP	CGP 55845
DCS	Direct Current Stimulation
EEG	Electroencephalogram
EF	Electric field
FR	Firing rate
GABA	γ-aminobutyric acid
GBZ	SR-95531 hydrobromide, Gabazine
IF	Infragranular
IPX	Iperoxo
K_v	Voltage-dependent K^+ channel
K_{v7}	Voltage gated K^+ channel 7
LFP	Local field potential
mAChR	Muscarinic Acetylcholine receptor
MUA	Multiunit activity
nAChR	Nicotinic Acetylcholine receptor
NE	Noradrenaline
NREM	Non-rapid eyed movement
PAI	Phthalimide-Azobenzene-Iperoxo
PCI	Perturbational Complexity Index
PSD	Power spectral density
SG	Supragranular
sPCI	*in vitro*, slice PCI
SWA	Slow wave activity
tDCS	Transcranial Direct Current Stimulation
TEA	Tetraethylammonium chloride
TMS	Transcranial Magnetic Stimulation
V1	Primary visual cortex
WM	White matter

Chapter 1

Introduction

1. Cortical rhythms

Throughout various brain states and subsequent cognitive processes, there is a complex interaction of billions of neurons, resulting in a collection of cortical rhythms (Gervasoni et al., 2004). These temporally coexist in the same or different cortical areas, with reciprocal interactions (Buzsáki and Draguhn, 2004), providing a temporal window of neuronal population cooperation necessary for cognitive processes (representation, processing, storage, and retrieval of information) and for switching the behavioral state (Csicsvari et al., 2003; Fogerson and Huguenard, 2016). Indeed, cortical rhythms are not pure oscillations. These consists of a combination by a combination of slow (<1 Hz), delta

(1-4 Hz), theta (4-7 Hz), alpha (7-12 Hz), beta (12-30 Hz), and gamma (30-100 Hz) rhythms (Mantini et al., 2007). Therefore, different cortical states are defined by distinct spatiotemporal profiles of spontaneous cortical activity (Casali et al., 2013; Steriade and Timofeev, 2003; Tremblay et al., 2016) and their alterations are associated with behavioral and cognitive disorders. Next, we describe the cortical activity during sleep and wakefulness, and patterns of aberrant cortical activity such as epilepsy or disorders of consciousness.

1.1. Slow wave activity and Awake states

During deep sleep (Non-rapid eye movement, NREM sleep) or anesthesia, brain potentials (electroencephalogram; EEG) are characterized by large-amplitude and slow rhythms, which is known as Slow Wave Activity (SWA) (Steriade et al., 2001) (**Figure 1**). This profile of cortical rhythm spontaneously appears with similar properties from the level of cortical slices *in vitro,* to the intact neocortex of the sleeping human (Sanchez-Vives and McCormick, 2000; Sanchez-Vives et al., 2017) (**Figure 2**). Therefore, SWA has

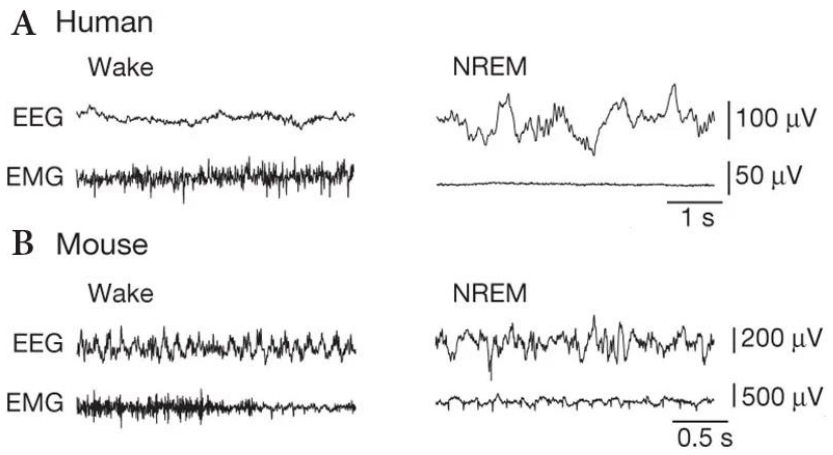

Figure 1. From bistable SWA, global activity varies to asynchronous awake states. *Examples from a human (**A**) and a mouse (**B**) electroencephalogram (EEG) and electromyogram (EMG) recordings during wakefulness and NREM sleep. Modified from* Nature Review Neuroscience (Weber and Dan, 2016).

been considered as a multiscale phenomenon which mainly depends on local and recurrent cortical connectivity of the neocortex (Constantinople et al., 2011; Fernandez et al., 2016; Massimini et al., 2005; Neske, 2016; Sanchez-Vives et al., 2017; Zagha and McCormick, 2014).

SWA is a bistable state whose neural population are (1) highly coordinated and synchronized (**Figure 1** and **Figure 2**) (Constantinople et al., 2011; Duarte et al., 2017; Hirata and Castro-Alamancos, 2010); and (2) alternates between periods of activity or neural firing (Up-states), with periods of silence (Down-states), at a frequency of 1Hz (Sanchez-Vives and McCormick, 2000; M Steriade et al., 1993b; Steriade, 2006) (**Figure 1** and **Figure 2**). Indeed, neural firing during Up-state has a similar temporal structure to the activity during wakefulness states (i.e. synchronized beta (12-30 Hz) and gamma (30-100 Hz) rhythms) (Destexhe et al., 2007; Steriade et al., 1996).

From synchronized regimes of SWA during sleep, global activity shifts to widespread spatiotemporal cortical rhythms during awake states, in which neurons fire irregularly and nearly independently (**Figure 1**) (Andalman et al., 2019; Chen et al., 2009; Constantinople et al., 2011; Duarte et al., 2017; Poulet and Crochet, 2019; Steriade et al., 2001). Unlike SWA, wakefulness activity is characterized by persistent depolarization, high frequency activity (gamma band) and low amplitude of EEG signals (**Figure 1**). These periods of activity have been related with high-order brain functions (i.e. perception, attention, sensory binding and storage and recall of information) (Dugladze et al., 2013) which require the activation of subcortical areas (Lee and Dan, 2012).

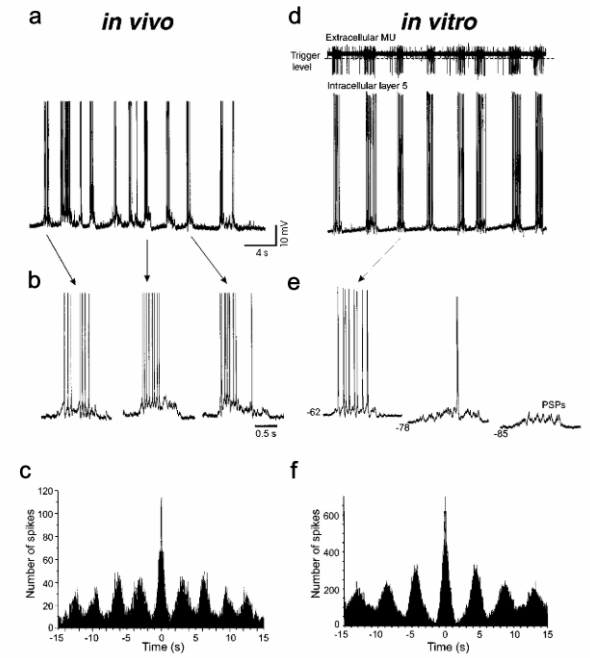

Figure 2. SWA in vivo and in vitro. a-d. *Intracellular recording showing depolarization periods (*Up*-states) and hyperpolarization periods (Down-states) of a single neuron in the anesthetized cat (a) and in a slice from ferret cortex (d). Extracellular multiunit activity (D, top).* ***b-e****. Up-state examples from a and d.* ***c-f****. Periodicity of the oscillation represented in autocorrelograms of the intracellular recordings. Source from* Nature Neuroscience *(Sanchez-Vives and McCormick, 2000).*

1.2. Altered cortical activity patterns: Epilepsy and Disorders of consciousness

Different cortical states are defined by distinct spatiotemporal profiles of spontaneous cortical activity (Casali et al., 2013; Steriade and Timofeev, 2003; Tremblay et al., 2016). Alterations in these profiles are associated with disorders such as epilepsy (Kalemaki et al., 2018; Lundstrom et al., 2019; Pinto et al., 2005), or disorders of consciousness e.g. following stroke or traumatic brain injury (Bodien et al., 2017; Casali et al., 2013; Malinowska et al., 2013).

While epilepsy is characterized by recurrent unprovoked seizures, caused by abnormally excessive and synchronous neuronal activity of the brain (Chabolla, 2002; Devinsky et al., 2018; Pinto et al., 2005), disorders of consciousness have been defined as

altered states of pathologic consciousness, and may be caused by disconnection of the thalamocortical system (Bayne et al., 2016; Malinowska et al., 2013; Xia et al., 2018). Although epilepsy and disorders of consciousness are different behavioral disorders they have something in common, both are associated with systematic changes in oscillatory rhythms (Boly et al., 2017; Englot et al., 2010; Fattinger et al., 2015; Lundstrom et al., 2019; Pellegrino et al., 2017; Wislowska et al., 2017). It has been demonstrated that, (1) during wakefulness or sleep states, low frequencies are enhanced during epilepsy episodes (Boly et al., 2017; Englot et al., 2010; Fattinger et al., 2015; Lundstrom et al., 2019; Pellegrino et al., 2017; Wislowska et al., 2017); (2) disorders of consciousness' patients show significant correlation between patients' behavioral diagnoses and impairment in cognitive processes, with alterations in EEG patterns including SWA and higher frequencies (Bai et al., 2017b; Lehembre et al., 2012; Malinowska et al., 2013; Schiff et al., 2014; Wislowska et al., 2017). Thus, the study of spontaneous cortical activity and their regulatory mechanisms is relevant for diagnosis of the disorders and could reveal new therapeutic opportunities for these diseases

2. Cortical excitatory and inhibitory transmission and their role in cortical rhythms

Interaction of neurons result in a collection of cortical rhythms (Gervasoni et al., 2004) such as SWA or awake activity. Switches in the cortical rhythms are possible for three main reasons: (1) Cortical networks form a specific framework, organized in six layers and columns (Constantinople and Bruno, 2013). (2) Furthermore, there is a neuronal specificity (excitatory and inhibitory neurons) and specialized connectivity (local and long range connections) which organizes the flow of information in the cortical network and subsequent cortical rhythms (Douglas and Martin, 2004; Isaacson and

Scanziani, 2011). (3) Finally, neurons are sensitive to extracellular or intracellular molecules (e.g. neuromodulators, ion concentration) through the expression of membrane proteins (receptors and ion channels) (Spruston, 2008).

2.1. Structure of cortical frameworks

Cortical networks are compounded by thousands of neurons connected between them by billions of synapses (Lee et al., 2016). Cortical networks constitute a framework because it is organized in layers (layer 1, 2/3, 4, 5 and 6) and columns (**Figure 3A**). In primary somatosensory cortices, such as primary visual cortex (V1), layer 4 is called the internal granular layer because it is composed of granule cells. Therefore, layers 1 and 2/3 are called supragranular layers (SG), and layers 5 and 6 are called infragranular (IF) layers (Douglas and Martin, 2004; Yuste, 2015) (**Figure 3A**). Cortical networks also constitute a framework because it is divided into functional units (**Figure 3B**). There is a specialized connectivity for processing cortical inputs (**Figure 3B**) (Douglas and Martin, 2004; Yuste, 2015). In summary, layer 4 receives information from thalamus and projects to layer 2/3. layer 2/3 communicates with layer 5. Then layer 5 projects to Layer 6 and gives feedback to layer 2/3. Layer 6 finally projects to layer 4. Layer 1 receives input from subcortical nuclei and feedback connections from other cortical areas (**Figure 3B**) (Constantinople and Bruno, 2013; Douglas and Martin, 2004; Markram et al., 2015; Wester and Contreras, 2012).

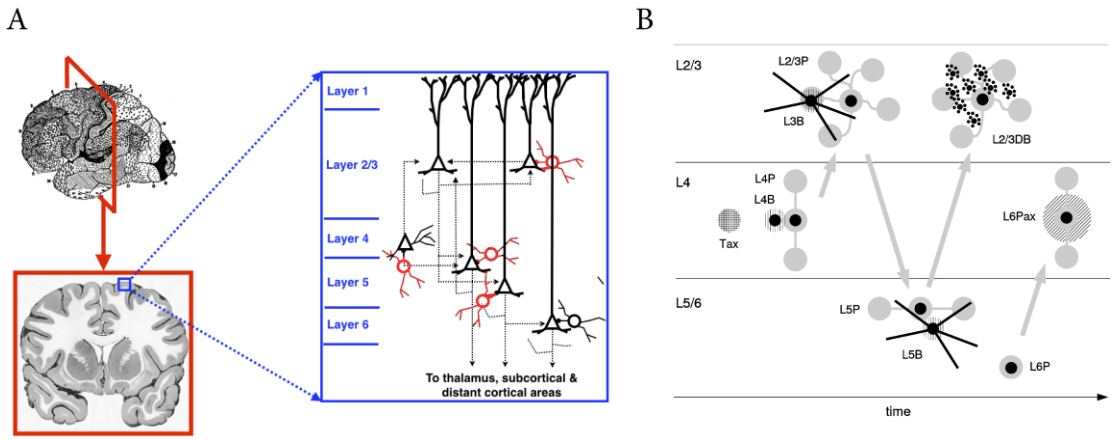

Figure 3. Division of layers in the neocortex and their laminar-temporal interactions between main neurons in the neocortex. A. *Illustration of layer division human neocortex. Modified from* Sinauer Associates (Blumenfeld, 2010). *Red cortical interneurons and Black marked cortical excitatory neurons.* ***B.*** *Time towards the right displaying 5 consecutive synaptic crossing. Gray circles, pyramidal cells. Black circles, interneurons. P: pyramidal cells. B: basket cells. Tax: thalamic afferents. L6Pax: Layer 6 pyramidal arbors projecting to layer 4. Reproduced from* Annual Review of Neuroscience (Douglas and Martin, 2004).

2.2. Elements of cortical frameworks: Inhibitory and excitatory components and their role in cortical rhythms

Within the cortical framework, there is a neuronal specificity (excitatory and inhibitory neurons) and specialized connectivity (local and long-range connections) which organizes the flow of information in the cortical network and subsequent cortical rhythms (Douglas and Martin, 2004; Isaacson and Scanziani, 2011). In summary, cortical units are classified mainly for glutamatergic excitatory neurons and GABAergic (γ-aminobutyric acid, GABA) inhibitory interneurons, which are functionally specialized based on their cortical location and distribution.

2.2.1. Glutamatergic excitatory neurons

Glutamatergic neurons form the excitatory connections between layers and are mainly involved in propagation signals (**Figure 3A**) (Constantinople and Bruno, 2013; Douglas and Martin, 2004; Markram et al., 2015; Naka and Adesnik, 2016; Thomson and

Lamy, 2007; Tremblay et al., 2016; Wester and Contreras, 2012). However, since excitatory neurons spontaneously oscillate with resonant firing at low frequencies, they have been also associated with a specific role in SWA. (1) It has been proposed that the initiation of SWA depends on cortical excitatory neurons from layer 5 and the thalamus (Beltramo et al., 2013; Gent et al., 2018; Neske, 2016; Sanchez-Vives and McCormick, 2000; Steriade et al., 1996; Wester and Contreras, 2012); and (2) the activation of glutamatergic ionotropic receptors and recurrent activation of excitatory synaptic activity is required for the maintenance of Up-states (McCormick et al., 2003; Neske, 2016; Sanchez-Vives and McCormick, 2000; Shu et al., 2003).

2.2.2. GABAergic inhibitory neurons

While glutamatergic cells mainly form the excitatory connections between layers, cortical GABAergic inhibitory neurons mainly form synapses within their local layer (**Figure 3A**) (Buzsáki et al., 2004; Douglas and Martin, 2004; Thomson and Lamy, 2007). In fact, excitatory neurons are inhibited by more than 50% of inhibitory neurons located within ~100 μm (Isaacson and Scanziani, 2011) and they can fire at higher rates than excitatory cells (Bartos et al., 2007; Cardin, 2018; Jones and Barth, 2002; Konstantoudaki et al., 2014; Orbán et al., 2001; Wright, 1997). Therefore, they play a critical role in processing information in the neocortex by gating signal flow and sculpting network rhythms. Among other functions, they have been associated with (1) controlling the temporal precision of excitatory cell firing, (2) regulation of firing rates and bursting, (3) synchronization and generation of cortical rhythms, and (4) the maintenance of the excitatory and inhibitory balance necessary for the transfer of information (Cobos et al., 2005; Guidotti et al., 2005; Konstantoudaki et al., 2014; Tremblay et al., 2016).

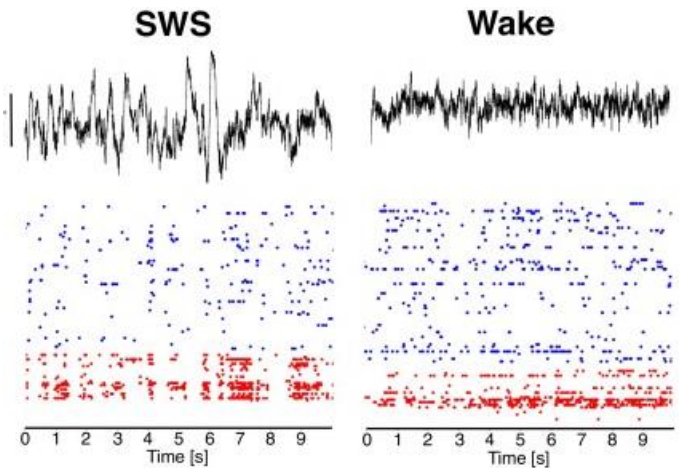

Figure 4. Neural firing presents different patterns across brain states in humans. *Local Field Potential (LFP) traces (top) and spiking activity from excitatory neurons (blue) and inhibitory neurons (red) (bottom) during SWA (SWS) and awake states (Wake).* From Current Opinion in Physiology (Susin and Destexhe, 2020)

Recent theories (Susin and Destexhe, 2020) proposed that excitatory and inhibitory neuron activity is persistent during awake states (**Figure 4**). However, during SWA, while both neurons are synchronized and almost silent during Down-states, during Up-states neuronal firing is similar to awake states (**Figure 4**) (Compte et al., 2009; Susin and Destexhe, 2020). Moreover, the participation of inhibitory neurons during gamma oscillation is higher during SWA than during awake states (Compte et al., 2008; Susin and Destexhe, 2020) and inhibitory neurons increased their activity to induce Up-state termination (Compte et al., 2003; Sanchez-Vives and McCormick, 2000; Schwindt et al., 1992; M Steriade et al., 1993b).

Thus, excitatory and inhibitory neuronal interaction constitutes a fundamental feature of cortical rhythms, required for cognitive processes and this is preserved across cortical states (Duarte et al., 2017; Poulet and Crochet, 2019; Singer, 1993; Zagha and McCormick, 2014). If, however, there is an imbalance in the interaction between excitation and inhibition neurons, aberrant cortical rhythms appear (Sanchez-Vives et al., 2010). In fact, it has been described that excessive excitation and synchronization during epilepsy is associated with a decrease in the number of inhibitory interneurons or with

faulty excitatory cells (Cardin, 2018; Kalemaki et al., 2018; Konstantoudaki et al., 2014; Marín, 2012; Tremblay et al., 2016; Yang et al., 2012). Therefore, it is fundamental to study about role of excitation and inhibition in spontaneous cortical activity for diagnosing these disorders and new therapeutic opportunities for these diseases could be revealed.

3. Endogenous modulation of cortical rhythms

Switches in the cortical network state are possible not only because cortical networks form a specific framework with specific types of neurons and connections, but also because neurons are sensitive to extracellular or intracellular molecules (e.g. neuromodulators, ion concentration) through the expression of membrane proteins (receptors and ion channels) (Spruston, 2008).

Neuromodulators from neuronal populations of subcortical areas target these membrane proteins, resulting in modification of several cellular functions (e.g. synaptic strength, firing rates, firing modes, dendritic excitability and intrinsic and network oscillations) (Spruston, 2008). Therefore, their liberation in the neocortex contribute in different ways to the transition into different cortical rhythms (Brown et al., 2012; Ding et al., 2016; Lee and Dan, 2012; Tremblay et al., 2016; Zhang, 2019) and precise modulation of activation/inactivation of these receptors and ion channels could be an approach for the study of the underlying mechanisms of cortical network states and their transitions.

3.1. GABA

GABA is the main inhibitory neurotransmitter in the neocortex (Wu and Sun, 2015) and GABAergic cortical neurons play a critical role in processing information (Cobos et al., 2005; Guidotti et al., 2005; Konstantoudaki et al., 2014; Tremblay et al., 2016). There

are two main types of GABA receptors in cortical neurons: (1) the ionotropic $GABA_A$ receptor (fast inhibition, ligand-gated ion channel) and (2) the metabotropic $GABA_B$ receptor (slow inhibition, G-protein coupled receptor) (Perez-Zabalza et al., 2020; Sanchez-Vives et al., 2020; Wu and Sun, 2015). Both are widely expressed in the brain (Kullmann et al., 2005; Princivalle et al., 2000) and both have an important role during sleep: (1) $GABA_A$ receptor activation balances the excitation during Up-states (Cardin, 2018; Li et al., 2017; Mann et al., 2009; Sanchez-Vives et al., 2010; Shu et al., 2003) and progressive pharmacological blockade of this receptor reduces Up-state duration (Mann et al., 2009; Sanchez-Vives et al., 2010); (2) blocking $GABA_B$ receptor inhibition results in a continuous increase in Up-state duration (Mann et al., 2009; Perez-Zabalza et al., 2020; Sanchez-Vives et al., 2020) which demonstrates that it contributes to the persistent activity during the Up-states (Cardin, 2018; Li et al., 2017; Mann et al., 2009; Perez-Zabalza et al., 2020).

Thus, deficits or excess of GABA release, or activation of its receptors, may underlie the aberrant patterns of cortical rhythms and behavioral states such us epilepsy (Kalemaki et al., 2018; Lundstrom et al., 2019; Pinto et al., 2005; Ruiz-Mejias et al., 2016), or disorders of consciousness (Bodien et al., 2017; Casali et al., 2013; Malinowska et al., 2013). While GABAergic signaling prevents the generation of high-frequency epileptiform bursts (Cardin, 2018; Mann et al., 2009) and drugs increasing this signaling could restore cortical activity in disorders of consciousness patients (Brown et al., 2010; Clauss, 2010; Salgado et al., 2011), blocking GABAergic receptor results in acute epileptic discharges (Cobos et al., 2005; Guidotti et al., 2005; Khazipov, 2016; Sanchez-Vives et al., 2010; Shiri et al., 2016). Thus, it is important to better understand the underlying mechanisms of GABA neuromodulation in the cortical rhythms and their transition.

3.2. Acetylcholine

To move cortical activity from one state to another requires neurotransmitter signals such as acetylcholine (ACh) from subcortical areas. During wakefulness states, this neuromodulatory system is highly activated, while during sleep, its activity is reduced or stopped (Jones, 2005; Lin, 2000). Therefore, liberation of this neurotransmitter in the neocortex contributes in different ways to the transition into different cortical rhythms (Lee and Dan, 2012) and behaviors. In fact, it has been shown that ACh plays an important role in several cognitive functions including arousal, working memory, and attention - all awake state processes. (Arroyo et al., 2014). ACh in the neocortex is mediated by two different types of receptors (AChRs), G-protein-coupled muscarinic AChRs (mAChRs,) and the ionotropic nicotinic AChRs (nAChRs, ligand-gated ion channel). Both participate in different ways in the sleep/awake transition. For example, it has been described that cholinergic release to neocortex (1) abolished Up-Down transitions through mAChRs, but not nAChRs signaling (McCormick and Williamson, 1989); and (2) eradicated SWA by the depression of cortico-cortical synaptic transmission and/or inhibition of excitatory neurons through the activation of mAChRs (Dasgupta et al., 2018; Eggermann et al., 2014; Poulet and Crochet, 2019). In addition, it has been described *in vitro* that activation of mAChRs are highly involved in the induction of persistent gamma frequency oscillations (Whittington et al., 2000). Thus, it is also fundamental to study the role of mAChR in cortical rhythms.

Five subtypes of mAChRs are classified in two different groups: M1-type receptors (M1, M3 and M5 subtype mAChRs), and M2-type receptors (M2 and M4 subtype mAChRs). The M1, M2, and M4 mAChRs subtypes are expressed in the neocortex and M1 subtype is the most predominant (Groleau et al., 2015; Muñoz and Rudy, 2014; Radnikow and Feldmeyer, 2018). M1 is the main excitatory mAChR subtype and enhances glutamatergic drive (Brown, 2010; Groleau et al., 2015; Muñoz and Rudy, 2014; Radnikow and Feldmeyer, 2018). However, M2 is a cholinergic inhibitory autoreceptor,

controlling extracellular levels of ACh and, on GABAergic terminals, it inhibits GABA release (Bereshpolova et al., 2011; Brown, 2010; Groleau et al., 2015). M2 receptors play a relevant role in several central nervous system disorders (Scarr, 2012), and regulating their activity and subsequent effects on cortical neuronal networks, may provide new therapeutic opportunities for these cholinergic diseases.

3.3. Ionic concentrations

Several of these neuromodulators modify cortical activity by activation of specific ionotropic or metabotropic receptors. Most of them result in a variation of extracellular/intracellular ion concentrations. Then, if ion concentration can be modulated, it could affect several cellular functions and modulates the cortical rhythms (Spruston, 2008). In fact, it has been demonstrated that increasing concentrations of extracellular K^+ were observed during arousal *in vivo,* and *in vitro* after infusion of a cocktail of neuromodulators such us carbachol. Indeed, imposing changes in extracellular ion concentrations alters local activity and behavioral state between sleep and wakefulness (Ding et al., 2016; Fröhlich et al., 2008; Krishnan et al., 2018).

Potassium channel are the most diverse of ion channels, and its expression is homogeneous among cortical inhibitory interneurons and excitatory neurons, and mostly underlie functions of neuronal excitability control (Greene and Hoshi, 2017). Simply raising the extracellular ion concentration increases the frequency of spontaneous oscillatory activity (Sancristóbal et al., 2016). These are also implicated in the modulation of some phases of the SWA such as Up-state initiation and termination (Compte et al., 2003; Contreras and Steriade, 1996; Cunningham et al., 2006; Neske, 2016; Phillis et al., 1975; Schwindt et al., 1992; Steriade et al., 1994). It has been proposed that voltage gated K^+ channel 7 (KCNQ or K_{v7}) is implicated in the termination of Up-states (Neske, 2016). Therefore, alterations of ion concentration or activation/inactivation of K^+ channels could represent the source of some patterns of aberrant cortical activity such as seizures. For example, some K^+ channelopathies include the generation of convulsions, and

activation of K_{v7} has been used as a treatment to alleviate them (Fröhlich et al., 2008). In fact, it has been demonstrated that seizure-like activity can be induced by blocking non-selective voltage dependent K^+ channels (K_v) (Shiri et al., 2016). Moreover, the extracellular K^+ concentration increases during seizures (Fröhlich et al., 2008; Somjen, 2002), and *in vitro* increased the amplitude of gamma burst (Subramanian et al., 2018). Therefore, it is important for better understanding of the underlying mechanisms of K^+ modulation in the cortical rhythms and their transition.

4. Exogenous modulation of cortical rhythms

In addition to subcortical areas sending neurotransmitters to the neocortex to evoke transition between cortical states, external methods have been used to evoke this transition such as anesthesia, electrical stimulation of cortical or subcortical networks, or new optical techniques such as optogenetics or photopharmacology.

4.1. Anesthesia

General anesthesia has been used for many years to stablish unconsciousness states in patients during surgical interventions. There are several types of anesthesia and they could affect one or more neuromodulatory systems (Van Dort et al., 2008). For example, they could enhance chloride current mediated by $GABA_A$ receptors (barbiturates or propofol) (Brown et al., 2011; Ma et al., 2002; Nelson et al., 2002; Rudolph and Antkowiak, 2004; Voss et al., 2019) or could disrupt the cholinergic neurotransmission (opioids or propofol). This was also observed in rats. It has been described that propofol administration to rats decreases cortical ACh release and produces unconsciousness (Lydic and Baghdoyan, 2005). Interestingly, it has been described that some anesthetics could have an effect even over K^+ channels such as Kv channels, which are inhibited by propofol (Li et al., 2018).

4.2. Direct current stimulation

As well as anesthetics externally neuromodulating cortical or subcortical circuits to induce changes in cortical rhythms, modulating altered brain circuits by chronic electric stimulation, can also induce variations and restore spontaneous cortical activity. For example, deep brain stimulation has been used as a treatment for motor disorders such as Parkinson disease, neuropsychological (depression, epilepsy, etc.) and for disorders of consciousness (Alkire et al., 2008; Freund et al., 2009; Kim et al., 2013; Kringelbach et al., 2007; Lemaire et al., 2014; Mina et al., 2013; Sankar et al., 2014).

Another way to electrically modulate cortical activity is through transcranial direct current stimulation (tDCS). tDCS is non-invasive perturbation that can be used to suppress epilepsy by decreasing cortical excitability in humans (Rahman et al., 2013; San-juan et al., 2015) and can effectively modulate cortical excitability in patients with disorders of consciousness (Bai et al., 2018, 2017a). This was also demonstrated *in vitro* (**Figure 5**). Direct current stimulation (DCS) generating homogenous electric field (EF) perpendicular to the layers (**Figure 5A**), could modulates the intrinsic properties of the neurons (such as depolarization/hyperpolarization, firing rate or spike timing) and the frequency of spontaneous oscillation (D'Andola et al., 2018; Fröhlich and McCormick, 2010; Kabakov et al., 2012; Rahman et al., 2013; Reato et al., 2010) (**Figure 5B**).

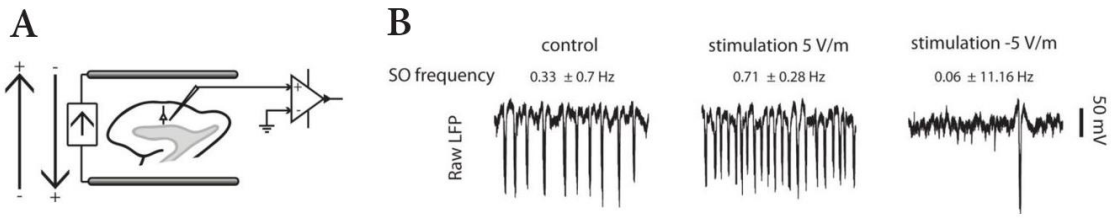

Figure 5. Direct current stimulation in vitro. A. *Modulation of network excitability was delivered by two parallel aligned silver/silverchlorided electrodes. They were placed parallel to the cortical layers in the slice, such that the direct current stimulation (DCS) generated homogenous electric field perpendicular to the layers.* ***B.*** *Raw LFP during control conditions, +5 V/m and -5 V/m DC fields. Source from* bioRxiv (D'Andola et al., 2018).

4.3. Photopharmacology, a new optical modulatory technique

The study of the modulation of cortical or subcortical circuits in neuroscience is possible thanks to bioactive molecules that have some selectivity to molecular targets. However, sometimes the interpretation is difficult if we look for high spatiotemporal precision of activation. Optogenetic substantially increases the selective activation of ion channels and receptors. It is a tool based on using light to achieve a gain or loss of function of well-defined events in specific cells of living tissue (Deisseroth, 2011) (**Figure 6A**). It is limited by the availability of suitable promoters and requires genetic manipulation. This problem is solved using photopharmacology (Barbero-Castillo et al., 2020; Riefolo et al., 2019).

Photopharmacology is based on synthetic ligands that target endogenous proteins, (**Figure 6B**). In addition, photoswitchable ligands can generally be used in multiple species, and their safety and regulation can be established as for other drugs. Indeed, it also allows to control at the spatiotemporal level (Broichhagen et al., 2015; Lerch et al., 2016; Riefolo et al., 2019). An important class of photoswitch is azobenzenes: *trans*-azobenzene gets converted into *cis*-azobenzene on exposure to ultraviolet (UV) light and the process is reversible when exposed to light of visible range (Broichhagen et al., 2015; Riefolo et al., 2019) (**Figure 10**). The application fields of photoswitchable molecules start from antimicrobials, diabetes, cellular toxicity to blocking carcinogenesis (Sarma and Medhi, 2017). Here we used a novel molecule Phthalimide-Azo-Iper (PAI) (Riefolo et al., 2019) that has been demonstrated to selectively activate M2 muscarinic ACh receptors (mAChRs) without requiring electric or genetic manipulation (**Figure 10**).

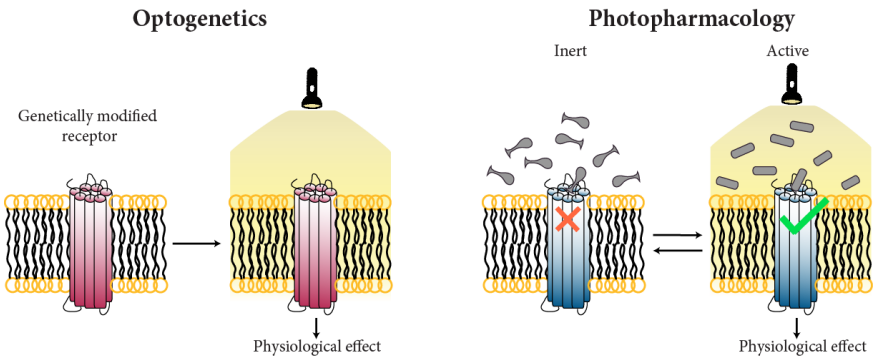

Figure 6. Illustration of light-controlled methods using a cell membrane receptor. *Optogenetics requires genetic manipulations to express light-sensitive receptors or channels. Photopharmacology uses photoswitchable drugs for interaction with their target receptors or channels.*

5. Measurements of cortical regime at different brain states

The effects of endogenous or exogenous modulation of cortical rhythms appear both in the spontaneous and evoked activity and at multiples scales, all of them with a role within global cortical activity. For this reason, it is important to study the underlying mechanisms of cortical rhythms and their transitions at multiple scales.

5.1. Spontaneous cortical activity

Switches of behavioral states are accompanied by changes in the cortical activity in many brain areas, which can be measured electrophysiologically (Gervasoni et al., 2004; Taub et al., 2013). Cortical activity under different brain states has been widely described from healthy human EEG (**Figure 1**) (Åkerstedt et al., 2002; Merica and Fortune, 2004; Saper et al., 2010), EEG from patients with disorders of consciousness (Wislowska et al., 2017) and also from *in vivo* anesthetized and implanted chronic animals in the local field potential (LFP) and Multiunit activity (MUA) (Fu et al., 2018; Hanrahan et al., 2013; Staba et al., 2017). While the physiological and electrophysiological changes in brain activity among different brain states have been well described, the causal mechanisms for the maintenance and its transitions are poorly understood. However, our *in vitro* (**Figure 2**) model is a good model to study these for three reasons: (1) cortical SWA, as well as awake

states, can be simulated in *in vitro* preparations (Markram et al., 2015; McKillop and Vyazovskiy, 2019; Sanchez-Vives and McCormick, 2000), (2) shifts between cortical rhythms can occur independently of thalamic inputs (3) and several neuromodulators act directly on neocortex (Constantinople et al., 2011; Lewis et al., 2015) in our *in vitro* preparation. Therefore, we can specifically activate or inactivate these ionic channels or ionic/metabotropic receptors to induce changes in the spontaneous or evoked activity and give some insights about the underling mechanisms controlling the transition between different cortical states.

5.2. Measurements of cortical complexity

Behavioral states can be distinguished based on the consciousness state. One of the network properties investigated to study the level of consciousness was the complexity, the level segregation and integration of information in cortical networks (Casali et al., 2013; D'Andola et al., 2017; Stratton and Wiles, 2015; Tononi et al., 1994).

The study of segregation and integration of information can be analyzed with a wide collection of tools and methods (Deco et al., 2015; Telesford et al., 2011). One such method is neural complexity, which is based on spontaneous activity. High levels of neural complexity correlates when the elements of a network are both functionally segregated and functionally integrated, as occurs in wakeful individuals (Bartels and Zeki, 2005; Casali et al., 2013; Sanders et al., 2012; Tononi, 2004). Otherwise, global random activity become either local (suggesting a loss of integration) or global but stereotypical (suggesting a loss of segregation) during loss consciousness states such as NREM sleep anesthesia (Gili et al., 2013; Monti et al., 2013) or patients with disorders of consciousness (Achard et al., 2012; Chennu et al., 2017, 2014). This was observed across multiple spatial scales, from a macro scale (intra- and inter-areal connections), to small groups of neurons (Casali et al., 2013; D'Andola et al., 2017; Pigorini et al., 2015).

Neural complexity can be studied based on spontaneous activity (Barbero-Castillo et al., 2019; Bettinardi et al., 2015; Tononi et al., 1994; Tononi and Edelman, 1998) or

measured based on a perturbational approach (**Figure 7**) like the Perturbational Complexity Index (PCI). It can measure effective connectivity (segregation) and to what extent subsets of neurons can interact causally as a whole (integration) to produce responses from a particular perturbation (Casarotto et al., 2016; D'Andola et al., 2017; Murphy et al., 2009) (**Figure 7**). PCI can distinguish levels of consciousness states in healthy and brain-injured patients from EEG response to Transcranial Magnetic Stimulation (TMS) (Casali et al., 2013) (**Figure 7**). PCI also distinguishes the level of cortical network *in vitro* (slice PCI, sPCI) (D'Andola et al., 2017) and *in vivo* at different levels of anesthesia measured through LFP responses to electrical stimulation (Dasilva et al., *under review*). sPCI adaptation was highly useful to simulate different regimes of network activity and their modulation by regulating the tone of different neurotransmitters involved in brain state transition (D'Andola et al., 2017).

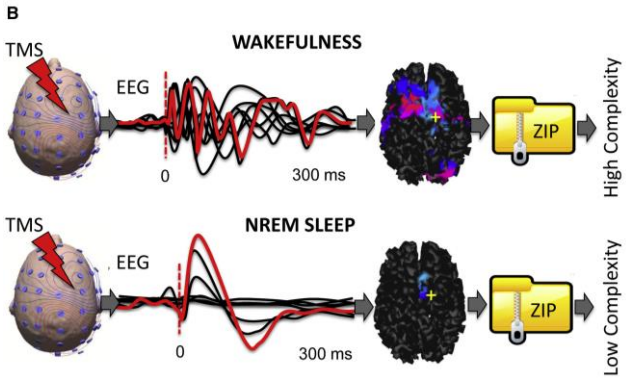

Figure 7. Perturbational Complexity Index in humans. *EEG responses after Transcranial Magnetic Stimulation (TMS) are more heterogeneous spatiotemporally during wakefulness states than during NREM sleep. Lempel-Ziv compression of significant evoked responses reveal high complexity during wakefulness states. Average of EEG responses following TMS (Red) and maximum current sources (color-coded according to their activation latency: light blue, 0 ms; red, 300 ms). Yellow cross: TMS target on the neocortex. Source from* Neuron (Sanchez-Vives et al., 2017)

Objectives

The global objective of this Thesis is to better understand the mechanisms underlying cortical network rhythms and generation of cortical network complexity *in vitro* and therefore the underpinnings of brain states. More specifically, the main objectives of this thesis are:

- ❖ To validate isolated cortical slices as a model of brain states and sPCI as a methodological tool for measuring network complexity.
- ❖ To study the contribution of excitatory and inhibitory components to cortical rhythms and complexity.
- ❖ To identify the cellular mechanisms underlying the modulation cortical states by regulating the levels of different neurotransmitters involved in brain state and complexity transitions.

Chapter 2

Material and Methods

We performed 4 different sets of experiments to achieve the objectives illustrated above:

1. We replicated SWA and awake-like activity regimes *in vitro* to validate isolated cortical slices as a model of brain states and analyzed sPCI as a methodological tool to quantify network complexity.
2. We pharmacologically blocked fast and slow inhibition during the abovementioned regimes of cortical activity *in vitro* to study the contribution of inhibitory components to maintenance of cortical rhythms and complexity.
3. We pharmacologically and electrically (through DCS) modulated level of excitability during the spontaneous SWA and evoked cortical activity *in vitro* to study the

contribution of excitatory and inhibitory balance to maintain cortical rhythms and complexity.

4. We pharmacologically modulated the activation of mAChRs and photopharmacologically controlled the activation of M2 mAChR during spontaneous SWA *in vitro* and *in vivo* to study their contribution to cortical activity and *in vitro* evoked activity to study M2 mAChR role in complexity

The following sections are common throughout all the experimental sets, with the exception of the modulation of cortical emergent activity section, which will be explained in separated subsections. All experiments were carried out in accordance with protocols approved by the Animal Ethics Committee of the University of Barcelona, which comply with the European Union guidelines on protection of vertebrates used for experimentation (Directive 2010/63/EU of the European Parliament and the Council of 22 September 2010).

1. Experimental procedure

1.1. The *in vitro* preparation

Cortical slices were prepared as previously described (Sanchez-Vives, 2012) (**Figure 2** and **Figure 8**). Briefly: adult ferrets (3-7 months old, either sex) were anesthetized with sodium pentobarbital (40 mg/kg) and decapitated. The entire forebrain was rapidly removed to oxygenated cold (4-10 ºC) bathing medium and cut into 400-μm-thick coronal slices from the occipital cortex containing primary and secondary visual cortical areas (areas 17, 18, and 19). To increase tissue viability, a modification of the sucrose-substitution technique developed by (Aghajanian and Rasmussen, 1989) was used during the preparation. Then, slices were placed in an interface style recording chamber (Scientific Systems Design, Inc.), and bathed for 30 minutes in an equal mixture of the sucrose-substituted solution and ACSF (Artificial Cerebro-Spinal Fluid). Afterwards slices were maintained for 2 hours in ACSF for recovery. Finally, an *in vivo*-like ACSF

solution was applied throughout the rest of the experiment. ACSF contained (in mM): NaCl, 126; KCl, 2.5; $MgSO_4$, 2; NaH_2PO_4, 1; $CaCl_2$, 2; $NaHCO_3$, 26; dextrose, 10. The modified ACSF had the same ionic composition except for different levels of (in mM): KCl, 4; $MgSO_4$, 1 and $CaCl_2$, 1. Solutions were aerated with 95% O2, 5% CO_2 to a final pH of 7.4 and temperature during experiment was maintained at 34.5-36°C. Electrophysiological recordings started after allowing at least 1-hour recovery.

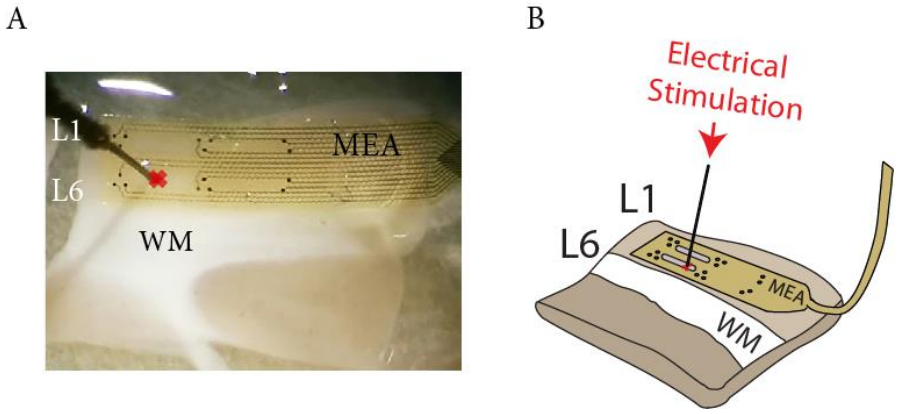

***Figure 8. Experimental set up. A**. Typical position of electrodes on a ferret coronal slice from V1 (layer 1, L1; layer 6 L6), white matter WM) for perturbational experiments **B.** Scheme of A. The recording array (MEA) was placed on the cortex, with 8 channels covering infragranular layers, and the remaining 8 spanning supragranular layers. Electrical stimulation was applied in the IF (red asterisk), with a concentric electrode touching the cortex through a hole in the recording electrode.*

1.2. The *in vivo* preparation

Cortical electrophysiology experiments were carried out in 2-3-month-old C57BL6/JR mice (*n*=3). Mice were kept under standard conditions (room temperature, 12:12-h light-dark cycle, lights on at 08:00 a.m.). Anesthesia was induced by intraperitoneal injection of ketamine (30 mg/kg) and medetomidine (100 mg/kg). After the reflex was removed, the mouse was placed in a stereotaxic frame, and continuously oxygenated with air enriched with oxygen. Body temperature was maintained at 37°C throughout the experiment (Ruiz-Mejias et al., 2011) with a water-circulating heating pad. All pressure points and tissues to be incised were infiltrated with lidocaine before

surgery. A craniotomy was performed in each mouse following Paxinos (Franklin and Paxinos, 2008): AP −2.5 mm, L 1.5 mm (primary visual cortex, V1). At the end of the experimental protocol, the animals were sacrificed by cervical dislocation (Castano-Prat et al., 2017).

2. Electrophysiological recordings of emergent activity

LFP recordings were obtained with two different type of electrode, depending on the experiment. *In vitro* recordings were obtained with a multielectrode array (MEA) of 16 gold electrodes plated with platinum black disposed on a flexible grid (**Figure 8** and **Figure 9A**). This grid was fabricated using SU-8 negative photoresist or polyamide. It also included an array of holes which allowed the oxygenation of the slices. Within this array of holes, two of them were bigger to place the stimulation electrode in the IF layers.

There were 2-3 electrodes in each of the recording points with 200 μm of distance between them in the MEA. This was placed (**Figure 8** and **Figure 9A**) to cover such that half of them (8 electrodes) would record from supragranular (SG) and the other half (8 electrodes) would record from infragranular (IG) layers (diodes / triodes were 750 μm apart in the vertical axis), as well as from 3 different cortical columns (1.5 mm apart in the horizontal axis). Each electrode was 50 μm in diameter, resulting in an impedance of $|Z|$~10 MΩ at 1kHz. Neural activity was referenced to an electrode placed at the bottom of the chamber in contact with the ACSF. The raw signal was amplified by 100 using a PGA16 Multichannel System (Multichannel System MCS GmbH - Harvard Bioscience Inc, Reutlingen, Germany) and digitized 10 kHz with the same Power1401. Activity was collected and monitored online by Spike2 (Cambridge Electronic Design, Cambridge, UK).

Spontaneous LFP recordings *in vivo* were obtained from deep layers of the cortex (depth: 0.6-0.7 mm) layers with 1–2 MΩ single tungsten electrode insulated with a plastic coating except for the tip (FHC, Bowdoin, ME, USA). The signal was amplified with a Multichannel System (Multichannel System MCS GmbH - Harvard Bioscience Inc, Reutlingen, Germany), digitized at 20 kHz with a CED acquisition board and acquired with Spike 2 (Cambridge Electronic Design, Cambridge, UK) unfiltered (Castano-Prat et al., 2017).

3. sPCI protocols

The sPCI protocol consisted of a single-pulse electrical stimulation applied using concentric electrodes (WPI, Aston, UK). Electrical pulses were triggered using a Power1401 ADC/DAC (Cambridge Electronic Design, Cambridge, UK) and converted to a current using a commercial stimulus isolator (360A, WPI, Aston, UK). The stimulation electrode was placed in IF layers (**Figure 9A**), following the notion that spontaneous Up-states are initiated in layer 5 (Sanchez-Vives and McCormick, 2000). Pulses had a duration of 0.1 ms, an intensity of 150–200 μA, and were applied every 10 s, with a random jitter from 0.5 to 1.5 s to avoid activity entrainment to the specific frequency of stimulation (D'Andola et al., 2017) (**Figure 9B**).

A binary spatiotemporal distribution of significant activity (SS(x,t)) was calculated from MUA signal and statistical differences from the baseline in response to the electrical stimulation were assessed by a bootstrap procedure as in D'Andola et al. (2017). The significance threshold was estimated as the one-tail (1-α) 99th percentile of the bootstrap distribution. Also, we first low-pass filtered (<10Hz) the trial average computed on the MUA signal, and considered significant only the periods in which the activity of each channel lay above the significance threshold for more than 50 ms, then, SS(x,t) = 1 for significant activity at channel x and time t, SS(x,t) = 0 otherwise (Casali et al., 2013). The

sPCI was then defined as the normalized Lempel-Ziv complexity of the binary matrix of significant evoked MUA spatiotemporal patterns (D'Andola et al., 2017) (**Figure 9C**).

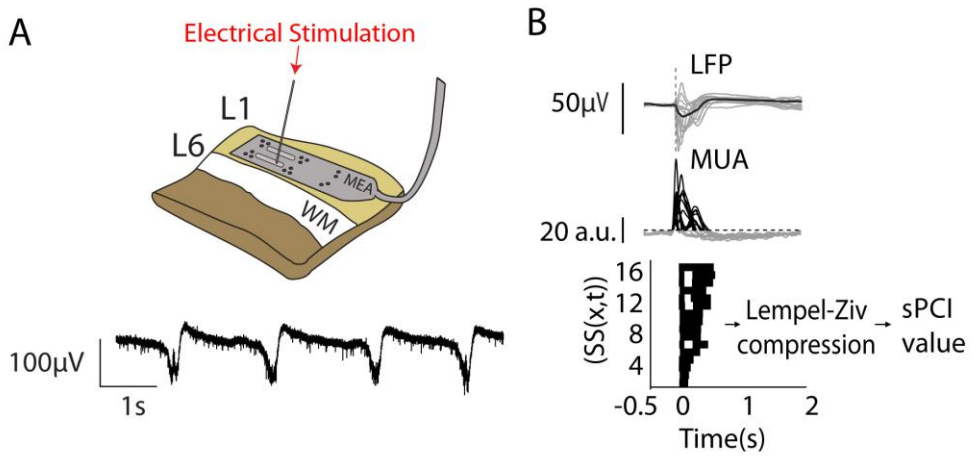

Figure 9. sPCI protocols. A. Top. *Experimental setup. A 16-channel multielectrode array was placed on a neocortical slice with a spatial distribution spanning infra- and supragranular layers. Electrical stimulation was delivered through a concentric electrode placed in IF layers (red arrow).* ***Bottom.*** *Representative LFP traces.* ***C.*** *sPCI was calculated from Lempel-Ziv compression of the significant multiunit activity (SS(x,t)) contained in a binary matrix.*

4. Modulation of cortical emergent activity

In order to study the underlying mechanisms controlling cortical rhythms and complexity, we modulated cortical emergent activity are as follows.

4.1. Classical pharmacology

In the first section of the results, we induced two different regimes of network activity. SWA appeared spontaneously as we described previously in the "*in vitro* preparation protocol". To induce awake-like activity we: (a) sequentially bath-applied AChR agonist Carbachol (CCh, 0.5 µM) and noradrenaline (NE, 50 µM) (D'Andola et al., 2017); (b) reduced the bath temperature from 36–37°C to 31–32°C (Reig et al., 2010); and

(c) modified extracellular calcium concentration levels from 1.2 mM to 0.8–0.9 mM (Markram et al., 2015). CCh and NE were obtained from Sigma-Aldrich.

In the second section we investigated the role of inhibition in the SWA and awake-like rhythms. We progressively blocked fast inhibition ($GABA_A$) with bicuculline methiodide (BMI: 0.2 µM, 0.4 µM, 0.6 µM, 0.8 µM and 1µM), obtained from Tocris Bioscience; and SR-95531 hydrobromide (gabazine, GBZ 50 nM, 100 nM, 150 nM and 200 nM), obtained from Sigma-Aldrich. We also progressively blocked slow inhibition ($GABA_B$) using CGP 55845 (CGP100 nM, 200 nM, 500 nM and 1 µM), obtained from Tocris Bioscience.

In the third section we examined the role of excitation in cortical rhythms. First, we increased the extracellular K^+ concentration ($[K^+]_{ec}$: 5 mM, 7 mM) and return to control condition with ACSF washout. In another set, we progressively blocked non-selective K^+ channel using Tetraethylammonium chloride (TEA: 1 mM, 5 mM and 10 mM), obtained from Sigma-Aldrich. We also gradually blocked non-selective K_v channel blocker using 4-Aminopyridine (4-AP: 25 µM and 50 µM), obtained from Tocris Bioscience. Finally, we blocked M-current usinge XE991 (100 µM) obtained from Tocris Bioscience.

We typically waited more than 1000 s after the application of each drug in order to let it act and to obtain a stable pattern of electrical activity.

4.2. Photopharmacology

In the last section, we modulated cholinergic effects on SWA *in vitro* by using novel molecules called photopharmacological agents (**Figure 6B**) (obtained from Nanoprobes and Nanoswitches group, Institute for Bioengineering of Catalonia (IBEC), Barcelona, Spain). These are bioactive molecules modified with photoswitches; that is, moieties that change their structure upon irradiation with light (Lerch et al 2016). First, we bath-applied non-photoresponsive muscarinic agonist Iperoxo (IPX: 10 nM to 100 nM)

(Riefolo et al., 2019) (**Figure 10**A). Then we used Phthalimide-Azobenzene-Iperoxo (PAI), which is a selective M2 mACh receptor agonist. White light was applied to obtain the *trans*-PAI (active molecule), which activates M2-mACh receptors and UV light (365nm) was applied to obtain the *cis*-PAI, which doesn't activate M2-mACh receptors (inactive molecule) (**Figure 10B,C**). PAI can be switched back to its on-state with blue or white light (**Figure 10B,C**). The high thermal stability of PAI inactive form (*cis*-PAI) allowed the administration of the inactive drug and subsequent activation of M2 receptors in the target region with white light (Riefolo et al., 2019). We first investigated the efficacy of PAI in cortical neuronal circuits *in vitro* by obtaining the dose-response curves of *trans*- and *cis*-PAI solutions applied separately. The more active PAI isomer (*trans*) was tested by applying its dark-adapted form (87 % of *trans*-PAI), and *cis*-PAI was obtained by illuminating 1 mM stock solutions with 365 nm light for 10 min (73% of *cis*-PAI) (Riefolo et al., 2019) (**Figure 10 C**). Increasing concentrations of both *trans*- and *cis*-PAI (10 nM, 100 nM, 300 nM and 1 μM) were bath applied in order to build up the dose-response curves.

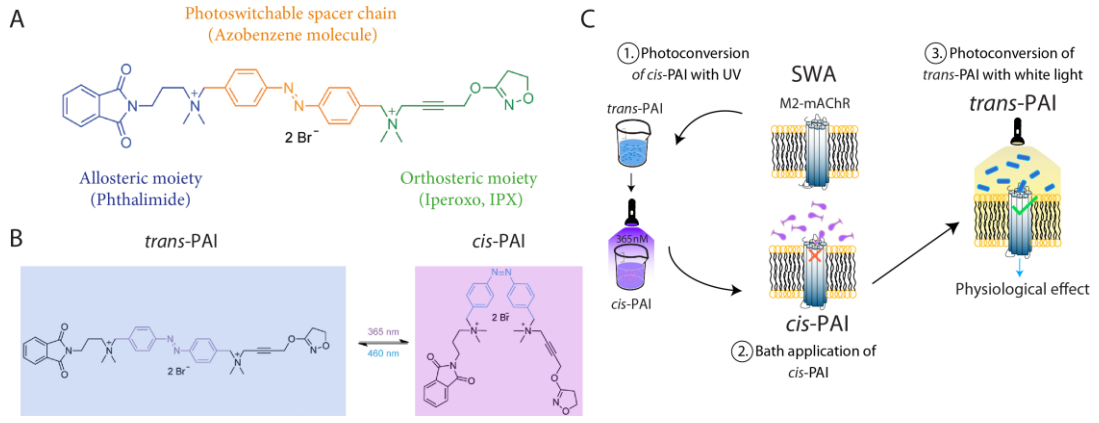

Figure 10. Photoswitchable molecule PAI and its photoconversion. ***A****. Phthalimide-Azobenzene-Iperoxo (PAI) molecules was compounded by Iperoxo as an orthosteric moiety Iperoxo, Azobenzene molecule as photoswithcable spacer chain and Phthalimide as an allosteric part. Source from American Chemical Society* (Riefolo et al., 2019). ***B.*** *2D representations of trans-PAI and cis-PAI isomers* (Riefolo et al., 2019)*. Irradiation of 365 nm was required to convert trans to cis-PAI and irradiation of 460nm was required to convert cis- to trans-PAI.* ***C.*** *PAI photoswitching protocol in vitro cortical slices. (1). Photoconversion from trans-PAI to cis-PAI with 10 min of UV irradiation; (2). Bath application of cis-PAI; (3). Photoconversion from cis-PAI to trans-PAI with White light irradiation.*

Spontaneous activity *in vivo* during anesthesia (control) was compared after application of the pre-illuminated, inactive drug form (*cis*-PAI) and application of white light to activate the drug (*trans*-PAI). *Cis*-PAI was locally delivered to the cerebral cortex surface and activity was recorded while applying a commercial red filter on the white light source to avoid the activation of the drug (Riefolo et al., 2019). The uncovered brain was illuminated with a white light source (Photonic Optics™ Optics Cold Light Source LED F1) in order to activate the drug *in situ* (*trans*-PAI).

4.3. Direct current stimulation

Electrical modulation of network excitability was delivered by a current between two parallel aligned silver/silverchlorided electrodes (1 mm diameter, 10 mm length) to create a constant EF. They were placed parallel to the cortical layers in the slice, such that DCS generated homogenous EF perpendicular to the layers (D'Andola et al., 2018; Fröhlich and McCormick, 2010) oriented parallel to the apical-dendritic axis of cortical pyramidal cells (**Figure 11A**) in order to assume maximum effect on the activity (Radman et al., 2009). The stimulation was triggered through a Power1401 ADC/DAC (Cambridge Electronic Design, Cambridge, UK). The applied EF was measured and calibrated before every experiment. EF intensity was calculated as the voltage gradient between two distant recording points (V/m). While positive EF induced depolarization by depolarizing fields oriented from white matter to cortical surface, negative EF hyperpolarized because depolarizing field went in the opposite direction (D'Andola et al., 2018) (**Figure 11**). We consistently alternated positive and negative EF to avoid tissue and electrode damage. First, 200 seconds of spontaneous activity was recorded, then the DCS was delivered alternating between ±3V/m, ±2V/m and ±5V/m intensities to exclude effects eventually coming from progressive current increases (**Figure 11B,C**). DCS periods were separated by recovery intervals of the same duration. DCS was applied during sPCI protocols (**Figure 11B,C**).

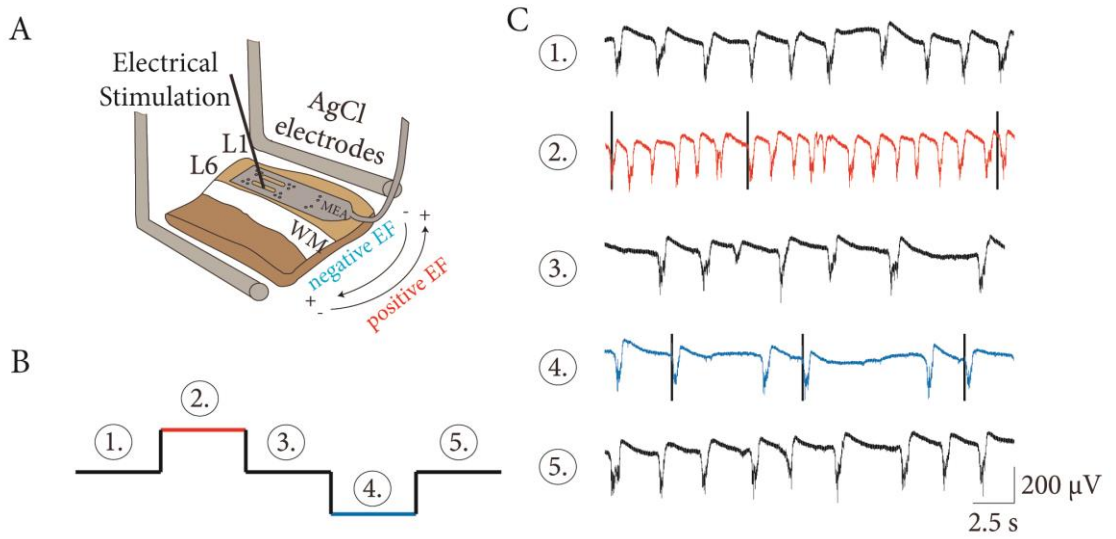

Figure 11. Direct current stimulation protocols. A*. Experimental set up. two parallel aligned silver/silverchlorided (AgCl) electrodes were place parallel to the cortical layers to create positive and negative EF. Cortical activity was recorded by 16 channels multielectrode arrays (MEA) and electrical stimulation was performed by concentric electrodes in the IF layers. White matter (WM), layer 1 (L1) and layer 6 (L6).* ***B****. Periods of 200 seconds were applied for each step of DCS protocol. (1) Control activity, (2) positive EF (red) and sPCI stimulation, (3) recovery interval, (4) negative EF (blue) and sPCI stimulation and (5) recovery interval.* ***C.*** *Representative LFP traces during above-mention conditions. Black line in 2. and 4. represents single pulse of electrical stimulation delivered during DCS periods.*

5. Data analysis

We analyzed the changes of spontaneous cortical activity from LFP and MUA (Herreras, 2016). We estimated the MUA from the LFP recordings and quantified Up and Down-states as previously described (Compte et al., 2008; D'Andola et al., 2017; Reig et al., 2010). The MUA was estimated from the extracellular recordings as the power change in the Fourier components at frequencies between 200 and 1500 Hz in 5 ms windows. We assumed that the spectrum at this band provides a good estimate of the population firing rate, because Fourier components at high frequencies have densities proportional to the spiking activity of the involved neurons (Mattia et al., 2010). To obtain MUA time series, MUA values were logarithmically scaled in order to balance the large fluctuations of the nearby spikes. The reported firing rate was estimated as the mean power in the Fourier

components at frequencies between 200 and 1500 Hz across time (in arbitrary units (a.u.)).

Up-state detection was performed by setting a threshold in the log(MUA) time series as previously described to quantify frequency of the SWA (Ruiz-Mejias et al., 2016; Sanchez-Vives et al., 2010). The relative firing rate (FR) of the Up-states was quantified from the transformed log(MUA) signal as the mean of absolute value of log(MUA). To study the variability of power spectral densities (PSD) of the local field potential, we used Welch's method with 50% overlapped Hamming window of 2 s and spectrograms were computed in 50% overlapping windows of 0.05 s using the LFP signal low-passed at 500 Hz. To estimate periodicity or regularity of the signal, autocorrelograms were performed from LFP signal and curve fitting was performed by ($y= e^{-\alpha x}$) selecting the first three peaks. Thus, the higher is the α-decay, the lower was the periodicity of the signal (more asynchronous). All off-line estimates and analyses, including estimation of sPCI, were implemented in MATLAB (The MathWorks Inc., Natick, MA, USA). All variables in the experimental conditions were compared with the control (no chemical added) condition.

To assess significant differences between sPCI and changes in the LFP and MUA after bath application of different drugs, we used the Friedman test and Wilcoxon post-hoc tests corrected for multiple comparisons (Benjamini and Hochberg, 1995) . *In vivo* statistical analysis was performed with the unpaired t-test, significance values were established with a * $p\text{-}value < 5 \cdot 10^{-2}$.

6. Histology *in vitro*

Nissl staining was used for visualizing lamination of the cortex and location of the electrical stimulation performed. Slices were marked where the array was positioned (**Figure 12A,B**) and fixed in paraformaldehyde (4%) for later Toluidine blue staining.

Slices (400 µm) were washed for 4-5 days in 0.1 M PB containing 30% saccharose. Then 80 µm thick slices were cut in a Thermo Scientific MICROM HM 450 microtome and placed on gelatin-coated glass slides. After drying overnight, slices were incubated for 2 hours in 70% ethanol for the subsequent double toluidine staining: first, nuclei were stained by an incubation of 15 minutes on toluidine blue and afterwards dehydrated with ascending alcohol series; 5 minutes incubation on xylene was done to clarify the tissue for the second staining. Second, similar incubations, 10-15 minutes toluidine and different increasing alcohols, finishing with two xylene incubations were used to stain cytoplasm. Finally, slices were mounted in DePeX medium. Images were visualized and taken with a light microscope. Infragranular (IF) and supragranular layers (SG) were limited according to density and size of the observed cells (Homman-Ludiye et al., 2010).

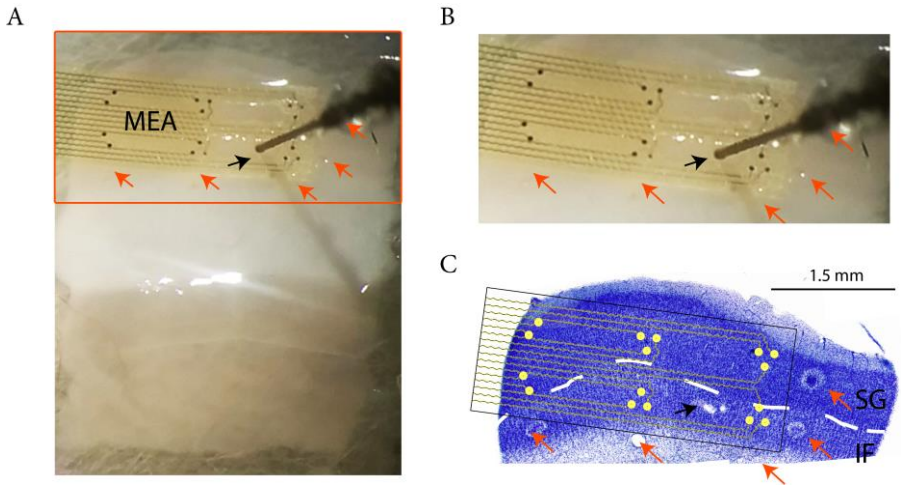

Figure 12. The electrical stimulation was successfully performed in the IF layers. A. *Slices were marked (red arrows) where the MEA was positioned and electrical stimulation was performed (black arrow).* ***B.*** *Zoom of A.* ***C.*** *Nissl staining and MEA illustration overlapped. Red arrows in the same position as A demonstrated where the marks were performed. Black arrow pointed to electrical stimulation position in the IF layers. White dashed line limit IF and SG layers.*

Chapter 3

Results

1. Isolated cortical slices display different regimes of network activity patterns and complexity

Given that isolated cortical slices can spontaneously display SWA (Sanchez-Vives and McCormick, 2000), it is possible to modulate the cortical activity through *in vitro* preparation; and it has been demonstrated that a shift between cortical rhythms can occur independently of thalamic inputs and due to neuromodulators acting directly on neocortex (Constantinople et al., 2011; Lewis et al., 2015). Here, we wanted to investigate whether cortical slices *in vitro* can display different regimes of network activity patterns and complexity, and if changes in the complexity can be detected using the sPCI method.

Spontaneous SWA was characterized as previously described. In summary, neurons within a local network fired in a bimodal distribution (**Figure 13A,B**) with neural firing during the Up-states and near silence during Down-states (Reig et al., 2010; Sanchez-Vives et al., 2017) (FRs: Appendix I (AI) **Table 1**, **Figure 13C**). Indeed, autocorrelograms demonstrated that this SWA was highly regular and periodical over time (α-decay: **Figure 13D, AI Table 1**) and with great presence of low frequencies (0.1-1 Hz) compared with other frequency bands (**Figure 13E**).

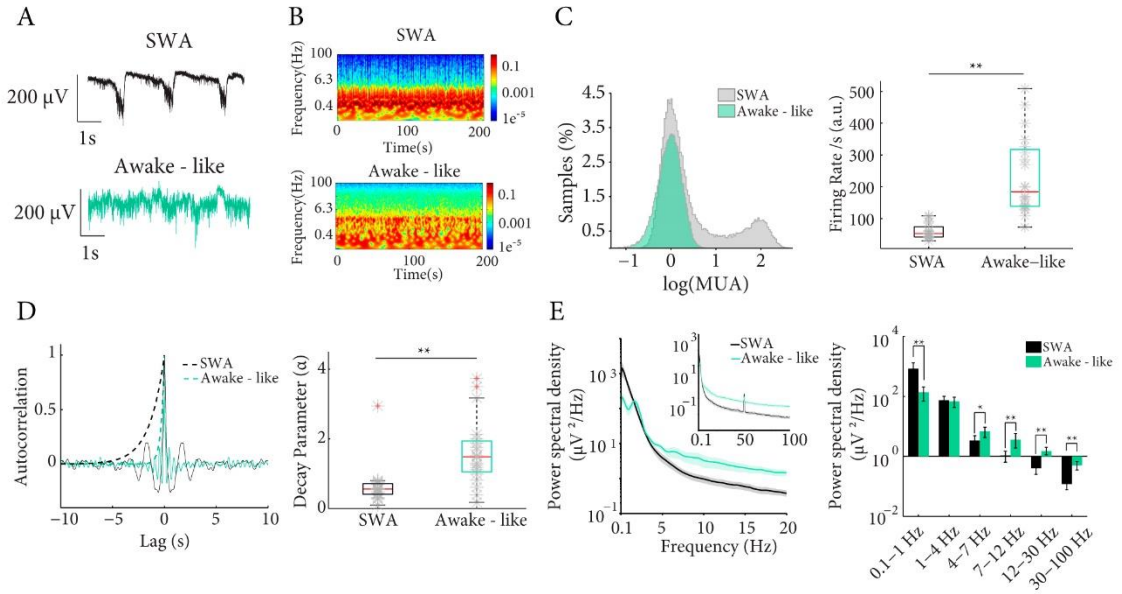

Figure 13. Cortical slices in vitro demonstrate different regimes of network activity. ***A****. Raw LFP recordings of spontaneous activity in cortical slices, control SWA (top) and awake-like activity (bottom) (n=20).* ***B.*** *Spectrogram of spontaneous activity under control SWA (top) and awake-like activity (bottom).* ***C.*** *Histogram distribution of log(MUA) was modulated from bimodal distribution of neural firing during SWA to homogeneous distribution during awake-like activity (left). The firing rate per second increased during awake-like activity (color code) (right).* ***D.*** *Autocorrelations of the LFP demonstrated an increment in the decay of exponential curve (α-decay) after we induced the awake-like activity (left). Population of values of exponential curve under control SWA and awake-like activity (right).* ***E.*** *Power spectral density of LFP under control and awake-like activity (color coded) (left). Mean power changes under control and awake-like activity revealed a decreased in low-frequency band and an enhancement in high-frequency bands. (* p-value < 0.05, **p-value < 0.01).*

Because it seemed that the presence of both ACh and NE can induce awake-like activity from synchronized SWA (Bennett et al., 2013; Constantinople et al., 2011; Reimer et al., 2016; M. Steriade et al., 1993), we a) sequentially bath-applied ACh agonist, CCh

(0.5 μM) and NE (50 μM) (D'Andola et al., 2017), b) reduced the bath temperature from 36-37 ºC to 31-32 ºC (Markram et al., 2015; Reig et al., 2010) and c) modified extracellular calcium concentration levels from 1.2 mM to 0.8-0.9 mM (Markram et al., 2015) (**Figure 13**).

Cortical slices (*n*=20) under awake-like regime led to the extinction of bistability, where neurons fired near independently (**Figure 13 A-C).** In addition, during this state, firing rate per second significantly increased (FRs: **AI Table 1**, *p*-value = 8.86 e^{-05}, **Figure 13C**) and the decay of the exponential curve of the autocorrelogram significantly increased, meaning that the oscillations during awake-like state was removed, appearing as asynchronous oscillations (α-decay: **AI Table 1**, *p*-value = 1.6286e^{-04}, **Figure 13D**) compared with SWA conditions. Moreover, this kind of activity revealed significant lower values of low-frequency band (0.1-1 Hz) and with higher significant values of high-frequency bands compared with SWA rhythms (*p*-value 0.1-1 Hz = 4.5523e^{-04}, *p*-value theta (4-7 Hz) = 0.0156, *p*-value alpha (7-12 Hz) = 0.0057, *p*-value beta (12-30 Hz) = 6.2920e^{-04}, *p*-value gamma (30-100 Hz) = 4.5523e^{-04}) (**Figure 13E**).

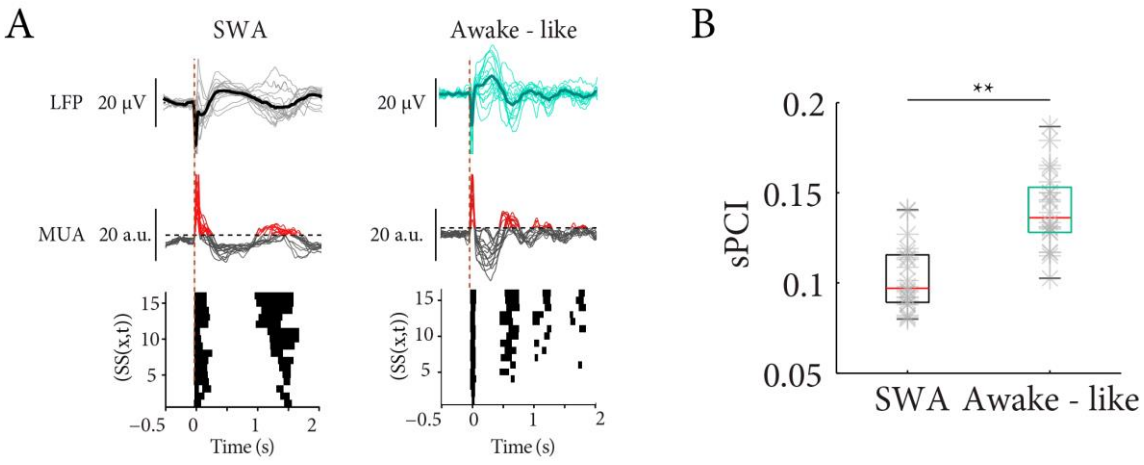

Figure 14. Extinction of bistability and regularity of neural firing at awake-like states induces higher complexity network dynamics. A. *Averaged LFP (top) and MUA (middle) responses to electrical stimulation during distinct regimes of activity. Binary matrix SS(x,t) (bottom) of significant sources of activity following a single electrical pulse.* ***B.*** *Population sPCI measured during control SWA and awake-like activity demonstrated an enhancement in the complexity of the spatiotemporal responses to an electrical stimulation (**p-value < 0.01).*

When we induced the awake-like activity, the bimodal distribution of SWA was also observed in the complexity *in vitro*. Spatiotemporal distributions of significant evoked responses were homogeneous and highly stereotypical (**Figure 14A**). After we induced the awake-like activity, we detected significant higher complexity values (sPCI: **AI Table 2**, *p*-value = $2.9280e^{-04}$), which was caused by a reduction of bistable responses (**Figure 14B**), displaying heterogeneous and irregular responses. Overall, these results indicated that bistable rhythms yield lower levels of neural firing and regular patterns than awake-like activity in cortical slices. Indeed, these results showed that bistable rhythms yield homogeneous, regular and uncomplex patterns of cortical activity than awake-like activity in cortical slices.

2. The role of inhibition in cortical rhythms and complexity

Switches in the cortical network rhythms are possible because cortical networks form a framework with excitatory and inhibitory neurons and specific connections. Here, we wanted to demonstrate whether the modulation of excitatory and inhibitory neurons by activation/inactivation of these receptors and ion channels can induce switches in cortical network rhythms and complexity. First, we studied the role of inhibition in cortical rhythms and complexity.

Given that progressive blockade of $GABA_A$ and $GABA_B$ modulates the characteristics of spontaneous SWA (Mann et al., 2009; Perez-Zabalza et al., 2020; Sanchez-Vives et al., 2010) and several studies demonstrated that GABAergic interneurons are essential for many cortical functions such as regime range modulation of cortical circuits or temporal precision of pyramidal cell firing (Tremblay et al., 2016), we decided to progressively remove $GABA_A$ and $GABA_B$ inhibition in brain slices displaying different regimes of network activity (SWA and awake-like).

From SWA or awake-like states, we bath-applied a range of different concentrations of Bicuculline methiodide (BMI 0.2, 0.4, 0.6, 0.8 and 1 μM, *n*=9 from SWA), SR-95531 hydrobromide (Gabazine, GBZ 50 nM, 100 nM, 150 nM and 200 nM, *n*=10 from awake-like and *n*=9 from SWA), to block $GABA_A$ receptors, and CGP55845 (CGP100 nM, 200 nM, 500 nM and 1 μM, *n*=7 from awake-like and *n*=11 from SWA), to block $GABA_B$ receptors. Under these conditions, we analyzed dynamical changes by studying the modulation of spontaneous LFP and MUA. We also studied the dynamical changes by studying the complexity alterations using sPCI.

2.1. Role of fast and slow inhibition in awake-like states and their control of activity patterns, excitability and complexity

First, we induced awake-like activity as we mentioned in the previous section and then we blocked either fast or slow inhibition. From the awake–like regime, when $GABA_A$ (fast inhibition) was blocked, the awake-like activity was removed. The decay of the exponential curve decreased, meaning that cortical activity progressively shifted to regular and periodical activity (α-decay: **AI Table 1**, *p*-value = 0.0107) with a bimodal distribution of neural firing (**Figure 15**) and the firing rate per second was as high as awake-like conditions (FRs: **AI Table 1**, *p*-value = 0.0107, **Figure 15C**). In addition, blocking $GABA_A$ increased the power in low-frequency bands (0.1-1 Hz, *p-value* = 0.011) with increasing power at high-frequency bands (*p*-value alpha (7-12 Hz) = 0.0148, *p*-value beta (12-30 Hz) = 0.0148 and *p*-value gamma (30-100 Hz) = 0.0149) (**Figure 15E**).

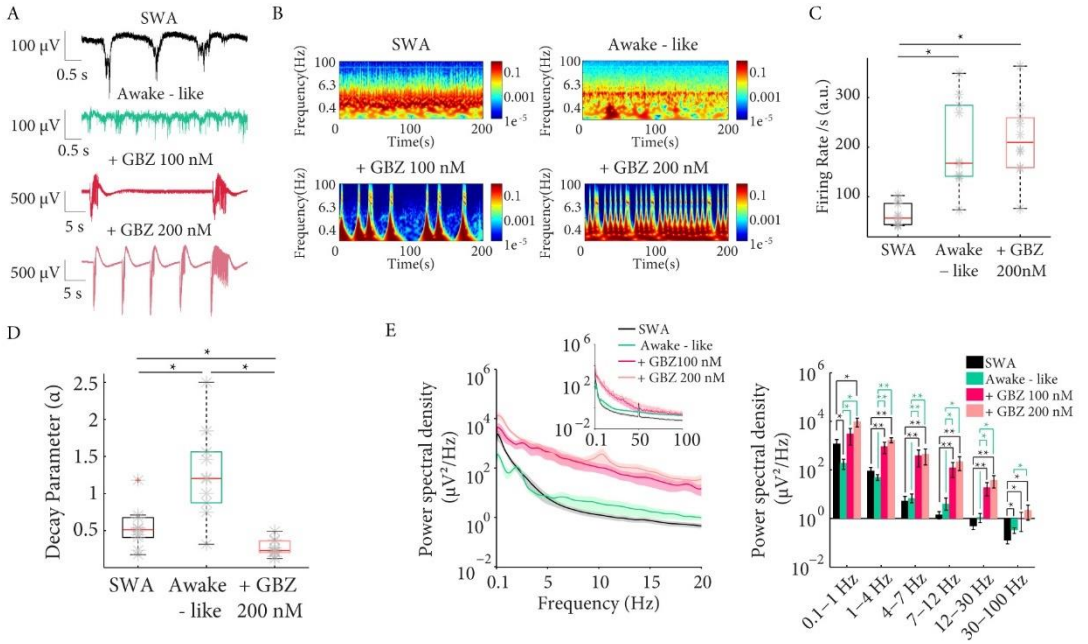

Figure 15. Fast inhibition is implicated in the maintenance of this irregular and heterogeneous regime of activity and controlled the level of neural firing. A. *Raw LFP recordings of spontaneous activity during control SWA, awake-like activity and progressive blockade of $GABA_A$ receptors by bath application GBZ (n=10).* ***B.*** *Spectrograms of spontaneous activity from A.* ***C.*** *Firing rate per second significantly increased and remained at high levels as awake-like conditions after blocking fast inhibition (+ GBZ 200 nM).* ***D.*** *Autocorrelations of the LFP demonstrated an increment in the decay of exponential curve after we induced the awake-like activity and significantly decreased after blocking fast inhibition (+ GBZ 200 nM).* ***E.*** *Power spectral density of LFP (color coded) (left). Mean power of low frequencies decreased from control to awake-like activity and increased in high-frequency bands. Finally, the power enhanced within all frequency bands after the bath application of GBZ 200 nM (Awake-like + GBZ 200 nM) (black comparing with SWA, green comparing with Awake-like) (right). (* p-value < 0.05, **p-value < 0.01).*

This shift to bistable and regular activity was not only observed in spontaneous cortical activity. When we analyzed complexity, from heterogeneous and irregular spatiotemporal distribution of significant responses during awake-like rhythms, responses became stereotypical and homogeneous when we blocked $GABA_A$ (**Figure 16 A**), correlating with low complexity values (sPCI: **AI Table 2**, *p*-value = 0.0223, **Figure 16 B**).

In summary, fast inhibition seems to be implicated in maintaining this irregular and heterogeneous activity and it controls the level of neural firing. Indeed, it seems that higher levels of neural firing are not required to induce higher complexity states.

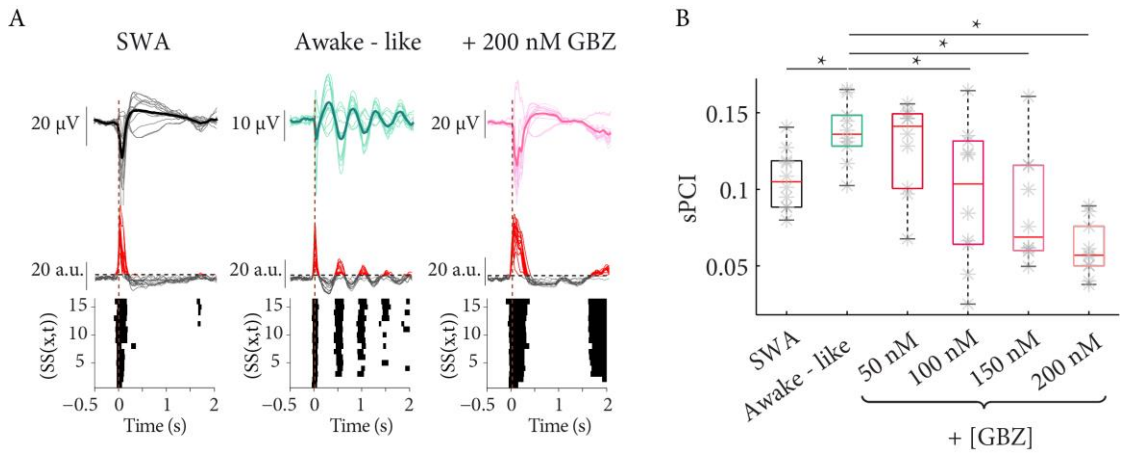

Figure 16. Fast inhibition maintains cortical activity within this irregular and heterogeneous complexity regime. A. *Averaged LFP (top) and MUA (middle) to electrical stimulation during distinct regimes of activity. Binary matrix SS(x,t) of significant sources of activity following a single electrical pulse (bottom).* ***B.*** *Population sPCI demonstrated an increase in the complexity of the spatiotemporal responses during awake-like states and stereotypical and reduced complexity responses after blocking fast inhibition (Awake-like + GBZ 200 nM) (* p-value < 0.05).*

After induced awake–like regime, blocking $GABA_B$ (**Figure 17**) removed the awake-like regime too. The decay of the exponential curve in the autocorrelograms decreased, showing more and periodical oscillations than awake-like regimes (α-decay: **AI Table 1**, *p*-value = 0.043) and cortical levels of firing rate per second remained at the same levels as awake-like condition rhythms (FRs: **AI Table 1**, *p*-value = 0.043, **Figure 17C**). In addition, there was an increment in high-frequency bands compared with the SWA regime (beta (12-30 Hz) ($p\text{-value}_{CGP1}$ = 0.0430) and gamma (30-100 Hz) ($p\text{-value}_{CGP1}$ = 0.0430) (**Figure 17E**) but without significant differences at low frequencies (0.1-1 Hz) and without significant differences to awake-like conditions.

These changes in the spontaneous activity were also observed at complexity. When $GABA_B$ was blocked, complexity responses became regular and homogeneous (**Figure 18A)** and sPCI progressively decreased but without significant differences, neither between SWA and CGP conditions (sPCI: **AI Table 2**, *p*-value =1.68) nor awake-like and CGP groups (sPCI: **AI Table 2**, *p*-value = 0.22) (**Figure 18A,B**).

In summary, fast inhibition seems to be implicated in maintaining this irregular and heterogeneous regime of activity and it controls the level of neural firing to a higher extent that slow inhibition.

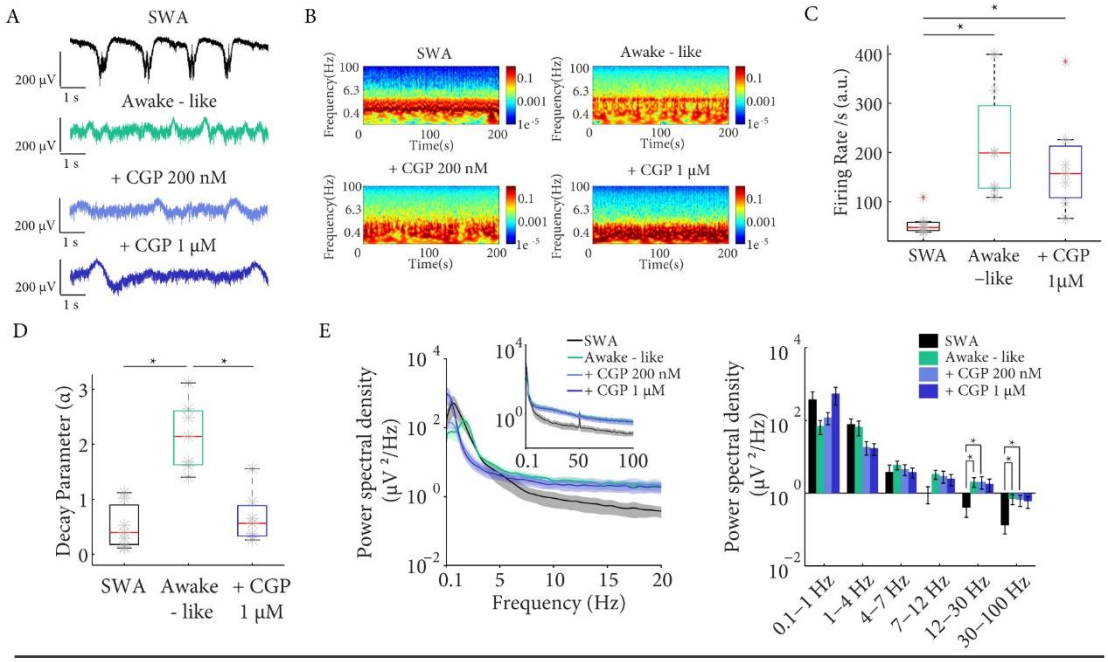

Figure 17. Slow inhibition also maintains cortical activity within this irregular and heterogeneous regimen, and it controls the level of neural firing. A. *Raw LFP recordings of spontaneous activity during control SWA, awake-like activity and blockade of $GABA_B$ receptors by bath application of increasing concentrations of CGP (n=7).* ***B.*** *Spectrograms of spontaneous activity shown in A.* ***C.*** *From SWA there was an increase in the firing rate per second during awake-like activity remained as higher values of firing rate per second as awake–like activity.* ***D.*** *Autocorrelations of the LFP demonstrated an increment in the decay of exponential curve after we induced the awake-like activity and significantly decreased after blocking slow inhibition (Awake-like + CGP 1 µM).* ***E.*** *Power spectral density of LFP (color coded) (left). Mean power of low-frequency band decreased from control to awake-like activity and an increased in high-frequency bands. Finally blocking slow inhibition (Awake-like + CGP 1 µM) induced an increased in low frequency band, decreased in 1-4 Hzpower and preserved high values of power at high-frequency bands (* p-value < 0.05).*

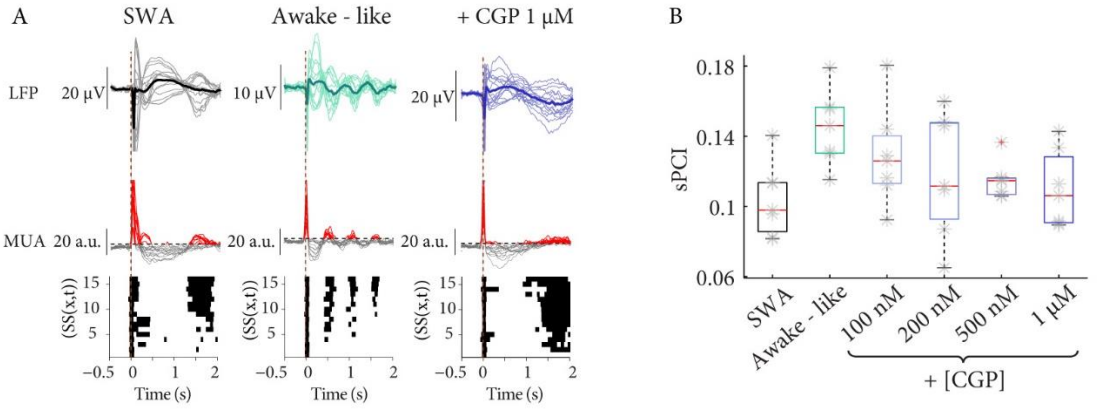

Figure 18. Slow inhibition also maintains cortical activity within this irregular and heterogeneous evoked activity but to a lower extent than fast inhibition. A. *Averaged LFP (top) and MUA (middle) responses to electrical stimulation during distinct regimes of activity. Binary matrix SS(x,t) of significant sources of activity following a single electrical pulse (bottom).* ***B.*** *Population sPCI demonstrated an enhancement in the complexity of the spatiotemporal responses to an electrical stimulation during awake-like states and stereotypical, reduced complexity responses after blocking slow inhibition (Awake-like + CGP 1 µM).*

2.2. Both fast and slow inhibition are required to maintain a physiological SWA regime

We observed that inhibition is important for the maintenance of cortical activity within this irregular and heterogeneous regime of activity and controls the level of neural firing and complexity. We therefore decided to block fast ($GABA_A$) and slow ($GABA_B$) inhibition during SWA regime.

After bath application of increasing concentrations of $GABA_A$ blocker BMI (0.2 µM, 0.4 µM, 0.6 µM, 0.8 µM, 1 µM) (n=9) (**Figure 19**) or GBZ (50 nM, 100 nM, 150 nM, 200 nM) (n=9) (**Figure 21**) cortical activity remained at the bistable regime and significantly increased the firing rate per second rate under increasing concentrations of BMI (FRs: **AI Table 3,** p-value = 0.0322, **Figure 19A-C**) and also under increasing concentrations of GBZ (FRs: **AI Table 3,** p-value = 0.0215) (**Figure 21A-C**). This increment in the firing occurred mainly during Up-states (FR Ups: BMI 1 µM: **AI Table 3,** p-value = 0.0089, **Figure 19C;** FR Ups: GBZ 200 nM: **AI Table 3,** p-value = 0.0039, **Figure 21C**) with a gradual shortening

of Up-states. In addition, the decay of the exponential curve in the autocorrelograms decreased, meaning that the regularity and periodicity of the oscillations increased under bath application of BMI (α-decay: **AI Table 3, Figure 19D**), with significant changes under bath application of GBZ (α-decay: **AI Table 3,** *p*-value= 0.0054, **Figure 21D**). In addition, there was also an enhancement in frequency bands from theta band comparing with BMI 1 μM (**Figure 19E**) (*p*-value theta (4-7 Hz) = 0.0107) and with GBZ 200 nM (*p*-value theta (4-7 Hz) = 0.0054) (**Figure 21E**).

Under these network regime, progressively blocking fast inhibition induced spatiotemporal distribution of cortical responses that were more stereotypical than the SWA condition (**Figure 20A** and **Figure 22A**), leading to a significant decreased in the complexity values at the highest concentration of BMI (sPCI: **AI Table 4**, *p-value* = 0.0117, **Figure 20B**) and after the bath application of 100nM of GBZ (sPCI: **AI Table 4**, *p-value* = 0.0039, **Figure 22B**).

In summary, without leaving the bistable regimen, fast inhibition is also required to maintain the network activity regime and complexity, controlling the levels of neural firing.

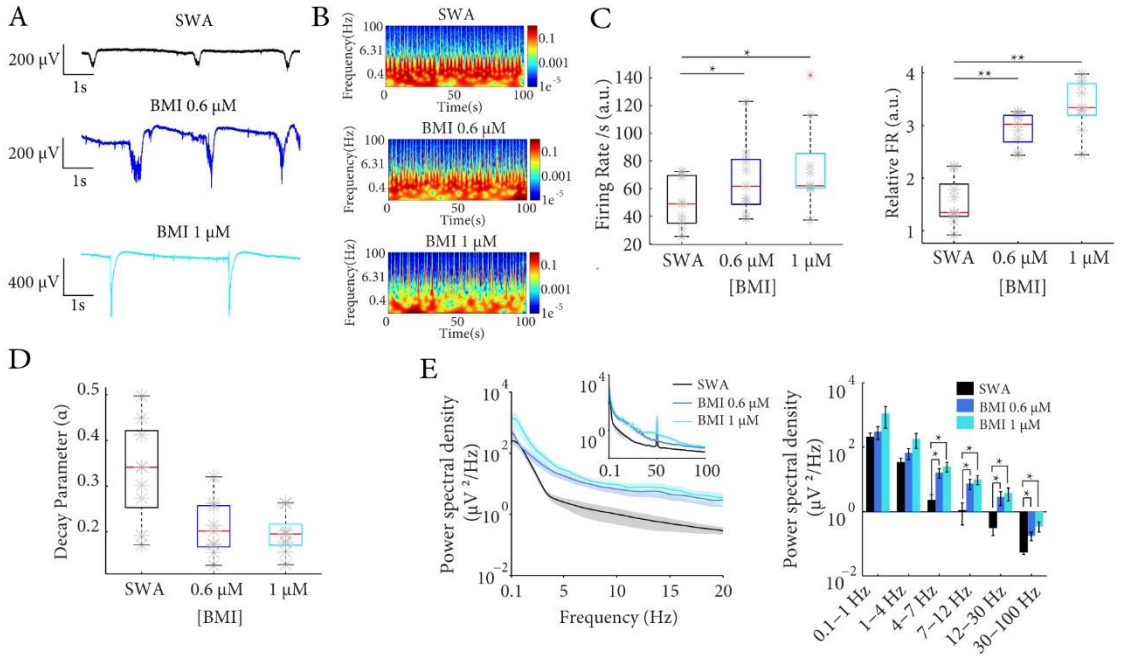

Figure 19. Without leaving bistable dynamics, fast inhibition is required to maintain the network activity regime and level of neural firing. A*. Raw LFP recordings of spontaneous activity in cortical slices, control SWA and blockade of $GABA_A$ receptors by bath application of increasing concentrations of BMI (n=9).* ***B****. Spectrograms of spontaneous activity from LFP recordings shown in A.* ***C.*** *Firing rate per second increased (left) after blocking fast inhibition (BMI 0.6 μM and 1 μM) and it mainly increased in the Up-states (right)* ***D.*** *Autocorrelations of the LFP demonstrated a progressive decrease in the decay of exponential curve blocking fast inhibition (BMI 0.6 μM and 1 μM).* ***E.*** *Power spectral density of LFP (color coded) (left). Mean power changes from control to progressive blocking fast inhibition (BMI 0.6 μM and 1 μM) induced enhancement of power within all frequency bands (right). (* p-value < 0.05, **p-value < 0.01).*

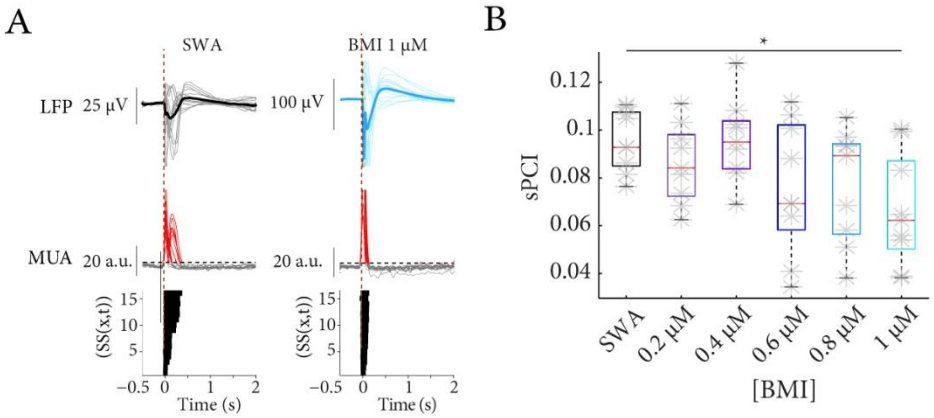

Figure 20. Fast inhibition is required to maintain the network activity regime during ongoing SWA. A*. Averaged LFP (top) and MUA (middle) to electrical stimulation during distinct regimes of activity. Binary matrix SS(x,t) (bottom) of significant sources of activity following a single electrical pulse.* ***B****. Population sPCI (right) demonstrated stereotypical and reduced complexity responses after blocking fast inhibition (BMI 0.6 μM and 1 μM). (* p-value < 0.05).*

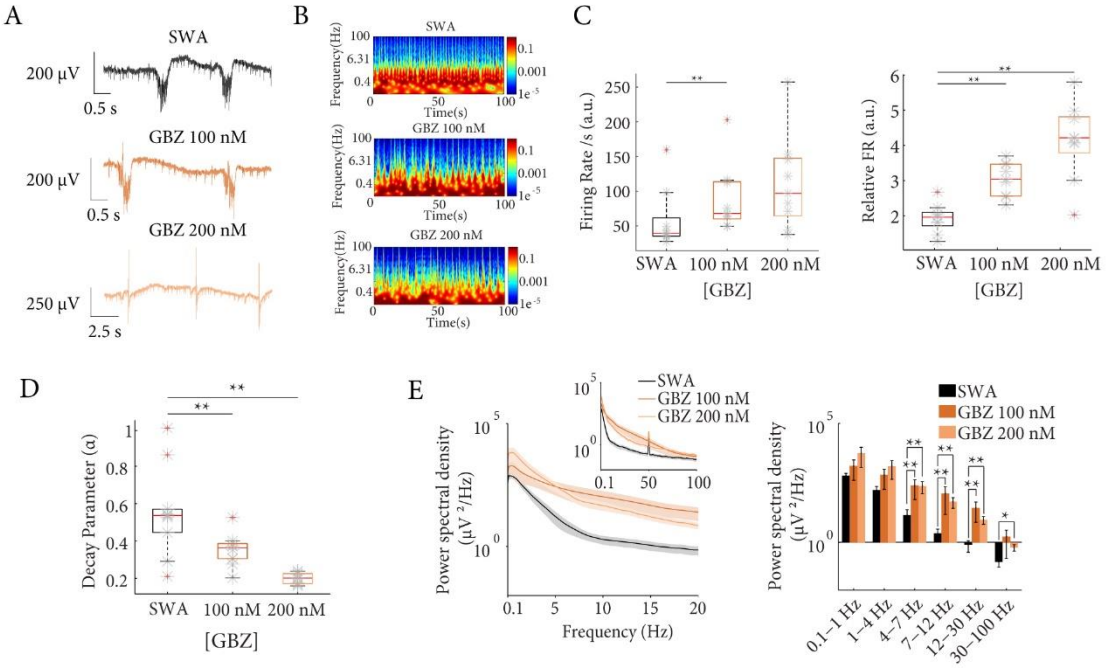

Figure 21. Without leaving bistable dynamics, fast inhibition is required to maintain the network activity regime and level of neural firing. A. *Raw LFP recordings of spontaneous activity during control SWA and blockade of $GABA_A$ receptors by bath application of increasing concentrations of GBZ (n=9).* ***B.*** *Spectrograms of spontaneous activity from LFP recordings shown in A.* ***C.*** *While neural firing measured by firing rate/s (left) remained within bistable levels after blocking fast inhibition (GBZ 100 nM and 200 nM), relative firing of the Up-states (right) demonstrated higher significant values.* ***D.*** *Autocorrelations of the LFP demonstrated a progressive decreased in the decay of exponential curve blocking fast inhibition (GBZ 100 nM and 200 nM).* ***E.*** *Power spectral density of LFP (color coded) (left). Mean power changes from control to progressive blocking fast inhibition (GBZ 100 nM and 200 nM) induced enhancement of power within all frequency bands (right). (* p-value < 0.05, **p-value < 0.01).*

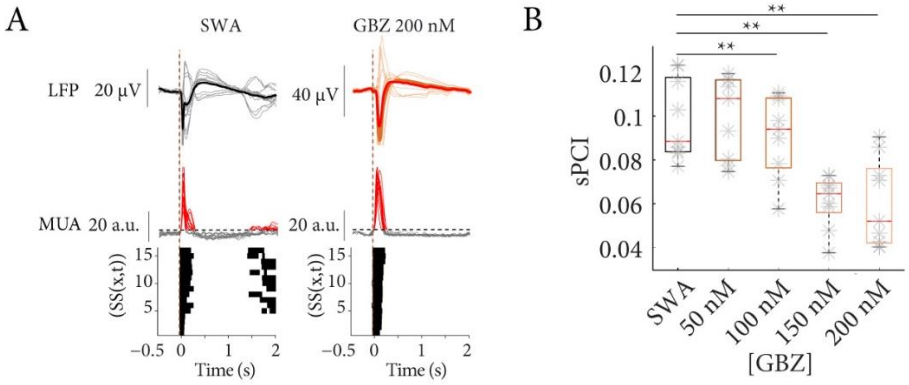

Figure 22. Without leaving bistable dynamics, fast inhibition is still required to maintain the network activity regime. A. *Averaged LFP (top) and MUA (middle) to electrical stimulation during distinct regimes of activity. Binary matrix SS(x,t) (bottom) of significant sources of activity following a single electrical pulse.* ***B.*** *Population sPCI demonstrated stereotypical and reduced complexity responses after blocking fast inhibition (GBZ 100 nM and 200 nM) (**p-value < 0.01).*

When we blocked the slow inhibition ($GABA_B$) with the bath application of increasing concentrations of CGP (100 nM, 200 nM, 500 nM and 1 μM) (n=11) (**Figure 23**) we also observed the importance of inhibition to maintain cortical rhythms. Equally to blocking fast inhibition, after removing slow inhibition, cortical activity remained bistable rhythms (**Figure 23A-C**) and the firing rate increased (FRs: **AI Table 3, Figure 23C**). This increase was observed during Up-states but it was just significant at the highest concentration of CGP (FR Ups: **AI Table 3,** p-value = 0.0098, **Figure 23C**) and the Up-states were longer and followed by prominent Down-states,. Indeed, the decay of the exponential curve decreased, meaning that it was an increase in the regularity and periodicity of the signal (α-decay: **AI Table 3**, **Figure 23D**) and modulation of low-frequency band (0.1-1 Hz, *p-value* = 0.0054) (**Figure 23E**).

In addition, the responses to the electrical stimulation were stereotypical (**Figure 24A**), showing lower values of sPCI with increasing concentrations of $GABA_B$ blocker (sPCI: **AI Table 4,** *p-value* = $9.7656e^{-04}$, **Figure 24B**).

In summary, without leaving the bistable regimen, fast inhibition is also required to maintain the network activity regime and controls the level of neural firing to a higher extent that slow inhibition. This also suggests that higher levels of neural firing are not required to induce higher complexity states.

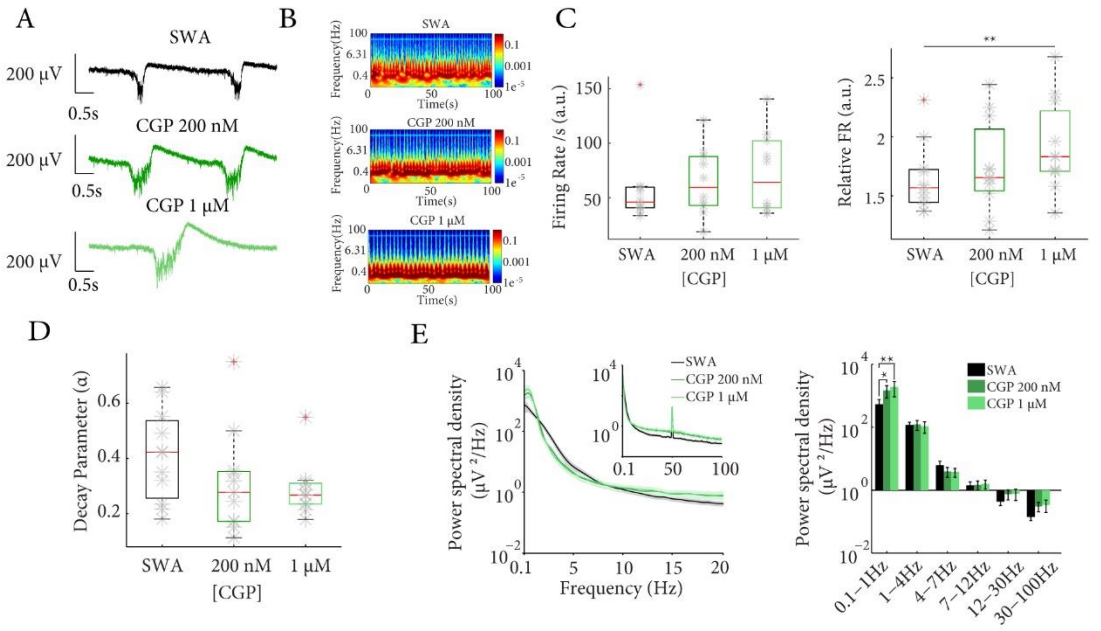

Figure 23. During ongoing SWA, slow inhibition is also required to maintain the network activity regime. A*. Raw LFP recordings of spontaneous activity during control SWA and blockade of $GABA_B$ receptors by bath application of increasing concentrations of CGP (n=11).* ***B.*** *Spectrograms of spontaneous activity from LFP recordings shown in A.* ***C.*** *While neural firing measured by firing rate per second (left) remained within bistable levels after blocking slow inhibition (CGP 200 nM and 1 µM), relative firing of the Up - states (right) demonstrate increasing significant values.* ***D****. Autocorrelations of the LFP demonstrated a progressive decrease in the decay of exponential curve blocking slow inhibition (CGP 200 nM and 1 µM).* ***E.*** *Power spectral density of LFP (color coded) (left). Mean power changes from control to progressive blocking slow inhibition (CGP 200 nM and 1 µM) induced increment of power within low and gamma band (right). (* p-value < 0.05, **p-value < 0.01).*

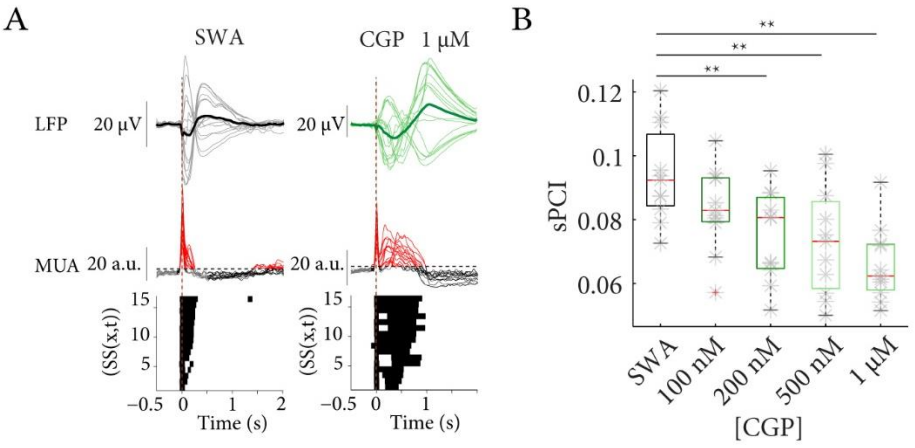

Figure 24. Without leaving bistable dynamics, slow inhibition is required to maintain the network activity regime. ***A.*** *Averaged LFP (top) and MUA (middle) to electrical stimulation during distinct regimes of activity. Binary matrix SS(x,t) (bottom) of significant sources of activity following a single electrical pulse.* ***B.*** *Population sPCI demonstrated stereotypical and reduced complexity responses after blocking slow inhibition (CGP 200 nM and 1 µM). (* p-value < 0.05, **p-value < 0.01).*

3. Excitatory and inhibitory balance to maintain cortical rhythms

After we observed that inhibition was relevant for the maintenance of cortical rhythms and complexity, we sought to determine whether the modulation of excitation can switch cortical rhythms and complexity. To do this, we first decided to modulate the level of neural firing by the modulation of extracellular K^+ concentration ($[K^+]_{ec}$) or inactivation of K^+ channels and then we modulated excitatory cortical neurons using DCS.

3.1. Activity-dependent K^+ channels are involved in the maintenance of cortical rhythms.

Potassium channels are the most diverse of ion channels, and their expression is homogeneous among cortical inhibitory and excitatory neurons and mostly underlie functions of neuronal excitability control (Greene and Hoshi, 2017; Sancristóbal et al., 2016). Indeed, K^+ channels are implicated in the modulation of some phases of the SWA such as Up-state initiation and termination (Ashford et al., 1988; Compte et al., 2003; Contreras and Steriade, 1996; Cunningham et al., 2006; Neske, 2016; Phillis et al., 1975; Sanchez-Vives and McCormick, 2000; Schwindt et al., 1992; M. Steriade et al., 1993; Steriade et al., 1994).

Increasing $[K^+]_{ec}$ (n=9) (**Figure 25**), without leaving the bistable regime (**Figure 25A,B**), significantly increased the firing rate per second (FRs: **AI Table 5**, p-value= 0.0215) and also significantly increased the frequency of oscillation (OF: **AI Table 5**, p-*value* = 0.0215, **Figure 25C,D**). Higher $[K^+]_{ec}$ increased the decay of the exponential curve in the autocorrelograms, meaning that the regularity and periodicity of the oscillations decreased (α-decay: **AI Table 5**, **Figure 25 E**). However, it did not reveal changes neither at

the level of relative firing rate of the Up-states (FR Ups: **AI Table 5**, **Figure 25 C**) nor in the

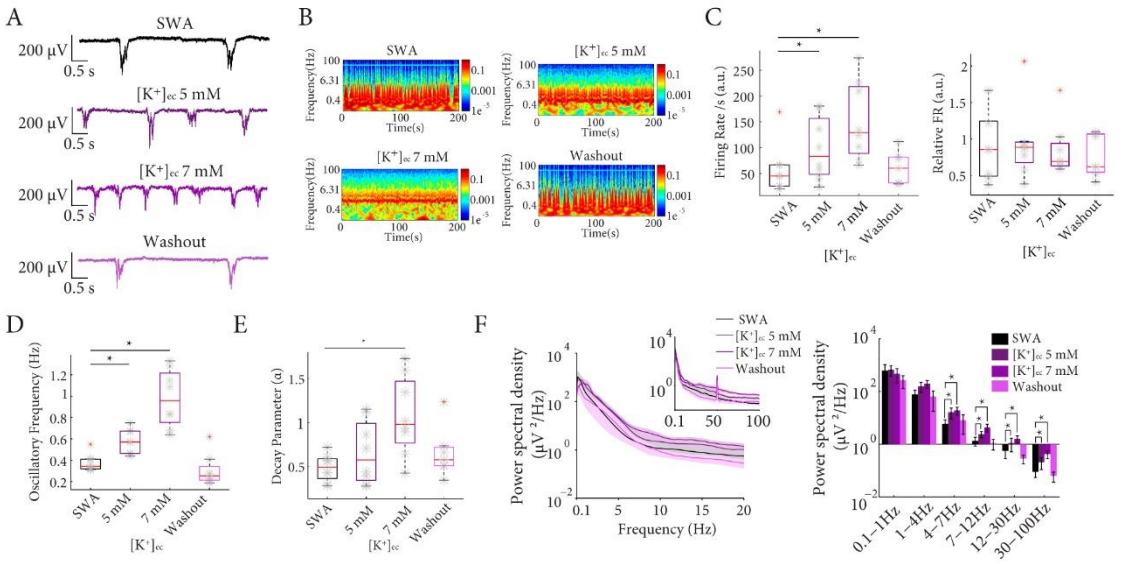

Figure 25. Cortical network regimes are modulated by excitability changes. ***A.*** *Raw LFP recordings of spontaneous activity during control SWA and increasing $[K^+]_{ec}$ (n=9).* ***B.*** *Spectrograms of spontaneous activity from LFP recordings shown in A.* ***C.*** *Firing rate per second increased (left) after the bath application of increasing $[K^+]_{ec}$ but firing rate during the Up-states did not demonstrate significant differences (right).* ***D.*** *Increasing $[K^+]_{ec}$ induced significant higher values of oscillatory frequency (right).* ***E.*** *Autocorrelations of the LFP demonstrated a progressive decrease in the decay of exponential curve after bath application of increasing concentrations of $[K^+]_{ec}$.* ***F.*** *Power spectral density of LFP (color coded) (left). Mean power changed from control to progressive increased all frequency bands without changes at low frequencies after bath application of increasing concentrations of $[K^+]_{ec}$.(* p-value < 0.05).*

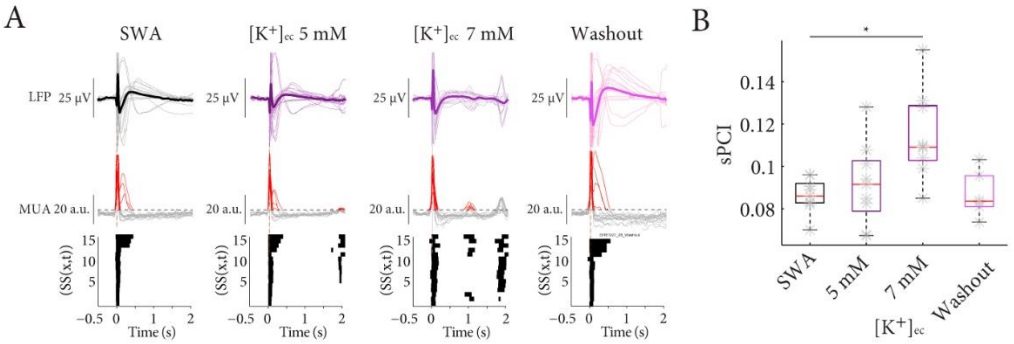

Figure 26. Cortical complexity is modulated by excitability changes. ***A.*** *Averaged LFP (top), MUA (middle) responses to electrical stimulation. Binary matrix SS(x,t) of MUA significantly higher than a threshold activity (bottom) under control, increasing $[K^+]_{ec}$ and washout.* ***B.*** *Population sPCI demonstrate heterogeneous and high complexity responses after bath application of increasing $[K^+]_{ec}$. (* p-value < 0.05).*

power of low frequencies band (0.1-1 Hz) (**Figure 25F**). However, the excitability increased was reflected in the enhancement of high-frequency bands compared with 7 mM K^+ (delta (1-4 Hz) *p-value* = 0.0215; theta (4-7 Hz) *p-value* = 0.0215; alpha (7-12 Hz) *p-value* = 0.0215; beta (12-30 Hz) *p-value* = 0.0215; and gamma (30-100 Hz) *p-value* = 0.0430) (**Figure 25F**).

Regarding the complexity of the responses, they were spatiotemporally heterogeneous and irregular (**Figure 26A**), increasing the cortical complexity in higher potassium concentration (sPCI: **AI Table 5**, *p-value* = 0.0215) (**Figure 26B**).

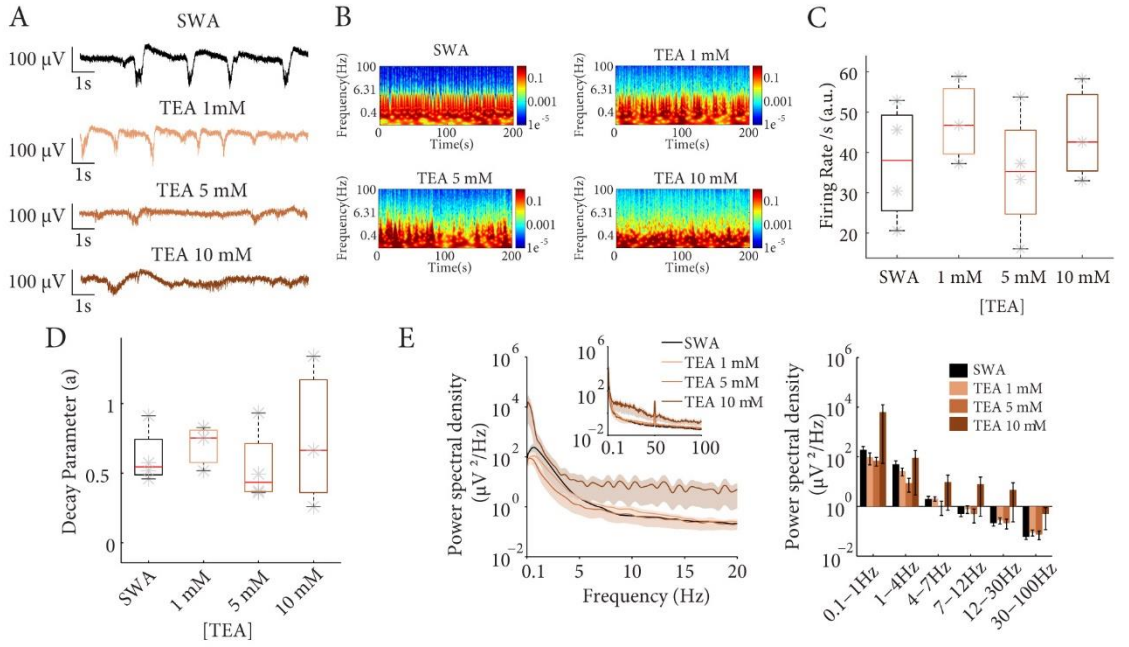

Figure 27. Blocking non-selective K^+ channels remove the cortical rhythms. A. *Raw LFP recordings of spontaneous activity during control SWA and increasing concentrations non-selective K^+ channel blocker (TEA 1 mM, 5 mM, 10 mM) (n=4).* ***B.*** *Spectrograms of spontaneous activity from LFP recordings shown in A.* ***C.*** *Bath application of non-selective K^+ channel blocker increased firing rate.* ***D.*** *Autocorrelations of the LFP demonstrated a decrease in the exponential curve after bath application increasing concentrations non-selective K^+ channel blocker.* ***E.*** *Power spectral density of LFP (color coded) (left). Mean power changed from control to progressive enhanced all frequency bands after bath application increasing concentrations non-selective K^+ channel blocker (TEA 1 mM, 5 mM, 10 mM) (right).*

Then, we analyzed cortical rhythms and complexity changes after bath application of increasing concentrations of K^+ channel blockers (TEA or 4-AP). Bath application of increasing concentrations of non-selective K^+ channel blocker (TEA 1 mM, 5 mM and 10

mM) (**Figure 27**) (*n*=4) removed the oscillatory patterns (α-decay: **AI Table 6**, **Figure 27D**) increased the firing rate per second (FRs: **AI Table 6**, **Figure 27A-C**) and there was an enhancement within all frequency bands (**Figure 27E**).

Those effects were also observed in the stereotypical spatiotemporal distribution of responses (**Figure 28A**), decreasing the complexity of the responses (sPCI: **AI Table 6**, **Figure 28B**).

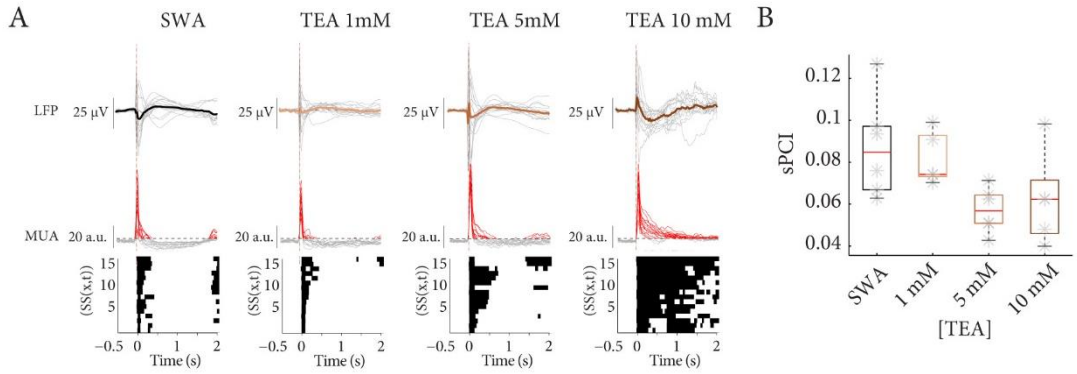

Figure 28. Network complexity decrease by blocking K⁺ channels. ***A.*** *Averaged LFP (top), MUA (middle) responses to electrical stimulation and binary matrix SS(x,t) of MUA significantly higher than a threshold activity (bottom) under control and increasing concentrations non selective K⁺ channel blocker (TEA 1 mM, 5 mM, 10 mM).* ***B.*** *Population sPCI demonstrated stereotypical spatiotemporal distribution of responses, losing the complexity of the responses.*

Blocking the non-selective K_v channel blocker (4-AP 25 μM and 50 μM, *n*=7) (**Figure 29**) we observed an increment in the firing rate (FRs: **AI Table 6**, **Figure 29A-C**) and the decay of the exponential curve in the autocorrelograms increased. There was then a decrease in the regularity and periodicity of the oscillation (α-decay: **AI Table 6**, **Figure 29 D**), and higher values in all frequency bands (**Figure 29E**).

As well as blocking non-selective K⁺ channels, the responses were more stereotypical (**Figure 30A**) reducing the complexity of the responses (sPCI: **AI Table 6**, **Figure 30B**).

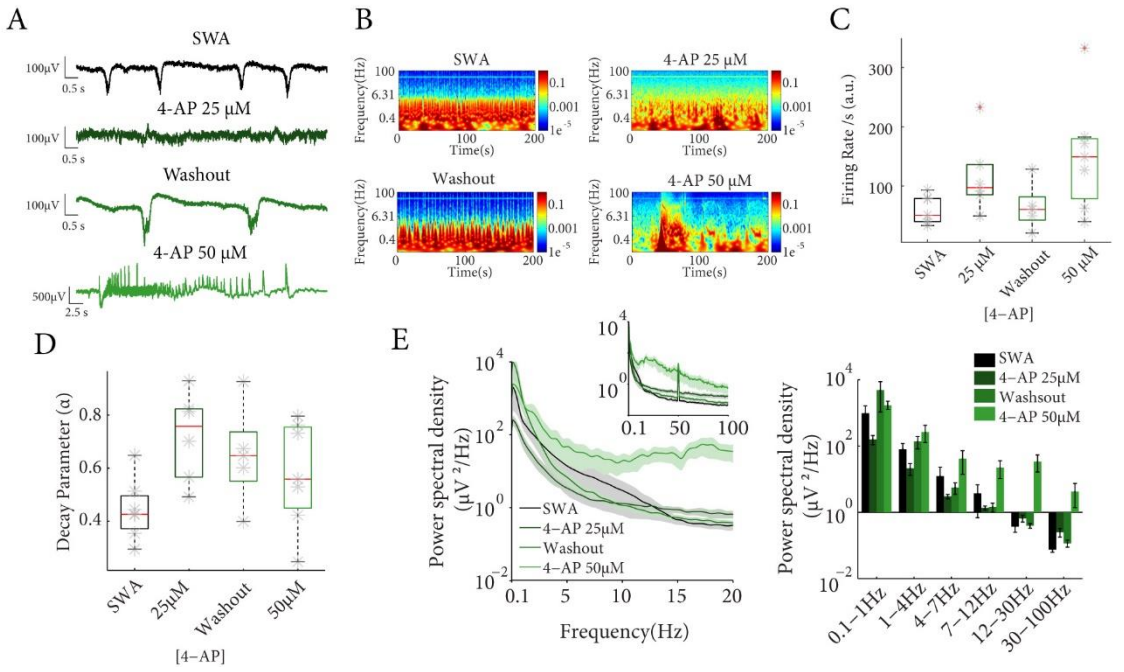

Figure 29. Cortical excitability increases and oscillations are removed by blocking voltage dependent K⁺ channels. ***A.*** *Raw LFP recordings of spontaneous activity in cortical slices, control SWA and increasing concentrations of voltage dependent K⁺ channels blockers (4-AP 25 µM and 50 µM), (n=7).* ***B.*** *Spectrograms of spontaneous activity from LFP recordings shown in A.* ***C.*** *From bimodal distribution of neural firing, blocking voltage dependent K⁺ channels (4-AP 25 µM and 50 µM) induced homogeneous distribution and decreased the firing rate (right).* ***D.*** *Autocorrelations of the LFP demonstrated a progressive increase in the decay of exponential curve after bath application increasing concentrations of voltage dependent K⁺ channels blockers (4-AP 25 µM and 50 µM).* ***E.*** *Power spectral density of LFP (color coded) (left). Mean power changed from control to progressive enhanced all frequency bands after bath application increasing concentrations of voltage dependent K⁺ channels blockers (50 µM) (right).*

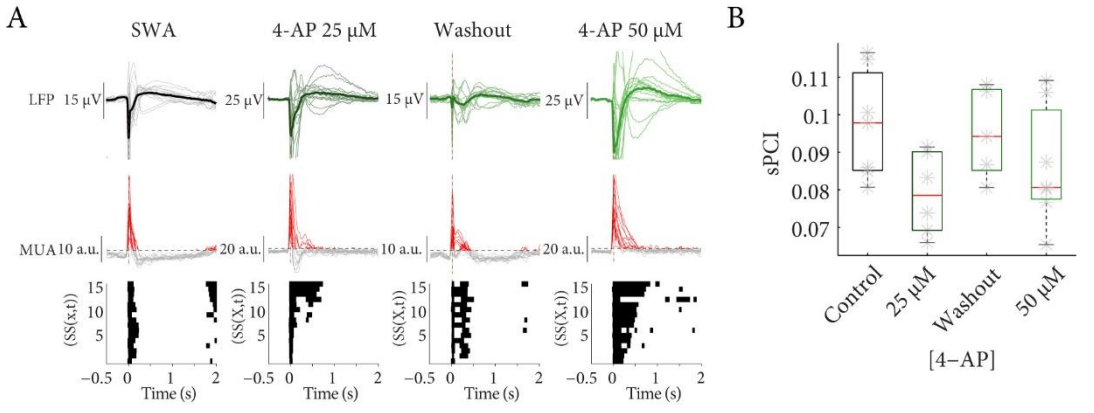

Figure 30. Network complexity decrease by blocking voltage dependent K⁺ channels. ***A*** *Averaged LFP (top), MUA (middle) responses to electrical stimulation and binary matrix SS(x,t) of MUA significantly higher than a threshold activity (bottom) under control and increasing concentrations of voltage dependent K⁺ channels blockers (4-AP 25 µM and 50 µM).* ***B.*** *Population sPCI demonstrated stereotypical spatiotemporal distribution of responses, losing the complexity of the responses.*

In summary, K^+ channels are involved in the control of the level of neural firing and increase the complexity in cortical networks. This suggested that certain levels of level of neural firing are required to induce higher complexity states. However, if this balance is disproportionally altered, segregation and integration balance is transformed and cortical complexity decay.

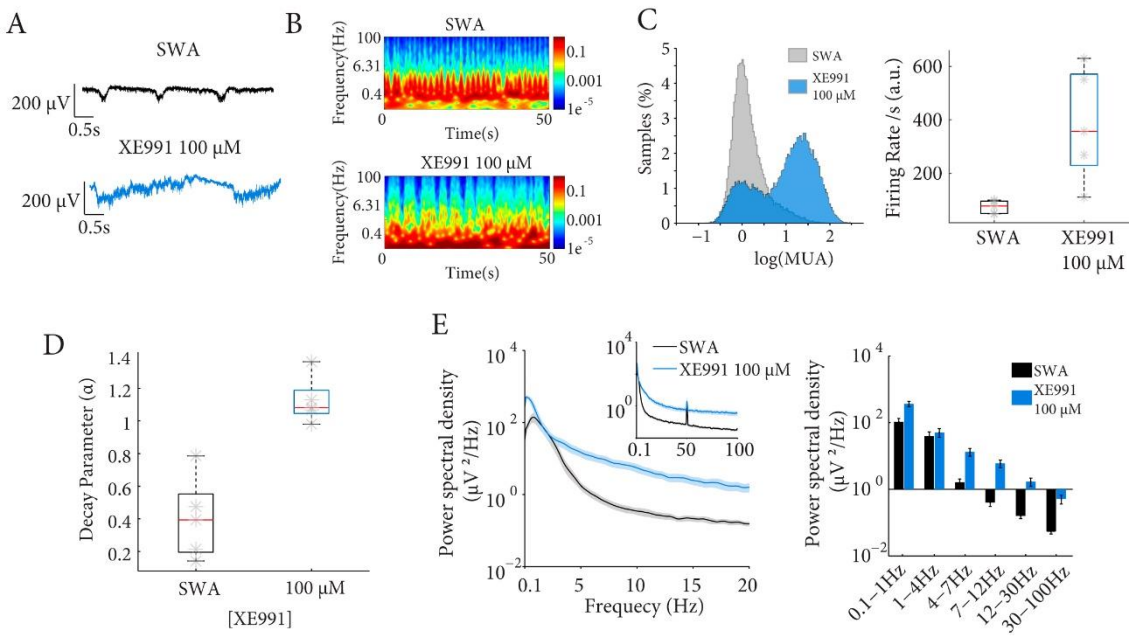

Figure 31. Kv7 blocking induces near asynchronous activity. A. *Raw LFP recordings of spontaneous activity during control SWA and blocking M-current (XE991 100 µM) (n=5).* ***B.*** *Spectrograms of spontaneous activity from LFP recordings shown in A.* ***C.*** *Histograms of log(MUA) distribution (left). From bimodal distribution of neural firing, blocking M-current (XE991 100 µM) induced an inverse bimodal distribution of neural firing where the periods of active states were longer than periods of silence and the average of firing rate didn't change (right).* ***D.*** *Autocorrelation of the LFP demonstrated that blocking M-current removed the oscillatory activity from SWA to a similar asynchronous pattern of cortical activity signal increasing the decay of the exponential curve.* ***E.*** *Power spectral density of LFP (color coded) (left). Mean power spectral density demonstrated an enhancement within high frequency band (right) but, unlike the asynchronous-like activity, the low-frequency bands tend to enhance.*

Considering these results, we decided to focus on one specific potassium channel, the voltage gated K^+ channel 7 (K_{v7}). This channel generates the M-current and is suppressed by the activation of mAChRs (M1 and M3 subtypes), leading to a transient increase in excitability and underlies some forms of cholinergic excitation (Brown, 2010; Radnikow and Feldmeyer, 2018). By blocking M-current with bath application of 100 µM of XE991

(*n*=5) (**Figure 31 A**), we observed that the bimodal distribution of firing submitted to an inversion, the periods of active states were longer than periods of silence, increasing the firing rate per second (FRs: **AI Table 6**, **Figure 31C**). Blocking M-current, the increase of the exponential curve in the autocorrelograms demonstrated that periodicity of oscillatory activity was removed from SWA to a similar awake-like pattern of cortical activity (α-decay: **AI Table 6**, **Figure 31D**), where high-frequency bands were enhanced but, unlike the awake-like activity, the low-frequency bands tend to be enhanced (**Figure 31E**).

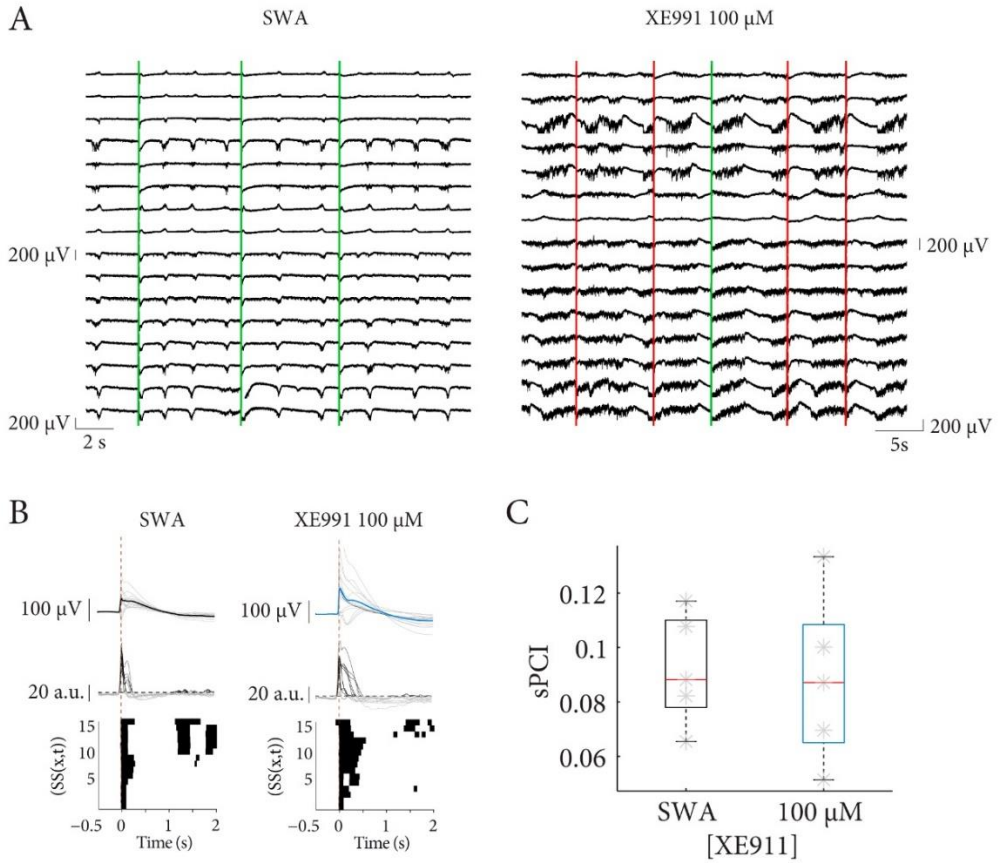

Figure 32. Kv7 blocking induce near asynchronous activity but its responses are still spatially uncomplex. A. *Representative LFP signals under SWA and blocking M-current (XE991 100 µM). Green and red lines represent effective or no effective responses of stimulation pulse respectively.* ***B.*** *Averaged LFP (top), MUA (middle) responses to electrical stimulation and binary matrix SS(x,t) of MUA significantly higher than a threshold activity (bottom) under control and blocking M-current (XE991 100 µM).* ***C.*** *Population sPCI demonstrated were mostly stereotypical at the spatial level and but it didn't reflect significant differences in cortical complexity.*

These complex patterns of cortical activity were difficult to analyze through sPCI method because they couldn't respond properly to the response in several electrical stimulation (**Figure 32A**). Probably, the high synchronized rhythms caused by blocking M-current, complicate the network recruitment to evoke a response. When they evoked a response, they were stereotypical (**Figure 32 A**) and it didn't reflect significant differences in cortical complexity (sPCI: **AI Table 6**, **Figure 32B,C**).

In summary, K^+ channels are involved in the control of the level of neural firing and increased complexity in cortical networks. It is difficult to precise exactly what is the mechanism at play because potassium channels blockers act on the network activity at many different levels: repolarization of individual action potentials, lengthening of the action potentials, they increase the entrance of calcium, therefore altering synaptic transmission, alter mechanisms of termination of Up-states, etc. Unlike the inhibition section, here we observed that modulation of excitability could induce changes in complexity. This suggested that certain levels of excitability were required to induce higher complexity states. However, if this balance is disproportionally altered (as occurred by blocking inhibition) cortical complexity decays even more than SWA regimes.

3.2. Orchestrated interventions of excitatory and inhibitory components are important for the maintenance of neural complexity

Given that excitability plays a role in the modulation of cortical rhythms, we decided to observe the contribution of cortical excitatory neurons. Thus, we decided to use DCS (n=13) (**Figure 11**), which mostly affects the excitatory components of cortical networks. Two parallel aligned silver/silverchlorided electrodes were placed parallel to the cortical layers in the slice, generating homogenous EF perpendicular to the layers (D'Andola et al., 2018; Fröhlich and McCormick, 2010) (**Figure 11A**) in the EF order and magnitude

that we mention in "Chapter 2 Material and Methods, 4.3. Direct current stimulation" (**Figure 11**).

Without leaving the bistable activity (**Figure 33A,B**), DCS proportionally varies the firing rate per second and significantly increased at +5 V/m of DCS (FRs: **AI Table 7**, *p-value* = 0.0446, **Figure 33C**). DCS also induced significantly higher values of frequency comparing with SWA conditions. At 0 V/m, SWA had a mean frequency of 0.30±0.05 Hz and significantly increased with the amplitude of the DCS as described previously (D'Andola et al., 2018) (OF: **AI Table 7**, *p-value* = 0.0107, **Figure 33C**). Furthermore, progressively increasing values of DCS demonstrate lower values of relative firing rate during the Up-states comparing with SWA conditions (FR Ups: **AI Table 7**, **Figure 33C**). In addition, the decay of the exponential curve increased, then the regularity and periodicity of oscillation proportionally decreased with the intensity of DCS, and it was significantly higher compared with +5 V/m (α-decay: **AI Table 7**, *p*-value= 0.0446, **Figure 33D**). Finally, when we observed changes in power components, we detected increasing significant differences at +5 V/m in almost all frequency bands comparing with 0 V/m of DCS (*p*-values comparing 0 V/m Vs +5 V/m: delta (1-4 Hz) *p-value* = 0.0215; theta (4-7 Hz) *p-value* = 0.0215; alpha (7-12 Hz) *p-value* = 0.0215; beta (12-30 Hz) *p-value* = 0.0215; and gamma (30-100 Hz) *p-value* = 0.0107) (**Figure 33E**).

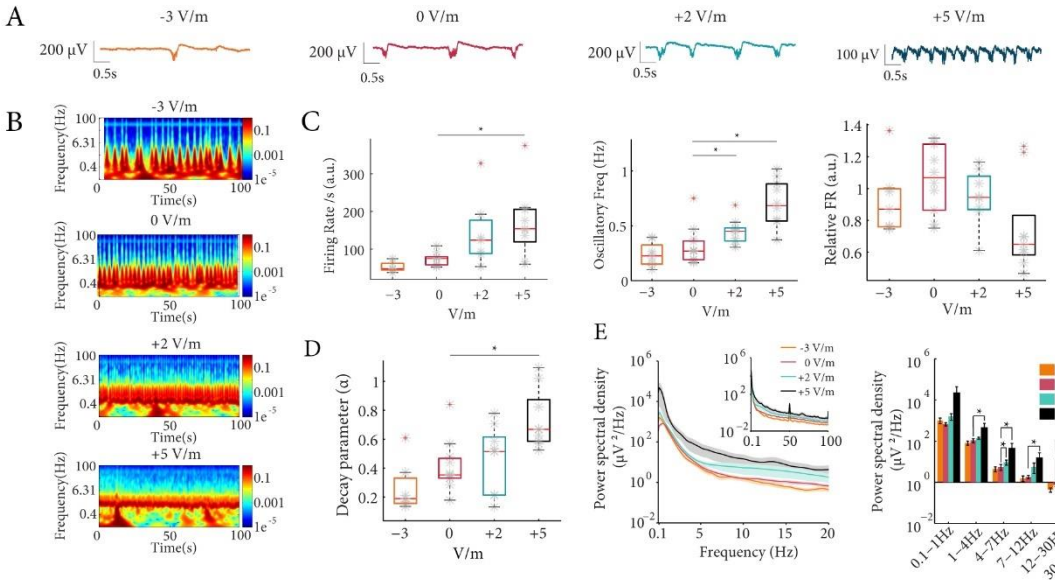

Figure 33. Mainly activation of excitatory neurons by DCS increases the excitability. A. *Raw LFP recordings of spontaneous activity in cortical slices, under different Electric fields (-3 V/m (n=8), +2 V/m (n=10) and +5 V/m (n=10)).* ***B.*** *Spectrograms of spontaneous activity from LFP recordings shown in A.* ***C.*** *Progressively, firing rate per second increased (left), oscillatory frequency increased (middle) and the relative firing rate during the Up-states decreased.* ***D.*** *Autocorrelations of the LFP demonstrated a progressive increment in the decay of exponential curve under different DCS.* ***E.*** *Power spectral density of LFP (color coded) (left). Mean power changed from control to progressive increased all frequency bands under +5 V/m DCS (* p-value < 0.05).*

Even under the modulation of cortical excitability by DCS, the spatiotemporal distribution of responses to electrical stimulation (n=5) were as homogeneous (**Figure 34A**) as SWA conditions, without significant differences in cortical complexity (sPCI: **AI Table 7**, **Figure 34B**).

In summary, DCS proportionally modulates the neural firing, oscillatory frequency and controls the periodicity of the oscillation. Even under those conditions, complexity did not change.

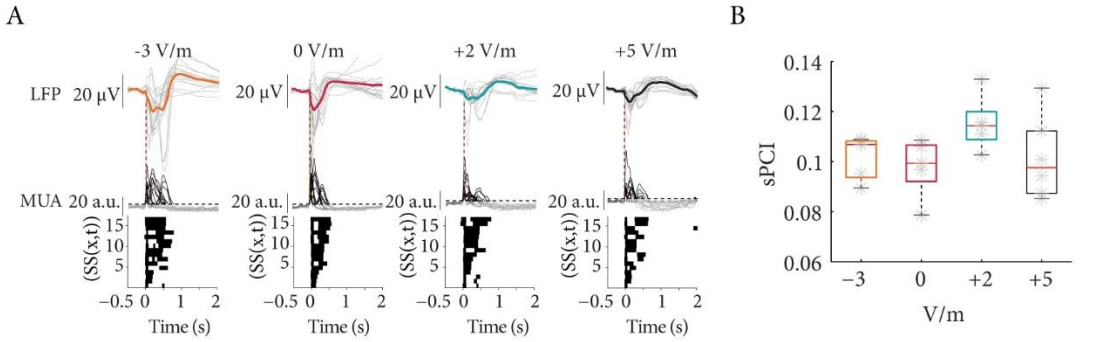

Figure 34. Activation of excitatory neurons by DCS does not modulate the complexity of the responses. A. *Averaged LFP (top), MUA (middle) responses to electrical stimulation and binary matrix SS(x,t) of MUA significantly higher than a threshold activity (bottom) under different electric fields (-3 V/m (n=5), +2 V/m (n=5) and +5 V/m (n=6)).* ***B.*** *Population sPCI under different electric fields demonstrate similar homogeneous and stereotypical responses than control conditions*

4. Cholinergic neurotransmission results in higher complexity states

We previously observed that excitatory and inhibitory neurons are required to stablish and maintain cortical rhythms. The activation of these neurons depends on the activation/inactivation of different receptors and ion channels expressed in their membranes which can affect various cellular functions. Neurotransmitters, such as ACh, are released in the neocortex to activate these channels and receptors, and shift the cortical activity from one state to another (Lee and Dan, 2012). Muscarinic acetylcholine receptors (mAChR) are implicated in the modulation of SWA and the transition from SWA to wakefulness (McCormick and Williamson, 1989; Poulet and Crochet, 2019). Then, we considered that mAChR activation could participate in the modulation of cortical rhythms and complexity in cortical networks.

On this basis, we studied *in vitro* the effect of (1) Iperoxo (IPX), a potent mAChR agonist (Barocelli et al., 2000), and (2) a novel IPX derivative photoswitchable molecule Phthalimide-Azobenzene-Iperoxo (PAI), a M2 mAChR agonist (Riefolo et al., 2019). In addition, because these molecules are a novel tool to modulate cortical activity, we wanted

to demonstrate whether photopharmacology can be used as a therapeutic tool to modulate cortical activity *in vitro* and *in vivo*, avoiding electric or genetic manipulation. Most of the following results have been published in (Barbero-Castillo et al., 2020).

4.1. Non-specific activation of mAChRs evokes neuronal hyperexcitability in cortical slices

First, we bath-applied a range of different concentrations of IPX (M1, M2, M3 mAChR agonist: 1 nM, 10 nM, 100 nM-200 nM) (**Figure 35**). The activation of mAChRs by IPX (n=4) resulted in a global change in the network's rhythms to a hyperexcitable activity (**Figure 35A,B**). At 100 nM IPX, the oscillatory frequency increased (OF: **AI Table 8, Figure 35C**), and bath application of the highest concentrations of IPX (100-200 nM) resulted in a seizure-like discharges (**Figure 35A,B**). Together with this, the relative firing rate during the Up-states decreased (FR Ups: **AI Table 8, Figure 35D**) and also the firing rate per second (FRs: **AI Table 8, Figure 35D**), but without significant differences compared with SWA conditions. Indeed, IPX abolished the periodicity of cortical oscillations (α-decay: **AI Table 8, Figure 35E**). Moreover, at concentrations equal or higher than 100 nM IPX, the oscillatory activity evolved to periods of seizure-like discharges which were characterized by low (<1 Hz), delta (1-4 Hz) and alpha (8-12 Hz) frequencies (**Figure 35F**).

In summary, given that IPX demonstrated an effect of cortical activity *in vitro*, IPX is a good design strategy to develop specific photoswitchable molecules for cortical mAChR. Indeed, activation of mAChR are involved in increasing the excitability of cortical networks, suggesting that great activation of mAChR underlies the seizure activity.

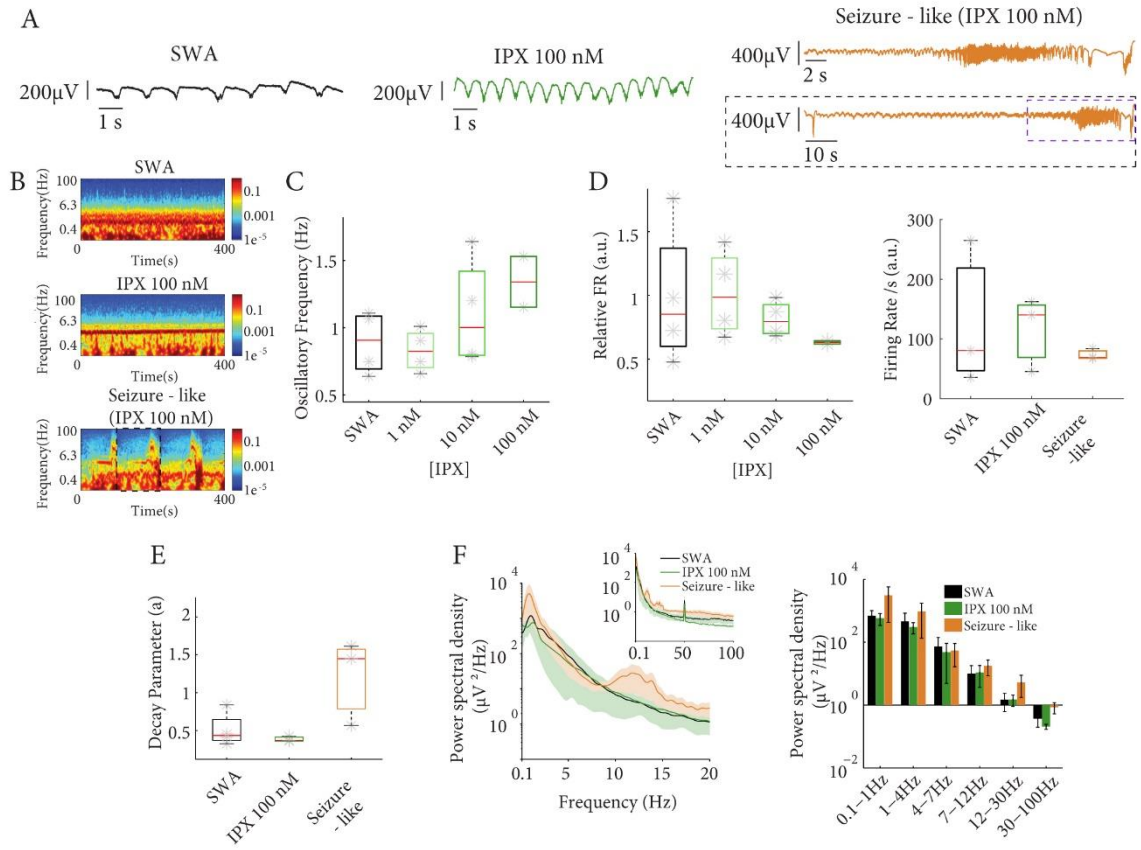

Figure 35. Non-specific activation of mAChRs evokes hyperexcitability in cortical slices. A. *Representative LFP traces showing the increasing of the oscillatory frequency during control, 100 nM IPX and periods of seizure-like discharges. Black square in marks the seizure-like discharge appeared in panel B.* ***B.*** *Spectrogram from the same time recording of LFP in panel A.* ***C.*** *Population of oscillatory frequency (Hz).* ***D.*** *Relative firing rate of the Up-state decreased (left) and firing rate per second (left) decreased with increasing concentrations of IPX.* ***E.*** *Non-specific activation of mAChRs removed periodicity.* ***F.*** *Power spectral density (PSD) values showing an enhancement of low, delta and theta frequency component.*

4.2. M2 agonists-PAI isomers effectively modulate cortical activity

After observing that cortical activity could be modulated by IPX derivate molecules, we decided to observe muscarinic neuromodulation using PAI, a photoswitchable IPX derivative that allows the reversible activation of M2 mAChRs with light (Riefolo et al., 2019). M2 mAChR plays relevant roles in several CNS disorders (Scarr, 2012), and regulating their activity and subsequent effects on cortical neuronal networks may provide new therapeutic opportunities for these cholinergic diseases.

We first built up the dose-response curves of the two drug forms separately, *trans*- (dark-adapted state) and *cis*-PAI (after UV irradiation) (10 nM, 100 nM, 300 nM, and 1 μM; *n*=6 for each PAI form, *trans* and *cis*) (**Figure 36A**), in order to find out the differences in cortical activity between the PAI-isoforms, and to identify the most convenient concentration range to manipulate cortical rhythms with light. In comparison to the SWA, the *trans*-PAI activity already showed alterations in the frequency of oscillations at 100 nM (OF: **AI Table 9**, **Figure 36B,C**). However, in comparison, *cis*-PAI displayed significantly weaker effects, in agreement with the reported PAI properties (Riefolo et al., 2019). At 100 nM and 300 nM, *cis*-PAI did not alter the spontaneous activity observed in SWA conditions (OF: **AI Table 9**, **Figure 36C**), in contrast to the strong alterations in oscillatory activity obtained with 100 nM and 300 nM *trans*-PAI, leading to significant differences between both isoforms at these concentrations (OF: **AI Table 9**, *p*-value = 0.0087). However, we did not observe significant differences in the decay of the exponential curve (**Appendix II (AII) Figure S1** and **Figure S2**). The activity of PAI at 100 nM and 1 μM in cortical slices did not strongly differ between *trans* (**AII Figure S1**) and *cis* (**AII Figure S2**) in terms of oscillatory activity. 100 nM applications of *trans* and *cis* did not mostly produce changes in neuronal firing comparison to the basal control situation (black line), as it was shown in the autocorrelograms graph (**AII Figure S1** and **Figure S2**). At 1 μM, both PAI isomers produce strong changes of the oscillatory activity (**AII Figure S1** and **Figure S2**). Indeed, we did not observe significant differences in the level of neural firing measured by firing rate per second. However, measuring level of neural firing by relative FR of the Up-states (FR Ups: **AI Table 9**, **Figure 36D**), we detected significant differences at the highest concentration of both drugs (FR Ups: **AI Table 9**, *p-value* = 0.0087, **Figure 36D**).

In summary, we demonstrated that PAI can be useful to modulate cortical rhythms by M2 mAChR activation. Here we observed that the differences in the physiological effects between *trans*- and *cis*-PAI emerged between 100 nM and 300 nM, and they were

observed in the OF (Hz) and Up-states relative firing rate (a.u.). We focused on these conditions in order to photomodulate cortical rhythms using PAI.

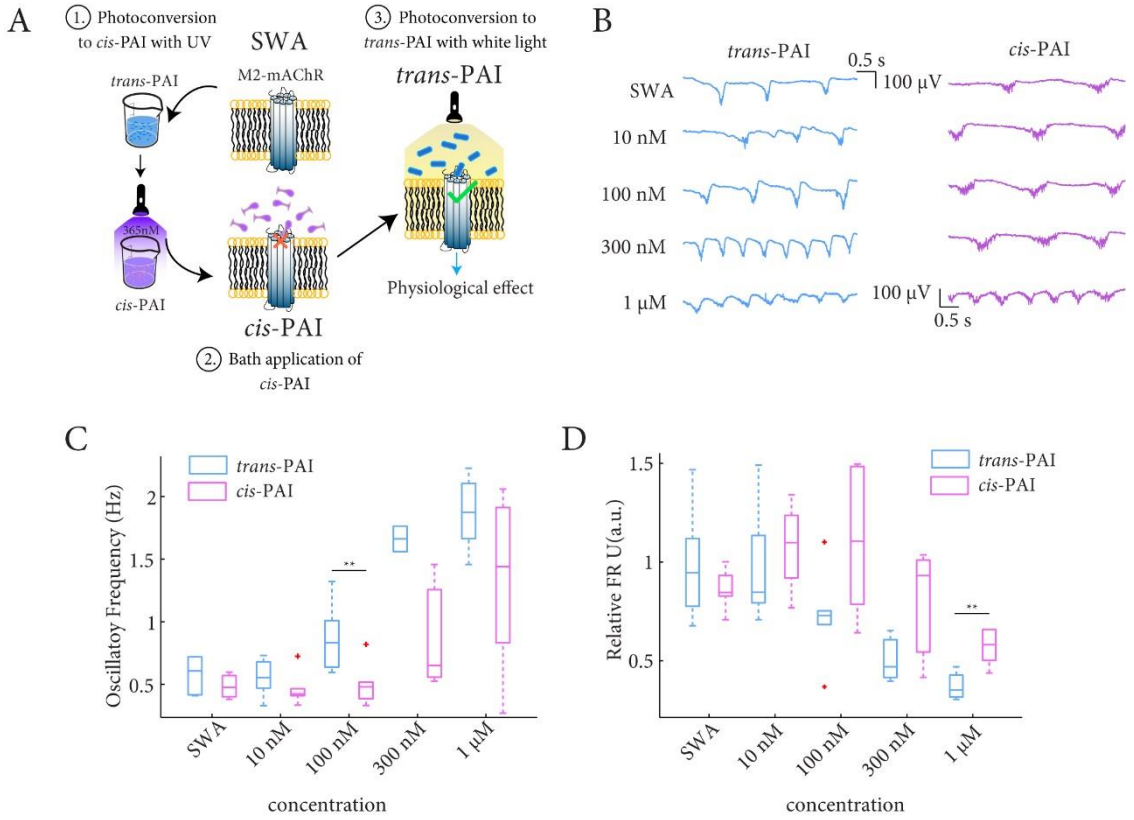

Figure 36. Dose response curve reflect significant differences in excitability between 100 nM and 1 µM of inactive and active PAI. A. *PAI photoswitching protocol. (1) Photoconversion from trans-PAI to cis-PAI with 10 min of UV irradiation; (2). Bath application of cis-PAI; (3). Photoconversion from cis-PAI to trans-PAI with White light irradiation.* ***B.*** *Representative local field potential traces showing the increasing of the oscillatory frequency.* ***C.*** *Population of oscillatory frequency demonstrated significant differences between isoforms at 100 nM.* ***D.*** *Population of relative firing rate of the Up-states demonstrated significant differences of both isoforms at 1 µM (**<0.01).*

4.3. Activation of M2 mAChR trigger activity higher excitable and complex states *in vitro*

Once the different oscillatory activity evoked by *cis*- and *trans*-PAI was quantified *in vitro*, we moved on to controlling cortical rhythms with light. We took advantage of the thermal stability of both PAI forms to apply initially the inactive one (*cis*-PAI) at 200 nM in cortical slices (n=17), in the absence of white light to avoid photoconversion to *trans*-PAI during the recordings (**Figure 37A**). As shown in **Figure 37B** and **Figure 37C**, 200

nM *cis*-PAI evoked an increase in the oscillatory frequency (OF: **AI Table 10,** *p*-value = 0.003), and no significant effects in the relative firing rate of the Up-states (FR Ups: **AI Table 10**). Subsequent illumination of the slices with white light produced a robust increase in the oscillatory frequency (OF: **AI Table 10,** *p*-value = 0.001, **Figure 37B**), and significantly decreased the relative firing rate of the Up-states (FR Ups: **AI Table 10,** *p*-value = 0.008, **Figure 37C**). In addition, it showed significant differences of firing rate per second between *cis*-PAI and SWA (FRs: **AI Table 10**, *p*-value = 0.045) and a robust and effective increase upon illumination compared with *cis*-PAI and SWA conditions (FRs: **AI Table 10,** *p*-value = 0.0178, **Figure 37D**). In spite *trans*-PAI had a significant effect in

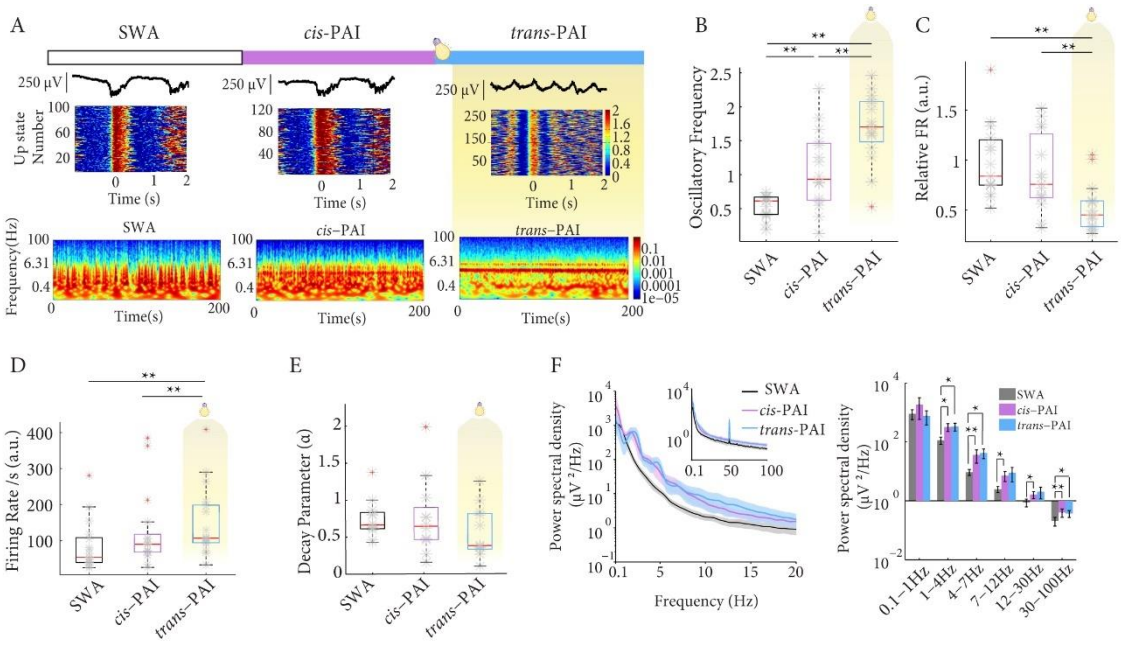

Figure 37. Modulation of brain waves in vitro using PAI, a light-regulated ligand, induces near awake activity. A. *Illustration of protocol activation of PAI (top) (n=17). Representative LFP traces (top) and corresponding raster plots of relative firing rate under SWA conditions, 200 nM of cis-PAI and 200 nM trans-PAI after light activation (middle). Representative spectrogram under SWA condition, 200 nM of cis-PAI after light activation (bottom)* ***B.*** *Population of oscillatory frequency (Hz) under mentioned conditions demonstrated a progressive increase after bath application of cis-PAI and higher frequency after light activation.* ***C.*** *Population of relative firing rate (a.u.) of the Up-states demonstrated a great decrease after light activation.* ***D.*** *Population of firing rate per second (a.u.) demonstrate significant higher values after light activation.* ***E.*** *Autocorrelograms of LFP from one channel and population of α-decay demonstrated no significant.* ***F.*** *Power spectral density (PSD) under control conditions, 200 nM of cis-PAI and 200 nM trans-PAI after white light activation (color code) demonstrated higher significant values at delta (1-4 Hz), theta (4-7 Hz) and gamma (30-100 Hz) comparing with SWA conditions. (* p-value < 0.05, **p-value < 0.01).*

the neural firing, no significant changes in the decay of the exponential curve were observed, which means that regularity and periodicity of the oscillations did no change (α-decay: **AI Table 10**, **Figure 37E, AII Figure S3**). In any case, here we can also observe that *cis*-PAI at 200 nM (pink line) in cortical slices did not evoke strong changes in terms of oscillatory frequency in comparison to the SWA situation (black line) without PAI application, as is shown in the autocorrelograms graph (**AII Figure S3**). After white light application, PAI switches to its active *trans* form (blue line), and strong changes in oscillatory activity are visible (**Figure S3**). Activation of M2 receptors with *trans*-PAI demonstrate higher values at delta (1-4 Hz), theta (4-7 Hz) and gamma (30-100 Hz) compared with SWA conditions (**Figure 37F**).

Finally, measuring cortical rhythms by means of cortical complexity, activation of M2 receptors reflected heterogeneous spatiotemporal responses (**Figure 38A**), leading to high-complexity rhythms (sPCI: **AI Table 10, Figure 38B**).

In summary, here we demonstrate that PAI can be used as tool to modulate cortical activity *in vitro* and activation of M2 mAChR induces highly excitable and complex states.

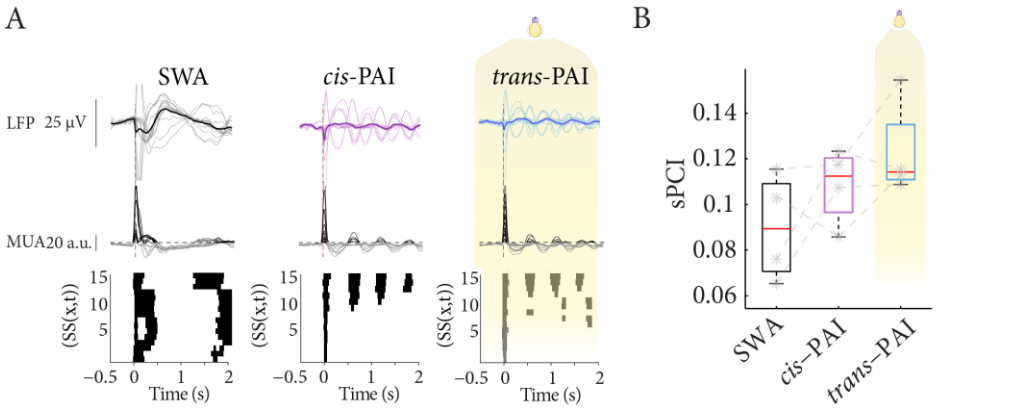

Figure 38. Modulation of brain waves in vitro using PAI enhances the cortical complexity. A. *Averaged LFP (top) and MUA (middle) to electrical stimulation during distinct regimes of activity and binary matrix SS(x,t) of significant sources of activity following a single electrical pulse (bottom).* ***B.*** *Population sPCI demonstrated heterogeneous and higher complexity responses after photoswitching with white light (trans-PAI).*

4.4. Photopharmacology tools can modulate cortical activity with light *in vivo*

Having established the ability of PAI to alter cortical oscillatory activity with light in slices, we then aimed to photocontrol cortical activity *in vivo*. Cortical activity was recorded in anesthetized C57BL6/JR mice (n=3) with an electrode inserted through a craniotomy across which we carried out the drug application and brain illumination (see Methods) (**Figure 39A**). SWA in anesthetized mice demonstrated an oscillatory frequency 0.63±0.08 Hz and relative firing rate of 0.87±0.29 a.u. As the dose-response curves of *cis*- and *trans*-PAI could be different from the *in vitro* conditions (**Figure 37** and **Figure 39**), we tested two different concentrations: 200 nM and 1 μM. 100 μL of 200 nM *cis*-PAI solution were initially applied to the brain surface, and the activity was recorded in the absence of white light, to avoid *cis* to *trans* photoisomerization of PAI. The oscillatory frequency and the frequencies power of the cortical oscillatory activity was not significantly altered by *cis*-PAI (OF: **AI Table 11, Figure 39B,D**) and caused a minor increase in the relative firing rate (FR Ups: **AI Table 11, Figure 39C**). Subsequently, we illuminated the brain using white light in the proximity of the recording electrode, in order to isomerize PAI to its active form (*trans*). An increase in the oscillatory frequency (OF: **AI Table 11, Figure 39B**) and in the power of the alpha (7-12 Hz) and gamma (30-100 Hz) frequency bands (**Figure 39D**) were observed under white light illumination, without changes in the relative firing rate (FR Ups: **AI Table 11, Figure 39C**). Applying a higher concentration of *cis*-PAI (1 μM), slightly reduced the frequency (OF: **AI Table 11, Figure 39B**) and increased power at low frequency band (0.1-1Hz) and decreased the power of alpha and gamma bands (**Figure 39D**), while the FR during the Up-states remained relatively elevated than the SWA condition (FR Ups: **AI Table 11, Figure 39C**). At this concentration, illumination significantly increased the oscillatory frequency (OF: **AI Table 11,** *p-value* = 0.042**, Figure 39B**) and again induced an increment of the alpha and gamma frequencies band (**Figure 39D)** while the FR during Up states was decreased

to the SWA values (FR Ups: **AI Table 11, Figure 39C**) following the tendency previously observed *in vitro*. By using two concentrations of the drug, we observed that the effect on the oscillatory frequency is nearly saturated at 200 µM, while the decrease of the FR during the Up-states occurs under 1 µM. This strategy allowed us to repeat twice the photocontrol of cortical activity by subsequent application of 1 µM *cis*-PAI and photoconversion to *trans*-PAI.

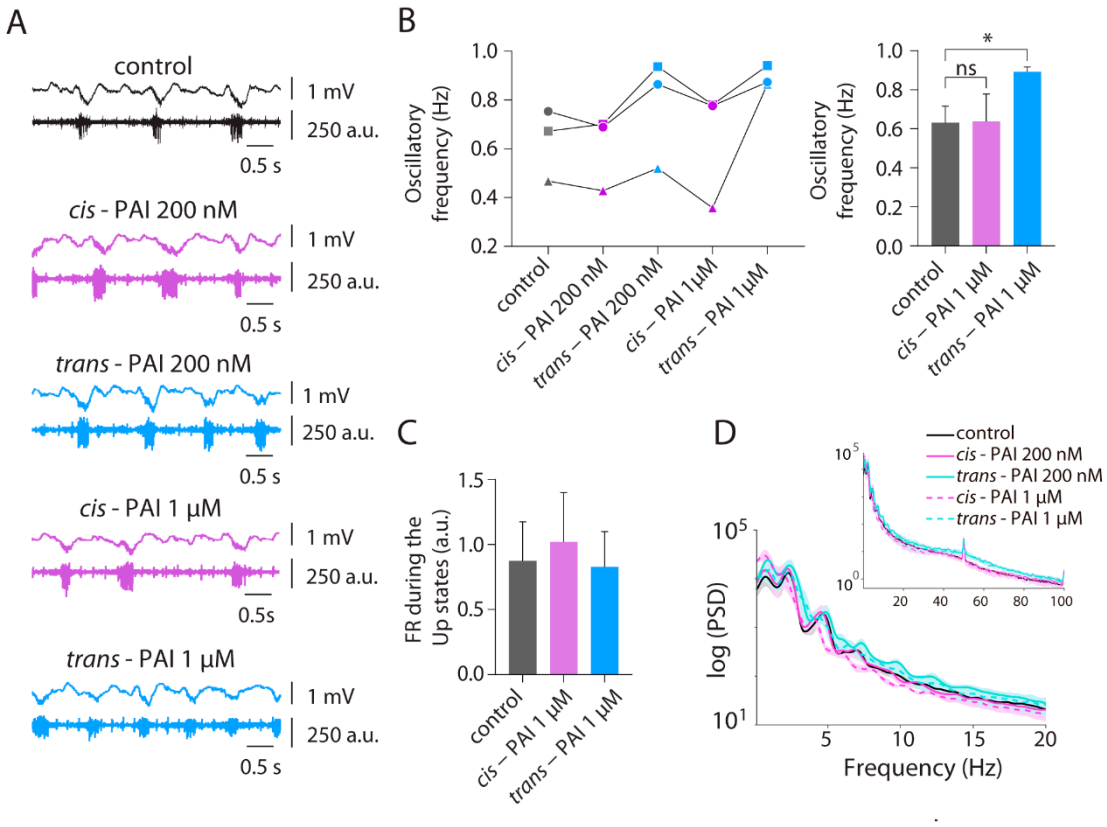

Figure 39. In vivo photomodulation of brain waves. ***A.*** *Representative raw traces of LFP (top, in mV) and MUA (bottom, a.u.), showing the differences in oscillatory frequency and FR during the Up-states between the control, 200 nM, and 1 µM cis-PAI (pre-irradiated with 365 nm), and after photoswitching with WL (trans-PAI).* ***B.*** *Individual (left) and mean (right) quantification of oscillatory frequency (Hz) at different concentrations.* ***C.*** *Mean quantification of FR during the Up-states (a.u.) at different concentrations.* ***D.*** *Power spectral density (PSD) of oscillatory activity at different concentrations displays an enhancement at high-frequency bands after WL activation. *p-value < 0.05.*

In summary, first we demonstrated that (1) IPX is a good design strategy to develop specific photoswitchable molecules for cortical mAChR; (2) non-specific activation of mAChR are involved in increasing the level of neural firing of cortical networks; (3) great activation of mAChR underlie the seizures activity; (4) PAI can be used as tool to modulate cortical activity *in vitro* and *in vivo;* (5) and activation of M2 mAChR induced highly excitable and complex states.

Chapter 4

Discussion

The aim of this PhD work was to explore the cortical emergent activity patterns and the mechanisms underlying cortical network complexity and therefore the underpinnings of brain states. To this end, we have used three approaches. (1) We replicated SWA and awake-like regimes to validate isolated cortical slices as a model of brain states and analyzed sPCI as a methodological tool to quantify network complexity. (2) We studied the contribution of excitatory and inhibitory components to the different cortical network regimes. (3) We identified cellular mechanisms underlying the modulation of cortical states by regulating the levels of ionic blockers and different neurotransmitters involved in brain state transitions. To do this, we modulated the cortical activity *in vitro* that spontaneously displays SWA, a hallmark of activity during deep sleep and anesthesia (Sanchez-Vives, 2020; Sanchez-Vives et al., 2017). It has been demonstrated that subcortical areas project several neuromodulatory inputs to the cortex

to induce cortical state switching (Lee and Dan, 2012). These mechanisms have been manipulated or replicated to externally induce cortical switching between brain states. For example, many anesthetics increase or decrease neurotransmitter release to the cortex to induce sedation or sleep states (Lydic and Baghdoyan, 2005). Other studies demonstrate that deep stimulation of subcortical areas in patients with disorders of consciousness could induce improvements in responsiveness (Schiff, 2008). Simulation of different cortical states and the study of spontaneous and evoked activity could provide insights about the underlying mechanisms controlling the cortical states, cortical complexity and their transitions. We demonstrated that isolated cortical slices can display different cortical activity patterns and levels of complexity detected by sPCI, as originally described (D'Andola et al., 2017). Using this model, we proved the disruption of inhibitory and excitatory balance has important effects over the regime of cortical activity and cortical complexity. We demonstrated that inhibition (both fast and slow) maintains these cortical activity patterns through the modulation of neural firing level and their oscillatory frequency. In addition, we demonstrated that certain levels of excitability are required to induce higher complexity states. When we induced changes in excitability through modulation of extracellular K^+ concentration or inactivation of K^+ channels (which affects both interneurons and excitatory neurons) (Greene and Hoshi, 2017) or activated M2-mACh receptors, or when we blocked inhibition, the network shifts from the bistable response to a state of increased excitability that can result in an epileptiform state (decreasing network complexity) or a more heterogeneous responses (increasing network complexity), respectively. These results agree with human studies of brain complexity showing that patients with consciousness disorders showed low complexity states and awake patients showed high complexity states (Casali et al., 2013). Thus, these results suggest that the inhibitory component alone or inhibitory and excitatory components together, are required for the maintenance of cortical rhythms and neural complexity at physiological levels.

1. Isolated cortical slices can display different regimes of network activity patterns and complexity

Given that isolated cortical slices can spontaneously display SWA (Sanchez-Vives and McCormick, 2000), and it is possible to modulate the cortical activity through *in vitro* preparation, we analyzed dynamical changes from spontaneous activity and complexity. We first observed that spontaneous SWA (**Figure 13**) was characterized as previously described in (D'Andola et al., 2017; Sanchez-Vives and McCormick, 2000). Neurons fired regular and periodically within a bimodal distribution of firing, with neural firing during the Up-states and almost silent during Down-states (Reig et al., 2010; Sanchez-Vives, 2020; Sanchez-Vives et al., 2017) and with high presence of low frequencies (0.1-1 Hz) compared with other frequency bands. As we expected, in our awake-like regime (**Figure 13**) neural firing increased where neurons fired nearly independently and irregularly. These results were similar to those obtained from *in vivo* experiments (Poulet and Crochet, 2019; Reyes-Puerta et al., 2016), therefore, we suggest that our *in vitro* model could be used as a model of brain states.

Together with these results, we considered whether we could use sPCI as a methodological tool to quantify network complexity (**Figure 14**). As expected, the spontaneous patterns of cortical activity supported the complex transfer of information occurring during awake-like states. Following neural complexity theory (Tononi, 2004) we suggested two possible scenarios: during the SWA regime, the cortical responses were homogeneous, mostly synchronized and spatially restricted (Pigorini et al., 2015; Tononi, 2004) in which interaction between different locations in the slice was probably reduced. Alternatively, awake-like regime displayed higher complexity states, perhaps because cortical network connections spans across other regions (enhancing integration), and cortical neurons fire nearly independently and irregularly, leading to rich responses by specific interactions. In fact, it has been proposed that the increase of the information processing power during awake states is possible because there is a decorrelation of

membrane potential between excitatory and inhibitory neurons, increasing the independence of individual neurons to process cortical information (Gentet et al., 2010; Poulet and Petersen, 2008) and perhaps also due to depolarizing mechanisms too. These results were in accordance with results obtained from complexity studies in human patients (Alkire et al., 2008; Casali et al., 2013) or *in vivo* experiments, where patients or mice under deep anesthesia, demonstrate lower complexity values than awake patients.

2. Inhibition maintains cortical rhythms through regulation of excitability and controls the equilibrium in cortical complexity

After observing that cortical slices *in vitro* could be used as a model of brain states and sPCI could detect complexity levels, we explored the role of inhibition (fast and slow inhibition) and excitation in the control of cortical rhythms and their transition and their role in the modulation of cortical complexity.

First, we progressively removed inhibition in isolated cortical slices displaying different regimes of network activity (SWA and awake-like). Removing fast inhibition (**Figure 15**) or slow inhibition (**Figure 17**) during awake-like states, the activity shifted to highly synchronous regular and periodical cortical activity, with the same levels of level of neural firing as the awake-like state, but with decreased the complexity (**Figure 16** and **Figure 18**). However, the effects of blocking fast inhibition were stronger than the effects of blocking slow inhibition. Indeed, cortical activity shifted to a bimodal distribution of neural firing after blocking fast inhibition, together with an increment in the power of low frequencies and high-frequency bands. Meanwhile, blocking slow inhibition during the awake-like regime, there were no changes in the modulation of low-frequency bands (0.1-1 Hz).

Then, blocking fast and slow inhibition during the SWA regime, analogous effects were observed in previous studies (Mann et al., 2009; Perez-Zabalza et al., 2020; Sanchez-Vives et al., 2020, 2010). Without leaving the bistable state, blocking fast (under bath application of BMI (**Figure 19**) or GBZ (**Figure 21**)) or slow inhibition (under bath application of CGP (**Figure 23**)), cortical levels of neural firing increased, mainly during Up-states. In addition, the regularity and periodicity of the oscillation increased. When blocking fast inhibition, a gradual shortening of Up-states was demonstrated, as previously (Mann et al., 2009; Sanchez-Vives et al., 2010) and blocking, slow inhibition led to longer Up-states followed by prominent Down-states, similarly to previous studies (Mann et al., 2009; Perez-Zabalza et al., 2020; Sanchez-Vives et al., 2020). Furthermore, when blocking fast (**Figure 20** and **Figure 22**) and slow inhibition (**Figure 24**), cortical complexity decreased (Sanchez-Vives et al., 2020).

In summary, inhibition seemed to be implicated in maintaining the awake-like or SWA regimes and controlling the level of neural firing. These coincide with previous suggestions (Buzsáki and Draguhn, 2004) which described that inhibitory interneurons in the cortex "clock" the networks oscillations and maintain the excitatory and inhibitory balance necessary for the transfer of information. Therefore, inhibition might play a critical role in processing information in the cortex by gating signal flow and sculpting network rhythms (Cobos et al., 2005; Compte et al., 2008; Guidotti et al., 2005; Konstantoudaki et al., 2014; Tremblay et al., 2016).

Indeed, we observed that higher excitability levels are not required to induce higher complexity states. In fact, it seemed that there was a break in the complexity balance. Following neural complexity theory (Tononi, 2004) we could speculate three possible scenarios: (1) during complex awake-like states, the network would be functionally integrated and segregated as we mentioned previously; (2) during low complexity SWA states, the cortical network would have low integration; however (3), by blocking inhibition, the network is fully integrated, while weakly segregated, giving rise

to activation waves that rapidly span the whole network, leading to faster and stereotypical responses (Sanchez-Vives et al., 2010). This suggests that inhibition, inducing prominent bistable activity, may break the causal interactions of the cortical network, decreasing the complexity. That was previously suggested in TMS/EEG studies (Pigorini et al., 2015). They observed that OFF-periods (Down-states) break the causal interactions among cortical areas, not only during sleep or anesthesia, but also in patients with disorders-of-consciousness (Casali et al., 2013; Pigorini et al., 2015). In previous disorders of consciousness studies (Wislowska et al., 2017) unconscious patients correlate with low complexity values while awake patients are correlated with high complexity values. Therefore, loss of consciousness can be correlated with a collapse of cortical connectivity (loss of integration), or with a breakdown of the collection of cortical activity patterns (loss of segregation), and also a dominance of slow oscillatory cortical activity (Alkire et al., 2008; Casali et al., 2013; Goldman et al., 2019; Massimini et al., 2009; Wislowska et al., 2017). Thus, the more prominent the Down-states, the lower the complexity. Pigorini et al., (2015) also suggested, and we demonstrated, that alterations in the balance of excitation/inhibition could induce low complexity states. In fact, when we studied the role of inhibition in complexity using a computational model, we observed how inhibition could induce changes at the integration/segregation balance in cortical networks. Furthermore, it has been demonstrated that some types of anesthetic induce their effect over the GABAergic system (Brown et al., 2011; Ma et al., 2002; Nelson et al., 2002; Rudolph and Antkowiak, 2004; Voss et al., 2019). Thus, suitable therapeutic targets for patients with disorders of consciousness such as $GABA_A$ and $GABA_B$ receptors might improve the behavioral responsiveness in vegetative patients. (Brown et al., 2010; Clauss, 2010; Salgado et al., 2011) by removing the bistability and restoring the balance between segregation and integration in the cortex.

3. Orchestrated interventions of excitatory and inhibitory is required to maintain cortical rhythms and complexity at physiological levels

After observing that inhibition was relevant to maintain cortical rhythms and complexity, we investigated some aspects of the excitatory component. To do this, we first decided to modulate the excitability through the modulation of extracellular K^+ concentration or inactivation of K^+ channels. K^+ channels are the most diverse of ion channels, their expression is homogeneous among cortical inhibitory and excitatory neurons and they mostly underlie functions of neuronal excitability control (Greene and Hoshi, 2017; Sancristóbal et al., 2016).

Increasing $[K^+]_{ec}$ (**Figure 25**) increases the neural firing and the frequency of oscillation and decreases the regularity and periodicity of the oscillations. In addition, the mean power of high frequencies increased too. However, it did not reveal changes neither at the level of relative firing rate of the Up-states, nor in the power of the low frequency bands (0.1-1 Hz). Unlike blocking inhibition, increasing excitability by increasing the $[K^+]_{ec}$, the responses were heterogeneous and irregular, resulting into high complexity values (**Figure 26**).

By blocking K^+ channels (non-selective K^+ channels (**Figure 27**), non-selective K_v channels (**Figure 29**) or K_{v7} channels (**Figure 31**)), cortical bistability was removed, decreasing the periodicity of the oscillations and increasing the neural firing. Under these conditions, cortical complexity was decreased after blocking K^+ channels (**Figure 28**, **Figure 30** and **Figure 31**). Interestingly, K_{v7} channels induced an inversion in the distribution of neural firing, where periods of neural firing were longer than periods of silence. It has already been proposed that the persistence of the Up-state depends on the activation of a specific potassium channel, K_{v7} (Neske, 2016). K_{v7} is a voltage-dependent potassium channel blocked by M1-type muscarinic receptors (Hu et al., 2007) implicated

in controlling of brain the excitability (Greene and Hoshi, 2017). Here we confirmed that the persistence of cortical Up-states was longer by blocking this channel. This was also reflected in the evoked responses, which were irregular but mostly stereotypical at the spatial distribution, so we would expect a decrease in cortical complexity. However, sPCI could not detect any changes to the level of complexity because of (1) technical difficulties, since several responses to electrical stimulation coincide during periods of neural firing and (2) the high synchronized rhythms caused by blocking M-current, complicate the network recruitment to evoke a response (**Figure 32**). Other measures of complexity should be used to assess how complexity varies after blocking K_{v7} channels.

In summary, K^+ channels are involved in the control of excitability and modulate the complexity in cortical networks. Distinct from blocking inhibition, here we observed that the modulation of excitability could induce changes in complexity. This suggests that certain levels of excitability are required to induce higher complexity states. However, if this balance were to be disproportionally altered (as occurred by blocking inhibition or K^+ channels) segregation and integration balance would be altered and cortical complexity would decay.

Given that the control of excitability plays a role in the modulation of cortical rhythms and complexity, we decided to observe the contribution of cortical excitatory neurons. Thus, we decided to use DCS (**Figure 11**), which mostly affects the excitatory components of cortical networks. Without leaving bistable activity, DCS (**Figure 33**) proportionally increased neural firing, the frequency of oscillations and the power of all frequency bands; and proportionally decreased the relative firing rate during Up-states and the regularity and periodicity of the oscillations. Even under the modulation of cortical excitability by DCS, the spatiotemporal distribution of responses to electrical stimulation were as homogeneous (**Figure 34**) as SWA conditions, without significant differences in cortical complexity within the explored range (Barbero-Castillo et al., 2019).

All of these results suggest that the inhibitory component alone or inhibitory and excitatory components together are required for the maintenance of cortical rhythms and neural complexity at physiological levels for different reasons. On the one hand, the modulation of excitatory neuron excitability by DCS did not demonstrate changes in network complexity measured by sPCI (Barbero-Castillo et al., 2019); although by measuring the complexity of propagation patterns (Barbero-Castillo et al., 2019), we were able to detect that complexity directly correlated with DCS intensity. We explain this by the fact that the network never left the bistable regime, preventing any detectable variation in the complexity of the response triggered by the perturbation (Barbero-Castillo et al., 2019; Pigorini et al., 2015). However, when we induced changes in excitability through activation/inactivation of K^+ channels (which affects both interneurons and excitatory neurons) (Greene and Hoshi, 2017), the network shifted from the bistable response to a homogeneous stereotypical epileptic response (decreasing network complexity state) or a more heterogeneous responses (increasing network complexity state). Therefore higher/lower complexity states are not the consequence of merely increasing/decreasing excitability, the excitatory and inhibitory neuronal interactions constitute a fundamental feature of switching between cortical rhythms and complexity.

As we mentioned previously, one of our limitations was that slight changes within the bistable regime might be difficult to detect with sPCI methods. sPCI is a method for quantifying the level of complexity but is limited by (1) the low number of recording channels to detect spontaneous and evoked activity; and (2) the fact that *in vitro* cortical slices constitute a small piece of the whole cortical network, where changes in the level of segregation and integration can be difficult to detect suing the sPCI method. In that sense, other methods for estimating complexity such as the estimation of the entropy of wave propagation patterns may be more sensitive, as we found in the case of DC fields stimulation.

4. Cholinergic neurotransmission results in higher complexity states

The final objective of this PhD work was to identify some of the cellular mechanisms underlying the modulation of cortical states by regulating the levels of different neurotransmitters involved in brain state transitions. This transition depends on the activation/inactivation of different receptors and ion channels expressed in their membranes which can affect various cellular functions. Neurotransmitters such as ACh, are released in the neocortex to activate these channels and receptors, and shift cortical activity from one state to another (Lee and Dan, 2012). During wakefulness states, this neuromodulatory system is highly activated while during sleep their activity is reduced or stopped (Jones, 2005; Lin, 2000). Muscarinic acetylcholine receptors (mAChR) are implicated in the modulation of SWA and the transition from SWA to wakefulness (McCormick and Williamson, 1989; Poulet and Crochet, 2019). In summary, we considered that mAChR activation could participate in the modulation of cortical rhythms and complexity in cortical networks. Most of the following results have been already published in (Barbero-Castillo et al., 2020).

First, we bath-applied a range of different concentrations of IPX (**Figure 35**) resulting in a global change in the network's rhythms to a hyperexcitable activity (**Figure 35A,B**). The oscillatory frequency increased and bath application of the highest concentrations of IPX (100-200 nM) resulted in seizure-like discharges, which were characterized by low (<1 Hz), delta (1-4 Hz) and alpha (7-12 Hz) frequencies. In addition, the relative firing rate during Up-states decreased, as did the estimated neural firing rate but without significant differences compared with control conditions.

In summary, given that IPX demonstrated an effect of cortical activity *in vitro*, IPX was a good design strategy to develop specific photoswitchable molecules for cortical mAChR. Indeed, activation of mAChR were involved in increasing the excitability of cortical networks, suggesting that high activation of mAChR underlies seizure activity.

This correlates with previous studies, which demonstrated that alterations of cholinergic system could increment the excitability leading to seizures and status epilepticus (Curia et al., 2008; Zimmerman et al., 2008). Indeed, it has been demonstrated that injections of the muscarinic agonist pilocarpine has been used to mimic this altered patterns of cortical activity (Curia et al., 2008; Zimmerman et al., 2008). It has also been observed that the cholinergic system participates in the control of generalized non-convulsive absence seizures that occur mainly during quiet wakefulness and transitions between wakefulness and slow-wave sleep (Danober et al., 1993). IPX derivative molecules could be a good design strategy to develop specific photoswitchable molecules that can act as cortical mAChR antagonists and for use it as a treatment against these hyperexcitable states.

After observing that cortical activity can be modulated by IPX derivate molecules, we decided to observed muscarinic neuromodulation using PAI, a photoswitchable IPX derivative that allows the reversible activation of M2 mAChRs with light (Riefolo et al., 2019). M2 mAChR plays relevant roles in several CNS disorders (Scarr, 2012), and regulating their activity and subsequent effects on cortical neuronal networks may provide new therapeutic opportunities for these cholinergic diseases. We first built up the dose-response curves of the two drug forms separately, *trans*- (dark-adapted state) and *cis*-PAI (after UV irradiation), in order to find out the differences in cortical activity between the PAI-isoforms, and to identify the most convenient concentration range to manipulate cortical rhythms with light. We demonstrated that PAI can be useful to modulate cortical rhythms by M2 mAChR activation. Once the different oscillatory activity evoked by *cis*- and *trans*-PAI was quantified *in vitro*, we moved on to control cortical rhythms with light (**Figure 37**). 200 nM *cis*-PAI evoked an increase in the oscillatory frequency and estimated neural firing, and no significant effects in the relative firing rate of the Up-states were seen. Subsequent illumination of the slices with white light produced a robust increase in the oscillatory frequency and significant decrease in relative firing rate of the Up-states and the estimated neural firing. In addition, activation of M2 receptors with *trans*-PAI demonstrated higher values at higher frequency bands.

This increment in the cortical level of neural firing was also reflected in the complexity. Activation of M2 receptor reflected heterogeneous spatiotemporal responses, leading to high complexity states (**Figure 38**).

Having established the ability of PAI to alter cortical oscillatory activity with light in slices, we then aimed to photocontrol cortical activity *in vivo* (**Figure 39**). As the dose-response curves of *cis*- and *trans*-PAI could be different from the *in vitro* conditions, we tested two different concentrations, 200 nM and 1 μM. By using two concentrations of the drug, we observed that the effect on the oscillatory frequency was already reached with 200 μM, while the tendency of the firing rate towards a decrease was more evident under 1 μM.

In summary, we demonstrated that (1) IPX was a good design strategy to develop specific photoswitchable molecules for cortical mAChR; (2) non-specific activation of mAChR were involved in increasing the excitability of cortical networks; (3) high activation of mAChR may underlie seizure activity; (4) PAI can be used as tool to modulate cortical activity *in vitro* and *in vivo;* (5) and activation of M2 mAChR induced high excitable and complex states. It is probably that activation of these receptors is involved in the induction of awake states in cortex. As we mentioned previously, during wakefulness states, this neuromodulatory system is highly activated while during sleep their activity is reduced or stopped (Jones, 2005; Lin, 2000). It has been described that the presence of ACh is required to induce arousal states, which increases their concentration in sensory cortices and modulates cortical activity. This modulation is specific for different types of cells and subcellular mechanisms. For example, it has been described that ACh enhanced thalamocortical synapsis over pyramidal cortical neurons while suppressing local inhibitory synapses during arousal states (Bennett et al., 2013; Reimer et al., 2016; M Steriade et al., 1993a). Indeed, it has been reported that the effect of anesthetic might be due to their effect over mAChR (Durieux, 1995; Lydic and Baghdoyan, 2005; Nagase et al., 1999; Van Dort et al., 2008). In summary, it would be

interesting to further investigate the effect of activation/inactivation of M2 mAChR in cortical activity *in vivo* or in human patients with some psychiatric disorders related with M2 mAChR. In addition, further investigations about other neuromodulatory mechanisms such as noradrenaline, serotonin and histamine, are required because they might underlie the of modulation cortical states and brain state transitions, and therefore cortical complexity.

Chapter 5

Conclusions

1. Isolated cortical slices can be used as a model for studying of cortical rhythms and complexity.

2. Synaptic inhibition is required to maintain the cortical slow oscillatory regime by regulating firing rates and by sculpting network rhythms.

3. Orchestrated intervention of inhibitory and excitatory components is required for the maintenance of physiological cortical rhythms and network complexity.

4. sPCI reliably distinguishes between different network states. However, slight changes within bistable regime might not be detectable using this method.

5. Inhibition is also required to regulate the excitatory/inhibitory balance necessary to generate cortical complexity. Alteration in this balance, results in a prominent bistable activity that breaks the causal interactions of cortical networks, resulting in a decrease in complexity.

6. Gradual $GABA_A$-Rs blockade resulted into higher synchronization and progressively reduced sPCI. Blocking $GABA_B$-Rs also resulted in a reduced sPCI while in synchronous conditions.

7. A certain level of excitability is required to induce higher complexity states. However, if there is a lack of inhibition or excess of excitation, the complexity balance is disproportionally altered, and the cortical complexity decays.

8. DCS proportionally modulates the neural firing and controls the frequency of the cortical oscillation, while sPCI is not affected within the investigated limits.

9. M-current is implicated in Up-state termination, underlying one of the mechanisms for the transition to higher complexity states.

10. Photopharmacology agents, such as PAI, can be used to selectively modulate SWA in cortical slices *in vitro* and *in vivo*.

11. IPX is a powerful modulator of cortical activity and a good design strategy to develop specific photoswitchable molecules for cortical mAChR.

12. mAChR are involved in increasing the excitability of cortical networks of mAChR and great non-specific activation of mAChR may underlie the seizure activity.

13. The photo-activation of M2 receptors induces a sudden transition from SWA to a higher oscillatory frequency both *in vitro* and *in vivo*.

14. Activation of M2-mACh receptors induced high excitable and complex states. It is probable that activation of this receptor is involved in the induction of awake states in the cortex.

Bibliography

Achard, S., Delon-Martin, C., Vértes, P.E., Renard, F., Schenck, M., Schneider, F., Heinrich, C., Kremer, S., Bullmore, E.T., 2012. Hubs of brain functional networks are radically reorganized in comatose patients. Proc. Natl. Acad. Sci. U. S. A. 109 (50), 20608–20613. https://doi.org/10.1073/pnas.1208933109

Aghajanian, G.K., Rasmussen, K., 1989. Intracellular studies in the facial nucleus illustrating a simple new method for obtaining viable motoneurons in adult rat brain slices. Synapse 3, 331–338. https://doi.org/10.1002/syn.890030406

Åkerstedt, T., Billiard, M., Bonnet, M., Ficca, G., Garma, L., Mariotti, M., Salzarulo, P., Schulz, H., 2002. Awakening from sleep. Sleep Med. Rev. 6, 267–286. https://doi.org/10.1053/smrv.2001.0202

Alkire, M.T., Hudetz, A.G., Tononi, G., 2008. Consciousness and anesthesia. Science 322, 876–80. https://doi.org/10.1126/science.1149213

Andalman, A.S., Burns, V.M., Lovett-Barron, M., Broxton, M., Poole, B., Yang, S.J., Grosenick, L., Lerner, T.N., Chen, R., Benster, T., Mourrain, P., Levoy, M., Rajan, K., Deisseroth, K., 2019. Neuronal Dynamics Regulating Brain and Behavioral State Transitions. Cell 177, 970-985.e20. https://doi.org/10.1016/j.cell.2019.02.037

Arroyo, S., Bennett, C., Hestrin, S., 2014. Nicotinic modulation of cortical circuits. Front. Neural Circuits 8, 30. https://doi.org/10.3389/fncir.2014.00030

Ashford, M.L., Sturgess, N.C., Trout, N.J., Gardner, N.J., Hales, C.N., 1988. Adenosine-5'-triphosphate-sensitive ion channels in neonatal rat cultured central neurones. Pflugers Arch. 412, 297–304. https://doi.org/10.1007/bf00582512

Bai, Y., Xia, X., Kang, J., Yang, Y., He, J., Li, X., 2017a. TDCS modulates cortical

excitability in patients with disorders of consciousness. NeuroImage Clin. 15, 702–709. https://doi.org/10.1016/j.nicl.2017.01.025

Bai, Y., Xia, X., Li, X., 2017b. A Review of Resting-State Electroencephalography Analysis in Disorders of Consciousness. Front. Neurol. 8, 471. https://doi.org/10.3389/fneur.2017.00471

Bai, Y., Xia, X., Wang, Y., Guo, Y., Yang, Y., He, J., Li, X., 2018. Fronto-parietal coherence response to tDCS modulation in patients with disorders of consciousness. Int. J. Neurosci. 128, 587–594. https://doi.org/10.1080/00207454.2017.1403440

Barbero-Castillo, A., Riefolo, F., Matera, C., Caldas-Martínez, S., Mateos-Aparicio, P., Weinert, J.F., Claro, E., Sánchez-Vives, M.V., Gorostiza, P., 2020. Control of brain state transitions with light. bioRxiv 793927. https://doi.org/10.1101/793927

Barbero-Castillo, A., Weinert, J.F., Camassa, A., Perez-Mendez, L., Caldas-Martinez, S., Mattia, M., Sanchez-Vives, M. V., 2019. Proceedings #31: Cortical Network Complexity under Different Levels of Excitability Controlled by Electric Fields. Brain Stimul. 12, e97–e99. https://doi.org/10.1016/j.brs.2018.12.200

Barocelli, E., Ballabeni, V., Bertoni, S., Dallanoce, C., De Amici, M., De Micheli, C., Impicciatore, M., 2000. New analogues of oxotremorine and oxotremorine-M: estimation of their in vitro affinity and efficacy at muscarinic receptor subtypes. Life Sci. 67, 717–23. https://doi.org/10.1016/s0024-3205(00)00661-5

Bartels, A., Zeki, S., 2005. Brain dynamics during natural viewing conditions—A new guide for mapping connectivity in vivo. Neuroimage 24, 339–349. https://doi.org/10.1016/j.neuroimage.2004.08.044

Bartos, M., Vida, I., Jonas, P., 2007. Synaptic mechanisms of synchronized gamma oscillations in inhibitory interneuron networks. Nat. Rev. Neurosci. 8, 45–56. https://doi.org/10.1038/nrn2044

Bayne, T., Hohwy, J., Owen, A.M., 2016. Are There Levels of Consciousness? Trends Cogn. Sci. 20, 405–413. https://doi.org/10.1016/j.tics.2016.03.009

Beltramo, R., D'Urso, G., Dal Maschio, M., Farisello, P., Bovetti, S., Clovis, Y., Lassi, G., Tucci, V., De Pietri Tonelli, D., Fellin, T., 2013. Layer-specific excitatory circuits differentially control recurrent network dynamics in the neocortex. Nat. Neurosci. 16, 227–234. https://doi.org/10.1038/nn.3306

Benjamini, Y., Hochberg, Y., 1995. Controlling the False Discovery Rate: A Practical and Powerful Approach to Multiple Testing. J. R. Stat. Soc. Ser. B. https://doi.org/10.2307/2346101

Bennett, C., Arroyo, S., Hestrin, S., 2013. Subthreshold Mechanisms Underlying State-Dependent Modulation of Visual Responses. Neuron 80, 350–357. https://doi.org/10.1016/J.NEURON.2013.08.007

Bereshpolova, Y., Stoelzel, C.R., Zhuang, J., Amitai, Y., Alonso, J.-M., Swadlow, H.A., 2011. Getting drowsy? Alert/nonalert transitions and visual thalamocortical network dynamics. J. Neurosci. 31, 17480–7. https://doi.org/10.1523/JNEUROSCI.2262-11.2011

Bettinardi, R.G., Tort-Colet, N., Ruiz-Mejias, M., Sanchez-Vives, M. V, Deco, G., 2015. Gradual emergence of spontaneous correlated brain activity during fading of general anesthesia in rats: Evidences from fMRI and local field potentials. Neuroimage 114, 185–198. https://doi.org/10.1016/j.neuroimage.2015.03.037

Blumenfeld, H., 2010. Neuroanatomy through Clinical Cases 2th Edition.

Bodien, Y.G., Chatelle, C., Edlow, B.L., 2017. Functional Networks in Disorders of Consciousness. Semin. Neurol. 37, 485–502. https://doi.org/10.1055/s-0037-1607310

Boly, M., Jones, B., Findlay, G., Plumley, E., Mensen, A., Hermann, B., Tononi, G., Maganti, R., 2017. Altered sleep homeostasis correlates with cognitive impairment in patients with focal epilepsy. Brain 140, 1026–1040. https://doi.org/10.1093/brain/awx017

Broichhagen, J., Frank, J.A., Trauner, D., 2015. A Roadmap to Success in Photopharmacology. Acc. Chem. Res. 48, 1947–1960. https://doi.org/10.1021/acs.accounts.5b00129

Brown, D.A., 2010. Muscarinic acetylcholine receptors (mAChRs) in the nervous system: some functions and mechanisms. J. Mol. Neurosci. 41, 340–6. https://doi.org/10.1007/s12031-010-9377-2

Brown, E.N., Purdon, P.L., Van Dort, C.J., 2011. General Anesthesia and Altered States of Arousal: A Systems Neuroscience Analysis. Annu. Rev. Neurosci. 34, 601–628. https://doi.org/10.1146/annurev-neuro-060909-153200

Brown, H.D., Baker, P.M., Ragozzino, M.E., 2010. The parafascicular thalamic nucleus concomitantly influences behavioral flexibility and dorsomedial striatal acetylcholine output in rats. J. Neurosci. 30, 14390–14398. https://doi.org/10.1523/JNEUROSCI.2167-10.2010

Brown, R.E., Basheer, R., McKenna, J.T., Strecker, R.E., McCarley, R.W., 2012. Control of Sleep and Wakefulness. Physiol. Rev. 92, 1087–1187. https://doi.org/10.1152/physrev.00032.2011

Buzsáki, G., Draguhn, A., 2004. Neuronal oscillations in cortical networks. Science 304, 1926–1929. https://doi.org/10.1126/science.1099745

Buzsáki, G., Geisler, C., Henze, D.A., Wang, X.-J., 2004. Interneuron Diversity series: Circuit complexity and axon wiring economy of cortical interneurons. Trends Neurosci. 27, 186–193. https://doi.org/10.1016/j.tins.2004.02.007

Cardin, J.A., 2018. Inhibitory Interneurons Regulate Temporal Precision and Correlations in Cortical Circuits. Trends Neurosci. 41, 689–700. https://doi.org/10.1016/j.tins.2018.07.015

Casali, A.G., Gosseries, O., Rosanova, M., Boly, M., Sarasso, S., Casali, K.R., Casarotto, S.,

Bruno, M.-A., Laureys, S., Tononi, G., Massimini, M., 2013. A Theoretically Based Index of Consciousness Independent of Sensory Processing and Behavior. Sci. Transl. Med. 5, 198ra105-198ra105. https://doi.org/10.1126/scitranslmed.3006294

Casarotto, S., Comanducci, A., Rosanova, M., Sarasso, S., Fecchio, M., Napolitani, M., Pigorini, A., G. Casali, A., Trimarchi, P.D., Boly, M., Gosseries, O., Bodart, O., Curto, F., Landi, C., Mariotti, M., Devalle, G., Laureys, S., Tononi, G., Massimini, M., 2016. Stratification of unresponsive patients by an independently validated index of brain complexity. Ann. Neurol. 80, 718–729. https://doi.org/10.1002/ana.24779

Castano-Prat, P., Perez-Zabalza, M., Perez-Mendez, L., Escorihuela, R.M., Sanchez-Vives, M. V., 2017. Slow and Fast Neocortical Oscillations in the Senescence-Accelerated Mouse Model SAMP8. Front. Aging Neurosci. 9, 141. https://doi.org/10.3389/fnagi.2017.00141

Chabolla, D.R., 2002. Characteristics of the Epilepsies. Mayo Clin. Proc. 77, 981–990. https://doi.org/10.4065/77.9.981

Chen, Y., Anand, S., Martinez-Conde, S., Macknik, S.L., Bereshpolova, Y., Swadlow, H.A., Alonso, J.M., 2009. The linearity and selectivity of neuronal responses in awake visual cortex. J. Vis. 9, 12–12. https://doi.org/10.1167/9.9.12

Chennu, S., Annen, J., Wannez, S., Thibaut, A., Chatelle, C., Cassol, H., Martens, G., Schnakers, C., Gosseries, O., Menon, D., Laureys, S., 2017. Brain networks predict metabolism, diagnosis and prognosis at the bedside in disorders of consciousness. Brain 140, 2120–2132. https://doi.org/10.1093/brain/awx163

Chennu, S., Finoia, P., Kamau, E., Allanson, J., Williams, G.B., Monti, M.M., Noreika, V., Arnatkeviciute, A., Canales-Johnson, A., Olivares, F., Cabezas-Soto, D., Menon, D.K., Pickard, J.D., Owen, A.M., Bekinschtein, T.A., 2014. Spectral Signatures of Reorganised Brain Networks in Disorders of Consciousness. PLoS Comput. Biol. 10, e1003887. https://doi.org/10.1371/journal.pcbi.1003887

Clauss, R.P., 2010. Neurotransmitters in Coma, Vegetative and Minimally Conscious

States, pharmacological interventions. Med. Hypotheses 75, 287–290. https://doi.org/10.1016/j.mehy.2010.03.005

Cobos, I., Calcagnotto, M.E., Vilaythong, A.J., Thwin, M.T., Noebels, J.L., Baraban, S.C., Rubenstein, J.L.R., 2005. Mice lacking Dlx1 show subtype-specific loss of interneurons, reduced inhibition and epilepsy. Nat. Neurosci. 8, 1059–1068. https://doi.org/10.1038/nn1499

Compte, A., 2003. Cellular and Network Mechanisms of Slow Oscillatory Activity (<1 Hz) and Wave Propagations in a Cortical Network Model. J. Neurophysiol. 89, 2707–2725. https://doi.org/10.1152/jn.00845.2002

Compte, A., Reig, R., Descalzo, V.F., Harvey, M.A., Puccini, G.D., Sanchez-Vives, M. V., 2008. Spontaneous High-Frequency (10-80 Hz) Oscillations during Up States in the Cerebral Cortex In Vitro. J. Neurosci. 28, 13828–13844. https://doi.org/10.1523/JNEUROSCI.2684-08.2008

Compte, A., Reig, R., Sanchez-Vives, M. V., 2009. Timing Excitation and Inhibition in the Cortical Network, in: Coherent Behavior in Neuronal Networks. Springer New York, New York, NY, pp. 17–46. https://doi.org/10.1007/978-1-4419-0389-1_2

Compte, A., Sanchez-Vives, M. V., McCormick, D.A., Wang, X.-J., 2003. Cellular and Network Mechanisms of Slow Oscillatory Activity (<1 Hz) and Wave Propagations in a Cortical Network Model. J. Neurophysiol. 89, 2707–2725. https://doi.org/10.1152/jn.00845.2002

Constantinople, C.M., Bruno, R.M., 2013. Deep Cortical Layers Are Activated Directly by Thalamus. Science (80-.). 340, 1591–1594. https://doi.org/10.1126/science.1236425

Constantinople, C.M., Bruno, R.M., 2011. Effects and Mechanisms of Wakefulness on Local Cortical Networks. Neuron 69, 1061–1068. https://doi.org/10.1016/J.NEURON.2011.02.040

Constantinople, C.M., Bruno, R.M., Kock, C.P. de, Kuner, T., Sakmann, B., Carandini, M., Lu, J., Lecea, L. de, 2011. Effects and mechanisms of wakefulness on local cortical networks. Neuron 69, 1061–8. https://doi.org/10.1016/j.neuron.2011.02.040

Contreras, D., Steriade, M., 1996. Synchronization of low-frequency rhythms in corticothalamic networks. Neuroscience 76, 11–24. https://doi.org/10.1016/S0306-4522(96)00393-4

Csicsvari, J., Jamieson, B., Wise, K.D., Buzsáki, G., 2003. Mechanisms of Gamma Oscillations in the Hippocampus of the Behaving Rat. Neuron 37, 311–322. https://doi.org/10.1016/S0896-6273(02)01169-8

Cunningham, M.O., Pervouchine, D.D., Racca, C., Kopell, N.J., Davies, C.H., Jones, R.S.G., Traub, R.D., Whittington, M.A., 2006. Neuronal metabolism governs cortical network response state. Proc. Natl. Acad. Sci. U. S. A. 103, 5597–601. https://doi.org/10.1073/pnas.0600604103

Curia, G., Longo, D., Biagini, G., Jones, R.S.G., Avoli, M., 2008. The pilocarpine model of temporal lobe epilepsy. J. Neurosci. Methods 172, 143–57. https://doi.org/10.1016/j.jneumeth.2008.04.019

D'Andola, M., Rebollo, B., Casali, A.G., Weinert, J.F., Pigorini, A., Villa, R., Massimini, M., Sanchez-Vives, M. V., 2017. Bistability, Causality, and Complexity in Cortical Networks: An In Vitro Perturbational Study. Cereb. Cortex 91, 1–10. https://doi.org/10.1093/cercor/bhx122

D'Andola, M., Weinert, J.F., Mattia, M., Sanchez-Vives, M. V., 2018. Modulation of slow and fast oscillations by direct current stimulation in the cerebral cortex in vitro. bioRxiv 246819. https://doi.org/10.1101/246819

Danober, L., Depaulis, A., Marescaux, C., Vergnes, M., 1993. Effects of cholinergic drugs on genetic absence seizures in rats. Eur. J. Pharmacol. 234, 263–268. https://doi.org/10.1016/0014-2999(93)90962-H

Dasgupta, R., Seibt, F., Beierlein, M., 2018. Synaptic Release of Acetylcholine Rapidly Suppresses Cortical Activity by Recruiting Muscarinic Receptors in Layer 4. J. Neurosci. 38, 5338–5350. https://doi.org/10.1523/JNEUROSCI.0566-18.2018

Dasilva, M., Perez-mendez, L., Pazienti, A., Navarro-Guzman, A., Camassa, A., Zamora-López, G., Mattia, M., Sanchez-Vives, M. V. Modulation of cortical slow oscillations and complexity across anesthesia levels. Neuroimage (under review).

Deco, G., Tononi, G., Boly, M., Kringelbach, M.L., 2015. Rethinking segregation and integration: Contributions of whole-brain modelling. Nat. Rev. Neurosci. 16, 430–439. https://doi.org/10.1038/nrn3963

Deisseroth, K., 2011. Optogenetics. Nat. Methods 8, 26–29. https://doi.org/10.1038/nmeth.f.324

Destexhe, A., Hughes, S.W., Rudolph, M., Crunelli, V., 2007. Are corticothalamic "up" states fragments of wakefulness? Trends Neurosci. 30, 334–342. https://doi.org/10.1016/j.tins.2007.04.006

Devinsky, O., Vezzani, A., O'Brien, T.J., Jette, N., Scheffer, I.E., de Curtis, M., Perucca, P., 2018. Epilepsy. Nat. Rev. Dis. Prim. 4, 18024. https://doi.org/10.1038/nrdp.2018.24

Ding, F., O'Donnell, J., Xu, Q., Kang, N., Goldman, N., Nedergaard, M., 2016. Changes in the composition of brain interstitial ions control the sleep-wake cycle. Science (80-.). 352, 550–555. https://doi.org/10.1126/science.aad4821

Douglas, R.J., Martin, K.A.C., 2004. Neuronal circuits of the neocortex. Annu. Rev. Neurosci. 27, 419–451. https://doi.org/10.1146/annurev.neuro.27.070203.144152

Duarte, R., Seeholzer, A., Zilles, K., Morrison, A., 2017. Synaptic patterning and the timescales of cortical dynamics. Curr. Opin. Neurobiol. 43, 156–165. https://doi.org/10.1016/J.CONB.2017.02.007

Dugladze, T., Maziashvili, N., Börgers, C., Gurgenidze, S., Häussler, U., Winkelmann, A.,

Haas, C.A., Meier, J.C., Vida, I., Kopell, N.J., Gloveli, T., 2013. GABA(B) autoreceptor-mediated cell type-specific reduction of inhibition in epileptic mice. Proc. Natl. Acad. Sci. U. S. A. 110, 15073–8. https://doi.org/10.1073/pnas.1313505110

Durieux, M.E., 1995. Inhibition by Ketamine of Muscarinic Acetylcholine Receptor Function. Anesth. Analg. 81, 57–62. https://doi.org/10.1097/00000539-199507000-00012

Eggermann, T., Heilsberg, A.-K., Bens, S., Siebert, R., Beygo, J., Buiting, K., Begemann, M., Soellner, L., 2014. Additional molecular findings in 11p15-associated imprinting disorders: an urgent need for multi-locus testing. J. Mol. Med. 92, 769–777. https://doi.org/10.1007/s00109-014-1141-6

Englot, D.J., Yang, L., Hamid, H., Danielson, N., Bai, X., Marfeo, A., Yu, L., Gordon, A., Purcaro, M.J., Motelow, J.E., Agarwal, R., Ellens, D.J., Golomb, J.D., Shamy, M.C.F., Zhang, H., Carlson, C., Doyle, W., Devinsky, O., Vives, K., Spencer, D.D., Spencer, S.S., Schevon, C., Zaveri, H.P., Blumenfeld, H., 2010. Impaired consciousness in temporal lobe seizures: role of cortical slow activity. Brain 133, 3764–3777. https://doi.org/10.1093/brain/awq316

Fattinger, S., Schmitt, B., Bölsterli Heinzle, B.K., Critelli, H., Jenni, O.G., Huber, R., 2015. Impaired slow wave sleep downscaling in patients with infantile spasms. Eur. J. Paediatr. Neurol. 19, 134–42. https://doi.org/10.1016/j.ejpn.2014.11.002

Fernandez, L.M.J., Comte, J.-C., Le Merre, P., Lin, J.-S., Salin, P.-A., Crochet, S., 2016. Highly Dynamic Spatiotemporal Organization of Low-Frequency Activities During Behavioral States in the Mouse Cerebral Cortex. Cereb. Cortex 1–19. https://doi.org/10.1093/cercor/bhw311

Fogerson, P.M., Huguenard, J.R., 2016. Tapping the Brakes: Cellular and Synaptic Mechanisms that Regulate Thalamic Oscillations. Neuron 92, 687–704. https://doi.org/10.1016/J.NEURON.2016.10.024

Franklin, K.B.J., Paxinos, G., 2008. The mouse brain in stereotaxic coordinates. Boston.

Freund, H.-J., Kuhn, J., Lenartz, D., Mai, J.K., Schnell, T., Klosterkoetter, J., Sturm, V., 2009. Cognitive functions in a patient with Parkinson-dementia syndrome undergoing deep brain stimulation. Arch. Neurol. 66, 781–5. https://doi.org/10.1001/archneurol.2009.102

Fröhlich, F., Bazhenov, M., Iragui-Madoz, V., Sejnowski, T.J., 2008. Potassium dynamics in the epileptic cortex: new insights on an old topic. Neuroscientist 14, 422–33. https://doi.org/10.1177/1073858408317955

Fröhlich, F., McCormick, D.A., 2010. Endogenous electric fields may guide neocortical network activity. Neuron 67, 129–43. https://doi.org/10.1016/j.neuron.2010.06.005

Fu, B., Wen, S., Wang, B., Wang, K., Zhang, J., Liu, S., 2018. Acute and chronic pain affects local field potential of the medial prefrontal cortex in different band neural oscillations. Mol. Pain 14, 174480691878568. https://doi.org/10.1177/1744806918785686

Gent, T.C., Bassetti, C. LA, Adamantidis, A.R., 2018. Sleep-wake control and the thalamus. Curr. Opin. Neurobiol. 52, 188–197. https://doi.org/10.1016/j.conb.2018.08.002

Gentet, L.J., Avermann, M., Matyas, F., Staiger, J.F., Petersen, C.C.H., 2010. Membrane Potential Dynamics of GABAergic Neurons in the Barrel Cortex of Behaving Mice. Neuron 65, 422–435. https://doi.org/10.1016/J.NEURON.2010.01.006

Gervasoni, D., Lin, S.-C., Ribeiro, S., Soares, E.S., Pantoja, J., Nicolelis, M.A.L., 2004. Global Forebrain Dynamics Predict Rat Behavioral States and Their Transitions. J. Neurosci. 24, 11137–11147. https://doi.org/10.1523/JNEUROSCI.3524-04.2004

Gili, T., Saxena, N., Diukova, A., Murphy, K., Hall, J.E., Wise, R.G., 2013. The Thalamus and Brainstem Act As Key Hubs in Alterations of Human Brain Network Connectivity Induced by Mild Propofol Sedation. J. Neurosci. 33, 4024–4031. https://doi.org/10.1523/JNEUROSCI.3480-12.2013

Goldman, J.S., Tort-Colet, N., di Volo, M., Susin, E., Bouté, J., Dali, M., Carlu, M., Nghiem, T.-A., Górski, T., Destexhe, A., 2019. Bridging Single Neuron Dynamics to Global Brain States. Front. Syst. Neurosci. 13, 75. https://doi.org/10.3389/fnsys.2019.00075

Greene, D.L., Hoshi, N., 2017. Modulation of Kv7 channels and excitability in the brain. Cell. Mol. Life Sci. 74, 495–508. https://doi.org/10.1007/s00018-016-2359-y

Groleau, M., Kang, J. Il, Huppé-Gourgues, F., Vaucher, E., 2015. Distribution and effects of the muscarinic receptor subtypes in the primary visual cortex. Front. Synaptic Neurosci. 7, 10. https://doi.org/10.3389/fnsyn.2015.00010

Guidotti, A., Auta, J., Davis, J.M., Dong, E., Grayson, D.R., Veldic, M., Zhang, X., Costa, E., 2005. GABAergic dysfunction in schizophrenia: new treatment strategies on the horizon. Psychopharmacology (Berl). 180, 191–205. https://doi.org/10.1007/s00213-005-2212-8

Hanrahan, S.J., Greger, B., Parker, R.A., Ogura, T., Obara, S., Egan, T.D., House, P.A., 2013. The effects of propofol]on local field potential spectra, action potential firing rate, and their temporal relationship in humans and felines. Front. Hum. Neurosci. 7, 136. https://doi.org/10.3389/fnhum.2013.00136

Herreras, O., 2016. Local Field Potentials: Myths and Misunderstandings. Front. Neural Circuits 10, 101. https://doi.org/10.3389/fncir.2016.00101

Hirata, A., Castro-Alamancos, M.A., 2010. Neocortex Network Activation and Deactivation States Controlled by the Thalamus. J. Neurophysiol. 103, 1147–1157. https://doi.org/10.1152/jn.00955.2009

Homman-Ludiye, J., Manger, P.R., Bourne, J.A., 2010. Immunohistochemical parcellation of the ferret (Mustela putorius) visual cortex reveals substantial homology with the cat (Felis catus). J. Comp. Neurol. 518 (21), 4439–4462. https://doi.org/10.1002/cne.22465

Hu, H., Vervaeke, K., Storm, J.F., 2007. M-Channels (Kv7/KCNQ Channels) That Regulate Synaptic Integration, Excitability, and Spike Pattern of CA1 Pyramidal Cells Are Located in the Perisomatic Region. J. Neurosci. 27, 1853–1867. https://doi.org/10.1523/JNEUROSCI.4463-06.2007

Isaacson, J.S., Scanziani, M., 2011. How inhibition shapes cortical activity. Neuron 72, 231–43. https://doi.org/10.1016/j.neuron.2011.09.027

Jones, B.E., 2005. From waking to sleeping: Neuronal and chemical substrates. Trends Pharmacol. Sci. 26 (11), 578–586. https://doi.org/10.1016/j.tips.2005.09.009

Jones, M.S., Barth, D.S., 2002. Effects of Bicuculline Methiodide on Fast (>200 Hz) Electrical Oscillations in Rat Somatosensory Cortex. J. Neurophysiol. 88, 1016–1025. https://doi.org/10.1152/jn.2002.88.2.1016

Kabakov, A.Y., Muller, P.A., Pascual-Leone, A., Jensen, F.E., Rotenberg, A., 2012. Contribution of axonal orientation to pathway-dependent modulation of excitatory transmission by direct current stimulation in isolated rat hippocampus. J. Neurophysiol. 107, 1881–1889. https://doi.org/10.1152/jn.00715.2011

Kalemaki, K., Konstantoudaki, X., Tivodar, S., Sidiropoulou, K., Karagogeos, D., 2018. Mice With Decreased Number of Interneurons Exhibit Aberrant Spontaneous and Oscillatory Activity in the Cortex. Front. Neural Circuits 12, 96. https://doi.org/10.3389/fncir.2018.00096

Khazipov, R., 2016. GABAergic Synchronization in Epilepsy. Cold Spring Harb. Perspect. Med. 6, a022764. https://doi.org/10.1101/cshperspect.a022764

Kim, J.P., Min, H.K., Knight, E.J., Duffy, P.S., Abulseoud, O. a., Marsh, M.P., Kelsey, K., Blaha, C.D., Bennet, K.E., Frye, M. a., Lee, K.H., 2013. Centromedian-parafascicular deep brain stimulation induces differential functional inhibition of the motor, associative, and limbic circuits in large animals. Biol. Psychiatry 74, 917–926. https://doi.org/10.1016/j.biopsych.2013.06.024

Konstantoudaki, X., Papoutsi, A., Chalkiadaki, K., Poirazi, P., Sidiropoulou, K., 2014. Modulatory effects of inhibition on persistent activity in a cortical microcircuit model. Front. Neural Circuits 8, 7. https://doi.org/10.3389/fncir.2014.00007

Kringelbach, M.L., Jenkinson, N., Owen, S.L.F., Aziz, T.Z., 2007. Translational principles of deep brain stimulation. Nat. Rev. Neurosci. 8, 623–635. https://doi.org/10.1038/nrn2196

Krishnan, G.P., González, O.C., Bazhenov, M., 2018. Origin of slow spontaneous resting-state neuronal fluctuations in brain networks. Proc. Natl. Acad. Sci. U. S. A. 115, 6858–6863. https://doi.org/10.1073/pnas.1715841115

Kullmann, D.M., Ruiz, A., Rusakov, D.M., Scott, R., Semyanov, A., Walker, M.C., 2005. Presynaptic, extrasynaptic and axonal GABAA receptors in the CNS: where and why? Prog. Biophys. Mol. Biol. 87, 33–46. https://doi.org/10.1016/j.pbiomolbio.2004.06.003

Lee, S.-H., Dan, Y., 2012. Neuromodulation of brain states. Neuron 76, 209–22. https://doi.org/10.1016/j.neuron.2012.09.012

Lee, W.-C.A., Bonin, V., Reed, M., Graham, B.J., Hood, G., Glattfelder, K., Reid, R.C., 2016. Anatomy and function of an excitatory network in the visual cortex. Nature 532, 370–374. https://doi.org/10.1038/nature17192

Lehembre, R., Marie-Aurélie, B., Vanhaudenhuyse, A., Chatelle, C., Cologan, V., Leclercq, Y., Soddu, A., Macq, B., Laureys, S., Noirhomme, Q., 2012. Resting-state EEG study of comatose patients: a connectivity and frequency analysis to find differences between vegetative and minimally conscious states. Funct. Neurol. 27, 41–7.

Lemaire, J.-J., Sontheimer, A., Nezzar, H., Pontier, B., Luauté, J., Roche, B., Gillart, T., Gabrillargues, J., Rosenberg, S., Sarret, C., Feschet, F., Vassal, F., Fontaine, D., Coste, J., 2014. Electrical modulation of neuronal networks in brain-injured patients with disorders of consciousness: a systematic review. Ann. Fr. Anesth. Reanim. 33, 88–97. https://doi.org/10.1016/j.annfar.2013.11.007

Lerch, M.M., Hansen, M.J., van Dam, G.M., Szymanski, W., Feringa, B.L., 2016. Emerging Targets in Photopharmacology. Angew. Chem. Int. Ed. Engl. 55, 10978–99. https://doi.org/10.1002/anie.201601931

Lewis, L.D., Voigts, J., Flores, F.J., Ian Schmitt, L., Wilson, M.A., Halassa, M.M., Brown, E.N., 2015. Thalamic reticular nucleus induces fast and local modulation of arousal state. Elife 4, 1–23. https://doi.org/10.7554/eLife.08760

Li, G., Henriquez, C.S., Fröhlich, F., 2017. Unified thalamic model generates multiple distinct oscillations with state-dependent entrainment by stimulation. PLOS Comput. Biol. 13, e1005797. https://doi.org/10.1371/journal.pcbi.1005797

Li, Y., Xu, J., Xu, Y., Zhao, X.-Y., Liu, Y., Wang, J., Wang, G.-M., Lv, Y.-T., Tang, Q.-Y., Zhang, Z., 2018. Regulatory Effect of General Anesthetics on Activity of Potassium Channels. Neurosci. Bull. 34, 887–900. https://doi.org/10.1007/s12264-018-0239-1

Lin, J.S., 2000. Brain structures and mechanisms involved in the control of cortical activation and wakefulness, with emphasis on the posterior hypothalamus and histaminergic neurons. Sleep Med. Rev. 4, 471–503. https://doi.org/10.1053/smrv.2000.0116

Lundstrom, B.N., Boly, M., Duckrow, R., Zaveri, H.P., Blumenfeld, H., 2019. Slowing less than 1 Hz is decreased near the seizure onset zone. Sci. Rep. 9, 6218. https://doi.org/10.1038/s41598-019-42347-y

Lydic, R., Baghdoyan, H.A., 2005. Sleep, Anesthesiology, and the Neurobiology of Arousal State Control. Anesthesiol. J. Am. Soc. Anesthesiol. 103, 1268–1295. https://doi.org/0000542-200512000-00024

Ma, J., Shen, B., Stewart, L.S., Herrick, I.A., Leung, L.S., 2002. The septohippocampal system participates in general anesthesia. J. Neurosci. 22, RC200. https://doi.org/10.1523/JNEUROSCI.22-02-J0004.2002

Malinowska, U., Chatelle, C., Bruno, M.-A., Noirhomme, Q., Laureys, S., Durka, P.J., 2013. Electroencephalographic profiles for differentiation of disorders of consciousness. Biomed. Eng. Online 12, 109. https://doi.org/10.1186/1475-925X-12-109

Mann, E.O., Kohl, M.M., Paulsen, O., 2009. Distinct roles of GABA(A) and GABA(B) receptors in balancing and terminating persistent cortical activity. J. Neurosci. 29, 7513–7518. https://doi.org/10.1523/JNEUROSCI.6162-08.2009

Mantini, D., Perrucci, M.G., Del Gratta, C., Romani, G.L., Corbetta, M., 2007. Electrophysiological signatures of resting state networks in the human brain. Proc. Natl. Acad. Sci. 104, 13170–13175. https://doi.org/10.1073/pnas.0700668104

Marín, O., 2012. Interneuron dysfunction in psychiatric disorders. Nat. Rev. Neurosci. 13, 107–120. https://doi.org/10.1038/nrn3155

Markram, H., Muller, E., Ramaswamy, S., Reimann, M.W., Abdellah, M., Sanchez, C.A., Ailamaki, A., Alonso-Nanclares, L., Antille, N., Arsever, S., Kahou, G.A.A., Berger, T.K., Bilgili, A., Buncic, N., Chalimourda, A., Chindemi, G., Courcol, J.-D., Delalondre, F., Delattre, V., Druckmann, S., Dumusc, R., Dynes, J., Eilemann, S., Gal, E., Gevaert, M.E., Ghobril, J.-P., Gidon, A., Graham, J.W., Gupta, A., Haenel, V., Hay, E., Heinis, T., Hernando, J.B., Hines, M., Kanari, L., Keller, D., Kenyon, J., Khazen, G., Kim, Y., King, J.G., Kisvarday, Z., Kumbhar, P., Lasserre, S., Le Bé, J.-V., Magalhães, B.R.C., Merchán-Pérez, A., Meystre, J., Morrice, B.R., Muller, J., Muñoz-Céspedes, A., Muralidhar, S., Muthurasa, K., Nachbaur, D., Newton, T.H., Nolte, M., Ovcharenko, A., Palacios, J., Pastor, L., Perin, R., Ranjan, R., Riachi, I., Rodríguez, J.-R., Riquelme, J.L., Rössert, C., Sfyrakis, K., Shi, Y., Shillcock, J.C., Silberberg, G., Silva, R., Tauheed, F., Telefont, M., Toledo-Rodriguez, M., Tränkler, T., Van Geit, W., Díaz, J.V., Walker, R., Wang, Y., Zaninetta, S.M., DeFelipe, J., Hill, S.L., Segev, I., Schürmann, F., 2015. Reconstruction and Simulation of Neocortical Microcircuitry. Cell 163, 456–92. https://doi.org/10.1016/j.cell.2015.09.029

Massimini, M., Boly, M., Casali, A., Rosanova, M., Tononi, G., 2009. A perturbational approach for evaluating the brain's capacity for consciousness. Prog. Brain Res. 177, 201–214. https://doi.org/10.1016/S0079-6123(09)17714-2

Massimini, M., Ferrarelli, F., Huber, R., Esser, S.K., Singh, H., Tononi, G., 2005. Breakdown of cortical effective connectivity during sleep. Science 309, 2228–32. https://doi.org/10.1126/science.1117256

Mattia, M., Ferraina, S., Del Giudice, P., 2010. Dissociated multi-unit activity and local field potentials: A theory inspired analysis of a motor decision task. Neuroimage 52, 812–823. https://doi.org/10.1016/j.neuroimage.2010.01.063

McCormick, D.A., Shu, Y., Hasenstaub, A., Sanchez-Vives, M., Badoual, M., Bal, T., 2003. Persistent Cortical Activity: Mechanisms of Generation and Effects on Neuronal Excitability. Cereb. Cortex 13, 1219–1231. https://doi.org/10.1093/cercor/bhg104

McCormick, D.A., Williamson, A., 1989. Convergence and divergence of neurotransmitter action in human cerebral cortex. Proc. Natl. Acad. Sci. U. S. A. 86, 8098–102. https://doi.org/10.1073/PNAS.86.20.8098

McKillop, L.E., Vyazovskiy, V. V, 2019. Sleep- and Wake-Like States in Small Networks In Vivo and In Vitro, in: Landolt, H.-P., Dijk, D.-J. (Eds.), Sleep-Wake Neurobiology and Pharmacology. Springer International Publishing, Cham, pp. 97–121. https://doi.org/10.1007/164_2018_174

Merica, H., Fortune, R.D., 2004. State transitions between wake and sleep, and within the ultradian cycle, with focus on the link to neuronal activity. Sleep Med. Rev. 8, 473–485. https://doi.org/10.1016/J.SMRV.2004.06.006

Mina, F., Benquet, P., Pasnicu, A., Biraben, A., Wendling, F., 2013. Modulation of epileptic activity by deep brain stimulation: a model-based study of frequency-dependent effects. Front. Comput. Neurosci. 7, 94. https://doi.org/10.3389/fncom.2013.00094

Monti, M.M., Lutkenhoff, E.S., Rubinov, M., Boveroux, P., Vanhaudenhuyse, A., Gosseries, O., Bruno, M.A., Noirhomme, Q., Boly, M., Laureys, S., 2013. Dynamic Change of Global and Local Information Processing in Propofol-Induced Loss and Recovery of Consciousness. PLoS Comput. Biol. https://doi.org/10.1371/journal.pcbi.1003271

Muñoz, W., Rudy, B., 2014. Spatiotemporal specificity in cholinergic control of neocortical function. Curr. Opin. Neurobiol. 26, 149–160. https://doi.org/10.1016/j.conb.2014.02.015

Murphy, M., Riedner, B. a, Huber, R., Massimini, M., Ferrarelli, F., Tononi, G., 2009. Source modeling sleep slow waves. Proc. Natl. Acad. Sci. 106, 1608–1613. https://doi.org/10.1073/pnas.0807933106

Nagase, Y., Kaibara, M., Uezono, Y., Izumi, F., Sumikawa, K., Taniyama, K., 1999. Propofol Inhibits Muscarinic Acetylcholine Receptor-Mediated Signal Transduction in Xenopus Oocytes Expressing the Rat M1 Receptor. Jpn. J. Pharmacol. 79, 319–325. https://doi.org/10.1254/jjp.79.319

Naka, A., Adesnik, H., 2016. Inhibitory Circuits in Cortical Layer 5. Front. Neural Circuits 10, 35. https://doi.org/10.3389/fncir.2016.00035

Nelson, L.E., Guo, T.Z., Lu, J., Saper, C.B., Franks, N.P., Maze, M., 2002. The sedative component of anesthesia is mediated by GABAA receptors in an endogenous sleep pathway. Nat. Neurosci. 5, 979–984. https://doi.org/10.1038/nn913

Neske, G.T., 2016. The Slow Oscillation in Cortical and Thalamic Networks: Mechanisms and Functions. Front. Neural Circuits 9, 1–25. https://doi.org/10.3389/fncir.2015.00088

Orbán, G., Kiss, T., Lengyel, M., Érdi, P., 2001. Hippocampal rhythm generation: Gamma-related theta-frequency resonance in CA3 interneurons. Biol. Cybern. 84, 123–132. https://doi.org/10.1007/s004220000199

Pellegrino, G., Tombini, M., Curcio, G., Campana, C., Di Pino, G., Assenza, G.,

Tomasevic, L., Di Lazzaro, V., 2017. Slow Activity in Focal Epilepsy During Sleep and Wakefulness. Clin. EEG Neurosci. 48, 200–208. https://doi.org/10.1177/1550059416652055

Perez-Zabalza, M., Reig, R., Manrique, J., Jercog, D., Winograd, M., Parga, N., Sanchez-Vives, M. V., 2020. Modulation of cortical slow oscillatory rhythm by GABA B receptors: an in vitro experimental and computational study. J. Physiol. JP279476. https://doi.org/10.1113/JP279476

Phillis, J.W., Kostopoulos, G.K., Limacher, J.J., 1975. A potent depressant action of adenine derivatives on cerebral cortical neurones. Eur. J. Pharmacol. 30, 125–129. https://doi.org/10.1016/0014-2999(75)90214-9

Pigorini, A., Sarasso, S., Proserpio, P., Szymanski, C., Arnulfo, G., Casarotto, S., Fecchio, M., Rosanova, M., Mariotti, M., Lo Russo, G., Palva, J.M., Nobili, L., Massimini, M., 2015. Bistability breaks-off deterministic responses to intracortical stimulation during non-REM sleep. Neuroimage 112, 105–113. https://doi.org/10.1016/j.neuroimage.2015.02.056

Pinto, D.J., Patrick, S.L., Huang, W.C., Connors, B.W., 2005. Initiation, Propagation, and Termination of Epileptiform Activity in Rodent Neocortex In Vitro Involve Distinct Mechanisms. J. Neurosci. 25, 8131–8140. https://doi.org/10.1523/JNEUROSCI.2278-05.2005

Poulet, J.F.A., Crochet, S., 2019. The Cortical States of Wakefulness. Front. Syst. Neurosci. 12, 64. https://doi.org/10.3389/fnsys.2018.00064

Poulet, J.F.A., Petersen, C.C.H., 2008. Internal brain state regulates membrane potential synchrony in barrel cortex of behaving mice. Nature 454, 881–885. https://doi.org/10.1038/nature07150

Princivalle, A., Regondi, M.C., Frassoni, C., Bowery, N.G., Spreafico, R., 2000. Distribution of GABA(B) receptor protein in somatosensory cortex and thalamus of adult rats and during postnatal development. Brain Res. Bull. 52, 397–405.

https://doi.org/10.1016/s0361-9230(00)00256-2

Radman, T., Ramos, R.L., Brumberg, J.C., Bikson, M., 2009. Role of cortical cell type and morphology in subthreshold and suprathreshold uniform electric field stimulation in vitro. Brain Stimul. 2 (4), 215-228.e3. https://doi.org/10.1016/j.brs.2009.03.007

Radnikow, G., Feldmeyer, D., 2018. Layer- and Cell Type-Specific Modulation of Excitatory Neuronal Activity in the Neocortex. Front. Neuroanat. 12, 1. https://doi.org/10.3389/fnana.2018.00001

Rahman, A., Reato, D., Arlotti, M., Gasca, F., Datta, A., Parra, L.C., Bikson, M., 2013. Cellular effects of acute direct current stimulation: somatic and synaptic terminal effects. J. Physiol. 591, 2563–2578. https://doi.org/10.1113/jphysiol.2012.247171

Reato, D., Rahman, A., Bikson, M., Parra, L.C., 2010. Low-Intensity Electrical Stimulation Affects Network Dynamics by Modulating Population Rate and Spike Timing. J. Neurosci. 30, 15067–15079. https://doi.org/10.1523/JNEUROSCI.2059-10.2010

Reig, R., Mattia, M., Compte, A., Belmonte, C., Sanchez-Vives, M. V, 2010. Temperature modulation of slow and fast cortical rhythms. J. Neurophysiol. 103, 1253–61. https://doi.org/10.1152/jn.00890.2009

Reimer, J., McGinley, M.J., Liu, Y., Rodenkirch, C., Wang, Q., McCormick, D.A., Tolias, A.S., 2016. Pupil fluctuations track rapid changes in adrenergic and cholinergic activity in cortex. Nat. Commun. 7, 13289. https://doi.org/10.1038/ncomms13289

Reyes-Puerta, V., Yang, J.-W., Siwek, M.E., Kilb, W., Sun, J.-J., Luhmann, H.J., 2016. Propagation of spontaneous slow-wave activity across columns and layers of the adult rat barrel cortex in vivo. Brain Struct. Funct. 221(9), 4429–4449. https://doi.org/10.1007/s00429-015-1173-x

Riefolo, F., Matera, C., Garrido-Charles, A., Gomila, A.M.J., Sortino, R., Agnetta, L., Claro, E., Masgrau, R., Holzgrabe, U., Batlle, M., Decker, M., Guasch, E., Gorostiza, P.,

2019. Optical Control of Cardiac Function with a Photoswitchable Muscarinic Agonist. J. Am. Chem. Soc. jacs.9b03505. https://doi.org/10.1021/jacs.9b03505

Rudolph, U., Antkowiak, B., 2004. Molecular and neuronal substrates for general anaesthetics. Nat. Rev. Neurosci. 5, 709–720. https://doi.org/10.1038/nrn1496

Ruiz-Mejias, M., Ciria-Suarez, L., Mattia, M., Sanchez-Vives, M. V., 2011. Slow and fast rhythms generated in the cerebral cortex of the anesthetized mouse. J. Neurophysiol. 106, 2910–2921. https://doi.org/10.1152/jn.00440.2011

Ruiz-Mejias, M., Martinez de Lagran, M., Mattia, M., Castano-Prat, P., Perez-Mendez, L., Ciria-Suarez, L., Gener, T., Sancristobal, B., García-Ojalvo, J., Gruart, A., Delgado-García, J.M., Sanchez-Vives, M. V, Dierssen, M., 2016. Overexpression of Dyrk1A, a Down Syndrome Candidate, Decreases Excitability and Impairs Gamma Oscillations in the Prefrontal Cortex. J. Neurosci. 36, 3648–59. https://doi.org/10.1523/JNEUROSCI.2517-15.2016

Salgado, H., Garcia-Oscos, F., Patel, A., Martinolich, L., Nichols, J.A., Dinh, L., Roychowdhury, S., Tseng, K.-Y., Atzori, M., 2011. Layer-specific noradrenergic modulation of inhibition in cortical layer II/III. Cereb. Cortex 21, 212–21. https://doi.org/10.1093/cercor/bhq081

San-juan, D., Morales-Quezada, L., Orozco Garduño, A.J., Alonso-Vanegas, M., González-Aragón, M.F., Espinoza López, D.A., Vázquez Gregorio, R., Anschel, D.J., Fregni, F., 2015. Transcranial Direct Current Stimulation in Epilepsy. Brain Stimul. 8, 455–464. https://doi.org/10.1016/j.brs.2015.01.001

Sanchez-Vives, M. V., 2012. Spontaneous Rhythmic Activity in the Adult Cerebral Cortex In Vitro. Humana Press, Totowa, NJ, pp. 263–284. https://doi.org/10.1007/978-1-62703-020-5_8

Sanchez-Vives, M. V., Barbero-Castillo, A., Perez-Zabalza, M., Reig, R., 2020. GABAB receptor-modulation of thalamocortical dynamics and synaptic plasticity. Neuroscience.

https://doi.org/10.1016/J.NEUROSCIENCE.2020.03.011

Sanchez-Vives, M. V., Mattia, M., Compte, A., Perez-Zabalza, M., Winograd, M., Descalzo, V.F., Reig, R., 2010. Inhibitory Modulation of Cortical Up States. J. Neurophysiol. 104, 1314–1324. https://doi.org/10.1152/jn.00178.2010

Sanchez-Vives, M. V., McCormick, D.A., 2000. Cellular and network mechanisms of rhytmic recurrent activity in neocortex. Nat. Neurosci. 3, 1027–1034. https://doi.org/10.1038/79848

Sanchez-Vives, M. V, 2020. Origin and dynamics of cortical slow oscillations. Curr. Opin. Physiol. 15, 217–223. https://doi.org/10.1016/J.COPHYS.2020.04.005

Sanchez-Vives, M. V, Massimini, M., Mattia, M., 2017. Shaping the Default Activity Pattern of the Cortical Network. Neuron 94, 993–1001. https://doi.org/10.1016/j.neuron.2017.05.015

Sancristóbal, B., Rebollo, B., Boada, P., Sanchez-Vives, M. V., Garcia-Ojalvo, J., 2016. Collective stochastic coherence in recurrent neuronal networks. Nat. Phys. 12, 881–887. https://doi.org/10.1038/nphys3739

Sanders, R.D., Tononi, G., Laureys, S., Sleigh, J.W., 2012. Unresponsiveness ≠ Unconsciousness. Anesthesiology 116, 946–959. https://doi.org/10.1097/ALN.0b013e318249d0a7

Sankar, T., Lipsman, N., Lozano, A.M., 2014. Deep Brain Stimulation for Disorders of Memory and Cognition. Neurotherapeutics 11, 527–534. https://doi.org/10.1007/s13311-014-0275-0

Saper, C.B., Fuller, P.M., Pedersen, N.P., Lu, J., Scammell, T.E., 2010. Sleep State Switching. Neuron 68, 1023–1042. https://doi.org/10.1016/j.neuron.2010.11.032

Sarma, P., Medhi, B., 2017. Photopharmacology. Indian J. Pharmacol. 49, 221–222. https://doi.org/10.4103/0253-7613.215730

Scarr, E., 2012. Muscarinic Receptors: Their Roles in Disorders of the Central Nervous System and Potential as Therapeutic Targets. CNS Neurosci. Ther. 18, 369–379. https://doi.org/10.1111/j.1755-5949.2011.00249.x

Schiff, N.D., 2008. Central thalamic contributions to arousal regulation and neurological disorders of consciousness. Ann. N. Y. Acad. Sci. 1129, 105–118. https://doi.org/10.1196/annals.1417.029

Schiff, N.D., Nauvel, T., Victor, J.D., 2014. Large-scale brain dynamics in disorders of consciousness. Curr. Opin. Neurobiol. 25, 7–14. https://doi.org/10.1016/j.conb.2013.10.007

Schwindt, P.C., Spain, W.J., Crill, W.E., 1992. Calcium-dependent potassium currents in neurons from cat sensorimotor cortex. J. Neurophysiol. 67, 216–226. https://doi.org/10.1152/jn.1992.67.1.216

Shiri, Z., Manseau, F., Lévesque, M., Williams, S., Avoli, M., 2016. Activation of specific neuronal networks leads to different seizure onset types. Ann. Neurol. 79, 354–365. https://doi.org/10.1002/ana.24570

Shu, Y., Hasenstaub, A., McCormick, D.A., 2003. Turning on and off recurrent balanced cortical activity. Nature 423, 288–293. https://doi.org/10.1038/nature01616

Singer, W., 1993. Synchronization of Cortical Activity and its Putative Role in Information Processing and Learning. Annu. Rev. Physiol. 55, 349–374. https://doi.org/10.1146/annurev.ph.55.030193.002025

Somjen, G.G., 2002. Ion regulation in the brain: Implications for pathophysiology. Neuroscientist 8, 254–267. https://doi.org/10.1177/1073858402008003011

Spruston, N., 2008. Pyramidal neurons: dendritic structure and synaptic integration. Nat. Rev. Neurosci. 9, 206–221. https://doi.org/10.1038/nrn2286

Staba, R.J., Bragin, A., Aibel-Weiss, S., van't Klooster, M.A., Engel, J.B.T.-R.M. in N. and

B.P., 2017. Oscillatory Activity: Neuronal Networks Generating Pathological High Frequency Oscillations. Elsevier. https://doi.org/10.1016/B978-0-12-809324-5.00171-1

Steriade, M., 2006. Grouping of brain rhythms in corticothalamic systems. Neuroscience 137, 1087–1106. https://doi.org/10.1016/j.neuroscience.2005.10.029

Steriade, M., Amzica, F., Contreras, D., 1996. Synchronization of fast (30-40 Hz) spontaneous cortical rhythms during brain activation. J. Neurosci. 16, 392–417. https://doi.org/10.1523/JNEUROSCI.16-01-00392.1996

Steriade, M., Amzica, F., Nunez, A., 1993. Cholinergic and noradrenergic modulation of the slow (approximately 0.3 Hz) oscillation in neocortical cells. J. Neurophysiol. 70, 1385–1400. https://doi.org/10.1152/jn.1993.70.4.1385

Steriade, M., Contreras, D., Amzica, F., 1994. Synchronized sleep oscillations and their paroxysmal developments. Trends Neurosci. 17, 201–207. https://doi.org/10.1016/0166-2236(94)90105-8

Steriade, M, Contreras, D., Curró Dossi, R., Nuñez, A., Houtkooper, R.H., Auwerx, J., Franken, P., Tafti, M., 1993a. The slow (< 1 Hz) oscillation in reticular thalamic and thalamocortical neurons: scenario of sleep rhythm generation in interacting thalamic and neocortical networks. J. Neurosci. 13, 3284–99. https://doi.org/11124996

Steriade, M, Nuñez, A., Amzica, F., 1993b. A novel slow (< 1 Hz) oscillation of neocortical neurons in vivo: depolarizing and hyperpolarizing components. J. Neurosci. 13, 3252–65. https://doi.org/10.1523/JNEUROSCI.13-08-03252.1993

Steriade, M., Timofeev, I., 2003. Neuronal plasticity in thalamocortical networks during sleep and waking oscillations. Neuron 37, 563–576. https://doi.org/10.1016/S0896-6273(03)00065-5

Steriade, M., Timofeev, I., Grenier, F., 2001. Natural Waking and Sleep States: A View From Inside Neocortical Neurons. J. Neurophysiol. 85, 1969–1985.

https://doi.org/10.1152/jn.2001.85.5.1969

Stratton, P., Wiles, J., 2015. Global segregation of cortical activity and metastable dynamics. Front. Syst. Neurosci. 9, 119. https://doi.org/10.3389/fnsys.2015.00119

Subramanian, D., Pralong, E., Daniel, R.T., Chacko, A.G., Stoop, R., Babu, K.S., 2018. Gamma oscillatory activity in vitro: a model system to assess pathophysiological mechanisms of comorbidity between autism and epilepsy. Transl. Psychiatry 8, 16. https://doi.org/10.1038/s41398-017-0065-7

Susin, E., Destexhe, A., 2020. Cellular correlates of wakefulness and slow-wave sleep: evidence for a key role of inhibition. Curr. Opin. Physiol. 15, 68–73. https://doi.org/10.1016/j.cophys.2019.12.006

Taub, A.H., Katz, Y., Lampl, I., 2013. Cortical balance of excitation and inhibition is regulated by the rate of synaptic activity. J. Neurosci. 33, 14359–68. https://doi.org/10.1523/JNEUROSCI.1748-13.2013

Telesford, Q.K., Simpson, S.L., Burdette, J.H., Hayasaka, S., Laurienti, P.J., 2011. The Brain as a Complex System: Using Network Science as a Tool for Understanding the Brain. Brain Connect. 1, 295–308. https://doi.org/10.1089/brain.2011.0055

Thomson, A.M., Lamy, C., 2007. Functional maps of neocortical local circuitry. Front. Neurosci. 1, 19–42. https://doi.org/10.3389/neuro.01.1.1.002.2007

Tononi, G., 2004. An information integration theory of consciousness. BMC Neurosci. 5, 42. https://doi.org/10.1186/1471-2202-5-42

Tononi, G., Edelman, G.M., 1998. Consciousness and complexity. Science 282, 1846–51. https://doi.org/10.1126/science.282.5395.1846

Tononi, G., Sporns, O., Edelman, G.M., 1994. A measure for brain complexity: Relating functional segregation and integration in the nervous system. Neurobiology 91, 5033–5037. https://doi.org/10.1073/pnas.91.11.5033

Tremblay, R., Lee, S., Rudy, B., 2016. GABAergic Interneurons in the Neocortex: From Cellular Properties to Circuits. Neuron 91, 260–292. https://doi.org/10.1016/J.NEURON.2016.06.033

Van Dort, C.J., Baghdoyan, H.A., Lydic, R., 2008. Neurochemical modulators of sleep and anesthetic states. Int. Anesthesiol. Clin. 46, 75–104. https://doi.org/10.1097/AIA.0b013e318181a8ca

Voss, L.J., García, P.S., Hentschke, H., Banks, M.I., 2019. Understanding the Effects of General Anesthetics on Cortical Network Activity Using Ex Vivo Preparations. Anesthesiology 130, 1049–1063. https://doi.org/10.1097/ALN.0000000000002554

Weber, F., Dan, Y., 2016. Circuit-based interrogation of sleep control. Nature 538, 51–59. https://doi.org/10.1038/nature19773

Wester, J.C., Contreras, D., 2012. Columnar Interactions Determine Horizontal Propagation of Recurrent Network Activity in Neocortex. J. Neurosci. 32, 5454–5471. https://doi.org/10.1523/JNEUROSCI.5006-11.2012

Whittington, M.A., Traub, R.D., Kopell, N., Ermentrout, B., Buhl, E.H., 2000. Inhibition-based rhythms: Experimental and mathematical observations on network dynamics. Int. J. Psychophysiol. 38, 315–336. https://doi.org/10.1016/S0167-8760(00)00173-2

Wislowska, M., del Giudice, R., Lechinger, J., Wielek, T., Heib, D.P.J., Pitiot, A., Pichler, G., Michitsch, G., Donis, J., Schabus, M., 2017. Night and day variations of sleep in patients with disorders of consciousness. Sci. Rep. 7, 266. https://doi.org/10.1038/s41598-017-00323-4

Wright, J.J., 1997. EEG simulation: variation of spectral envelope, pulse synchrony and ≈40 Hz oscillation. Biol. Cybern. 76, 181–194. https://doi.org/10.1007/s004220050331

Wu, C., Sun, D., 2015. GABA receptors in brain development, function, and injury. Metab. Brain Dis. 30, 367–79. https://doi.org/10.1007/s11011-014-9560-1

Xia, X., Yang, Y., Guo, Y., Bai, Y., Dang, Y., Xu, R., He, J., 2018. Current Status of Neuromodulatory Therapies for Disorders of Consciousness. Neurosci. Bull. 34, 615–625. https://doi.org/10.1007/s12264-018-0244-4

Yang, H., Shew, W.L., Roy, R., Plenz, D., 2012. Maximal Variability of Phase Synchrony in Cortical Networks with Neuronal Avalanches. J. Neurosci. 32, 1061–1072. https://doi.org/10.1523/JNEUROSCI.2771-11.2012

Yuste, R., 2015. From the neuron doctrine to neural networks. Nat. Rev. Neurosci. 16, 487–497. https://doi.org/10.1038/nrn3962

Zagha, E., McCormick, D.A., 2014. Neural control of brain state. Curr. Opin. Neurobiol. 29, 178–86. https://doi.org/10.1016/j.conb.2014.09.010

Zhang, J., 2019. Basic Neural Units of the Brain: Neurons, Synapses and Action Potential.

Zimmerman, G., Njunting, M., Ivens, S., Tolner, E., Behrens, C.J., Gross, M., Soreq, H., Heinemann, U., Friedman, A., 2008. Acetylcholine-induced seizure-like activity and modified cholinergic gene expression in chronically epileptic rats. Eur. J. Neurosci. 27, 965–975. https://doi.org/10.1111/j.1460-9568.2008.06070.x

Appendix I

Table 1. Mean±SE of estimated FR (FRs) and the decay of exponential curve under SWA, awake-like conditions and after blocking $GABA_A$ (GBZ) and blocking $GABA_B$ (CGP 55845, CGP).

		FRs (a.u.)	α-decay (a.u.)
n=20	**SWA**	60.46±5.54	0.65±0.13
	Awake – like	232.78±27.63	1.61 ±0 .21
n=10	**SWA**	62.61±7.17	0.54±0.09
	Awake – like	203.93±28.67	1.27±0.19
	+ 200 nM GBZ	215.57±25.10	0.26±0.04
n=7	**SWA**	55.93±9.24	0.51±0.15
	Awake – like	213.11±41.73	2.15±0.24
	+ 1 µM CGP	177.94±39.69	0.66±0.17

Table 2. Mean±SE of sPCI after blocking $GABA_A$ (GBZ) and $GABA_B$ (CGP55845, CGP) during "awake-like" states.

sPCI SWA and "awake-like" state (*n*=20)			
SWA		0,103±0,004	
Awake-like		0,141±0,005	
+ GBZ sPCI (*n*=10)		**+ CGP 558845 sPCI (*n*=7)**	
SWA	0.107±0.006	**SWA**	0.104±0.008
Awake-like	0.137±0.006	**Awake-like state**	0.145±0.008
+ 50 nM GZB	0.128±0.009	**+ 100 nM CGP**	0.129±0.011
+ 100 nM GBZ	0.096±0.014	**+ 200 nM CGP**	0.118±0.013
+ 150 nM GBZ	0.086±0.011	**+ 500 nM CGP**	0.115±0.004
+ 200 nM GBZ	0.060±0.006	**+ 1 µM CGP**	0.109±0.008

Table 3. Mean±SE of estimated FR (FRs), relative Firing rate during the Up-states (FR Ups) and the decay of exponential curve (α-decay) under SWA and after blocking $GABA_A$ (BMI and GBZ) or $GABA_B$ (CGP55845, CGP).

	Concentration	FRs (a.u.).	FR Ups (a.u.)	α-decay (a.u.)
BMI (*n*=9)	SWA	49.54±5.97	1.55±0.15	0.33±0.04
	0.6 µM BMI	67.57±8.85	2.94±0.11	0.21 ±0.02
	1 µM BMI	76.13 ±1 0.64	3.39±0.16	0.19±0.01
GBZ (*n*=9)	SWA	58.31±14.43	1.92±0.14	0.55±0.07
	+ 100 nM GBZ	89.32±16.32	3.04±0.16	0.35±0.01
	+ 200 nM GBZ	112.37±22.65	4.12±0.36	0.20±0.01
CGP55845 (*n=11*)	SWA	57.59±11.02	1.64±0.09	0.54±0.09
	+ 200 nM CGP	64.62±9.81	1.75±0.12	0.30±0.06
	+ 1 µM CGP	72.34±11.83	1.91±0.12	0.29±0.03

Table 4. Mean±SE of sPCI after blocking $GABA_A$ (GBZ and BMI) and $GABA_B$ (CGP55845) during SWA.

SWA + Inhibition blockers					
$GABA_A$ blockers				$GABA_B$ blocker	
BMI (*n*=9)		GBZ (*n*=9)		CGP 55845 (*n*=11)	
SWA	0.096±0.004	SWA	0.098±0.006	SWA	0.094±0.004
0.2 µM	0.086±0.005	50 nM	0.099±0.006	100 nM	0.084±0.004
0.4 µM	0.096±0.006	100 nM	0.091±0.006	200 nM	0.075±0.004
0.6 µM	0.076±0.009	150 nM	0.061±0.004	500 nM	0.073±0.005
0.8 µM	0.077±0.008	200 nM	0.061±0.007	1 µM	0.066±0.004
1 µM	0.066±0.008				

Table 5. Mean±SE of estimated FR (FRs), relative Firing rate during the Up-states (FR Ups), oscillation frequency (OF), the decay of exponential curve under (α-decay) and sPCI under increasing concentrations of $[K^+]_{ec}$ (n=9).

Concentration	FRs (a.u.)	FR Ups (a.u.)	OF (Hz)	α-decay (a.u.)	sPCI
SWA	58.71±17.10	0.90±0.16	0.39±0.03	0.49±0.05	0.086±0.030
5 mM K^+	98.35±21.61	0.94±0.84	0.61±0.05	0.65±0.13	0.090±0.050
7 mM K^+	152.25±26.88	0.84±0.13	0.93±0.10	1.07±0.16	0.114±0.100
Washout	61.53±11.24	0.76±0.11	0.30±0.05	0.65±0.13	0.087±0.004

Table 6. Mean±SE of estimated FR (FRs), the decay of exponential curve under (α-decay) and sPCI under increasing concentrations of K^+ channel blockers.

	Concentration	FRs (a.u.)	α-decay (a.u.)	sPCI
TEA ***(n=4)***	**SWA**	37.54±7.29	0.61±0.10	0.087 ±0.010
	1 mM TEA	47.78±1.54	0.69±0.08	0.081 ±0.010
	5 mM TEA	35.26±7.73	0.54±0.13	0.057±0.004
	10 mM TEA	44.77±6.37	0.75±0.27	0.062 ±0.001
4-AP ***(n=6)***	**SWA**	59.60±8.91	0.44±0.04	0.097±0.010
	25 µM 4-AP	116.43±24.07	0.82±0.07	0.079±0.004
	Washout	65.09±14.91	0.75±0.15	0.095±0.010
	50 µM 4-AP	152.31±36.30	0.89±0.30	0.086±0.010
XE991 ***(n=5)***	**SWA**	73.95±10.87	0.40±0.11	0.092±0.01
	XE991	383.52±94.12	1.12±0.06	0.088±0.0139

Table 7. Mean±SE of estimated FR (FRs), relative Firing rate during the Up-states (FR Ups), oscillation frequency (OF), the decay of exponential curve under (α-decay) and sPCI under growing intensities of DCS.

Intentisy	FRs (a.u.)	FR Ups (a.u.)	OF (Hz)	α-decay (a.u.)	sPCI
-3 V/m (*n=8*)	52.67±32.90	0.93±0.08	0.23±0.04	0.26±0.06	0.10±0.01 (*n=5*)
0 V/m (*n=13*)	73.88±55.88	1.05±0.06	0.30±0.05	0.41±0.05	0.09±0.01 (*n=6*)
+ 2 V/m (*n=10*)	143.88±243.13	0.94±0.06	0.45±0.04	0.46±0.08	0.12±0.01 (*n=5*)
+ 5 V/m (*n=10*)	170.29±278.90	0.75±0.09	0.71±0.06	0.73±0.07	0.10±0.02 (*n=6*)

Table 8. Mean±SE of estimated FR (FRs), relative Firing rate during the Up-states (FR Ups), oscillation frequency (OF), the decay of exponential curve under (α-decay) under bath application non-selective muscarinic agonist (Iperoxo, IPX) in vitro.

Concentration	FRs (a.u.)	FR Ups (a.u.)	OF (Hz)	α-decay (a.u.)
SWA	127.03± 70.16	1.13±0.24	0.89±0.12	0.51±0.13
1 nM IPX	151.10± 77.90	0.75±0.03	0.83±0.08	0.78±0.20
10 nM IPX	256.19±102.89	0.67±0.08	1.11±0.20	0.68±0.02
100 nM IPX	116.03±35.88	0.10±0.02	1.34±0.19	0.38±0.02
Seizure (100 – 200 nM)	73.46±5.16			1.21±0.32

Table 9. Mean±SE of relative Firing rate during the Up-states (FR Ups) and oscillation frequency (OF) under the bath application of increasing concentrations of PAI isoforms (cis- and trans-PAI) in vitro.

Condition		OF (Hz)	FR Ups (a.u.)
***trans*-PAI (*n*=6)**	**SWA**	0.58±0.06	0.99±0.11
	10 nM	0.55±0.06	0.97±0.12
	100 nM	0.87±0.10	0.72±0.09
	300 nM	1.66±0.10	0.50±0.08
	1 µM	1.87±0.13	0.37±0.03
***cis*-PAI (*n*=6)**	**SWA**	0.48±0.04	0.86±0.04
	10 nM	0.46±0.05	1.07±0.08
	100 nM	0.52±0.07	1.10±0.14
	300 nM	0.88±0.25	0.79±0.19
	1 µM	1.37±0.27	0.74±0.19

Table 10. Mean±SE of estimated FR (FRs), relative Firing rate during the Up-states (FR Ups), oscillation frequency (OF), the decay of exponential curve under (α-decay) and sPCI under bath application of cis-PAI and upon illumination (trans-PAI) in vitro.

Condition	FRs (a.u.)	FR Ups (a.u.)	OF (Hz)	α-decay (a.u.)	sPCI
SWA	84.12±16.73	1.02±0.10	0.53±0.04	0.67±0.04	0.09±0.01
***cis*-PAI**	121.46±25.34	0.88±0.10	1.03±0.14	0.68±0.07	0.10±0.01
***trans*-PAI**	150.47±23.49	0.52±0.06	1.68±0.11	0.60±0.1	0.12±0.01

Table 11. Mean±SE of relative Firing rate during the Up-states (FR Ups) and oscillation frequency (OF) under the bath application of increasing concentrations of PAI isoforms (cis- and trans-PAI) in vivo.

Concentration		FR Ups (a.u.)	OF (Hz)
200 nM	**SWA**	0.87±0.29	0.63±0.08
	***cis*-PAI**	1.03±0.43	0.60±0.09
	***trans*-PAI**	1.06±0.38	0.77±0.13
1 µM	***cis*-PAI**	1.02±0.37	0.64±0.14
	***trans*-PAI**	0.82±0.27	0.89±0.02

Appendix II

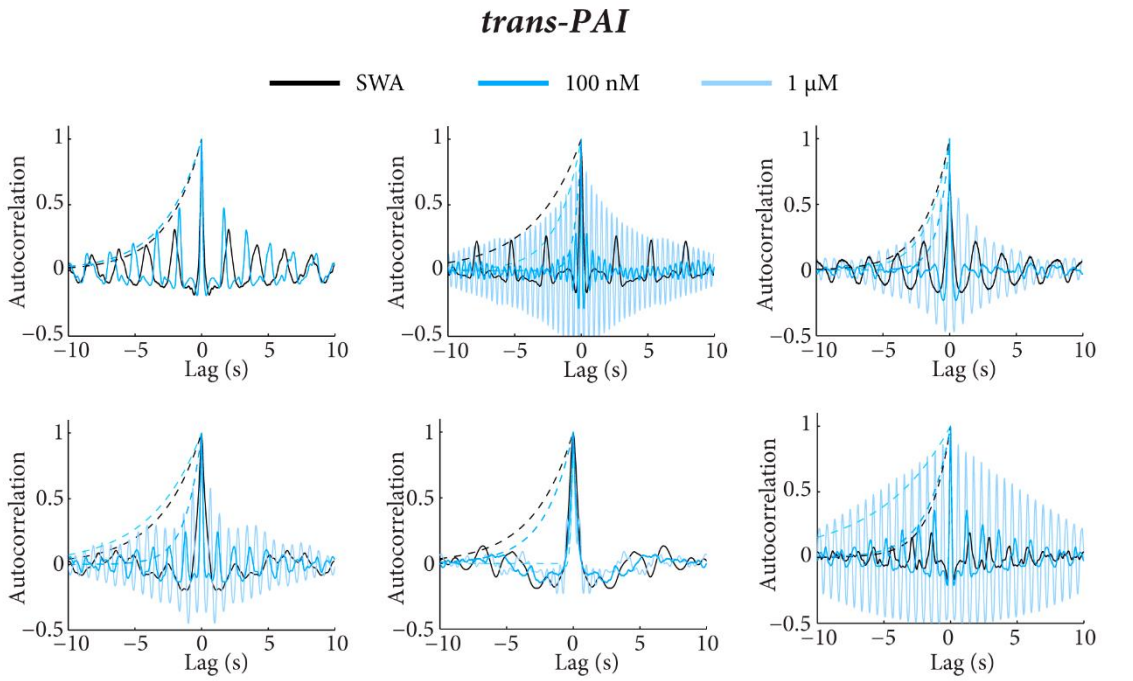

Figure S1. *Autocorrelograms of the rhythmicity of the neuronal oscillatory activity during SWA regime (black line), at 100 nM and 1 µM of trans-PAI (blue lines) applications*

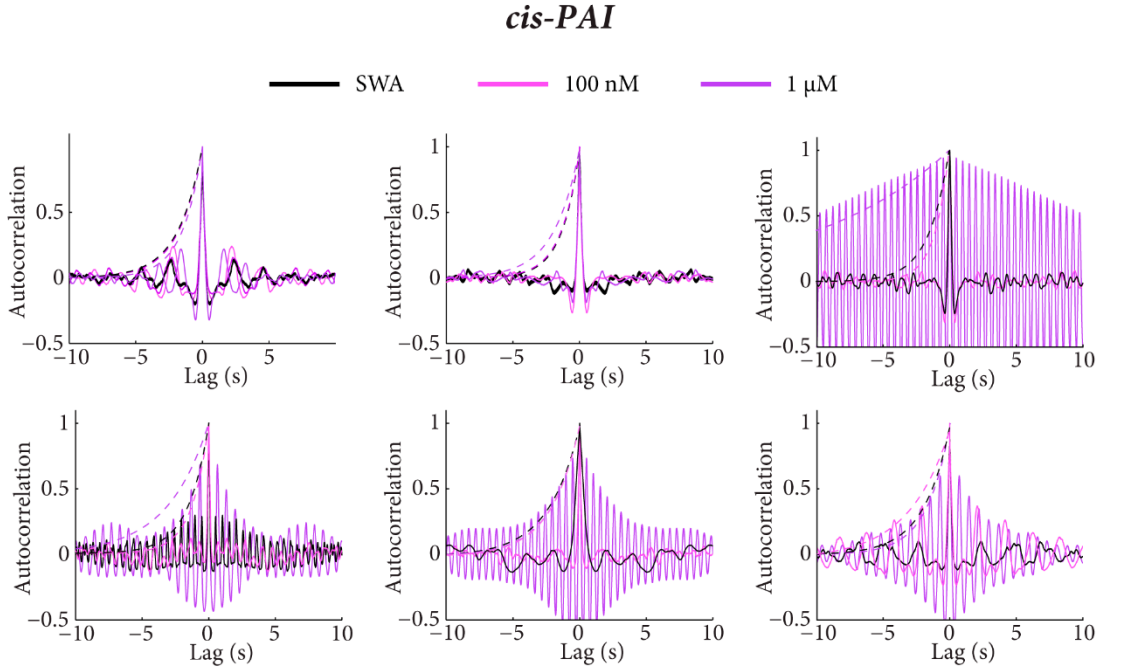

Figure S2 *Autocorrelograms of the rhythmicity of the neuronal oscillatory activity during SWA regime (black line), at 100 nM and 1 µM of cis-PAI (pink lines) applications.*

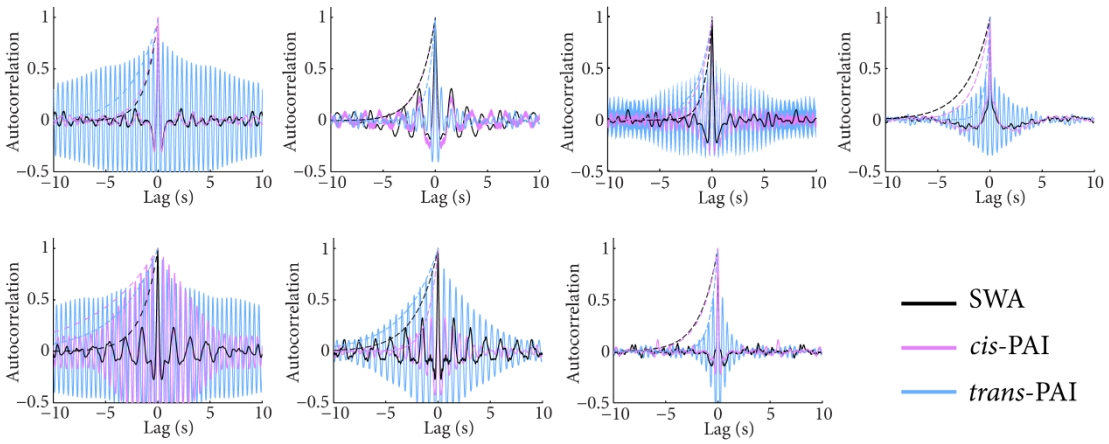

Figure S3. *PAI can light-modulate the neuronal oscillatory activity in cortical ferret slices. Autocorrelograms of the rhythmicity of the neuronal oscillatory activity during SWA regime (black line), under 200 nM cis-PAI application (pink line) and during white light irradiation (trans-PAI, blue line).*